DOI: 10.14750/ME.2025.027

Computational and Experimental Study of Antioxidant Polymer Additives

Ph.D. Dissertation

Dalal Karad Thbayh

Supervisor:
Dr. Béla Fiser

Antal Kerpely Doctoral School of Materials Science & Technology at the Faculty of Materials Science and Chemical Engineering

Institute of Chemistry
University of Miskolc
2025

DOI: 10.14750/ME.2025.027

بِسْمِ اللَّهِ الرَّحْمَٰنِ الرَّحِيمِ

"سَيَرْفَعُ اللَّهُ الَّذِينَ آمَنُوا مِنْكُمْ وَالَّذِينَ أُوتُوا الْعِلْمَ دَرَجَاتٍ ۚ وَاللَّهُ بِمَا تَعْمَلُونَ خَبِيرٌ"

القرآن الكريم [سورة المجادلة، الآية 11]

"Allah will raise those who have believed among you and those who were given knowledge, by degrees. And Allah is Acquainted with what you do."

The Noble Qur'an [Chapter 28- Al-Mujadila, Verse 11]

DOI: 10.14750/ME.2025.027

Supervisor's Recommendation for

Dalal Karad Thbayh

for her doctoral dissertation entitled as

Computational and Experimental Study of Antioxidant Polymer Additives

It was a great honor to work with Dalal Karad Thbayh over the last four years. She has been involved in several projects, many of which she initiated.

It was just nice to witness her growth in leadership roles and how she managed various research tasks. During this period, I have observed her consistently improving in all areas of research and soft skills.

Over the last four years, Dalal Karad has contributed to 22 articles, four of which were closely related to her PhD topic. In these instances, she was the first author of the publications which were accepted in internationally recognized scientific journals (e.g., Q1). She has also contributed to conferences and workshops with 15 oral and poster presentations. Furthermore, Dalal was involved in patent preparation, demonstrating that her results are not only scientifically significant but also have industrial relevance.

During her PhD studies, Dalal proved the applicability of several natural antioxidants in polymeric formulations using a combined computational and experimental approach.

Her ability to conduct research in different frameworks is further supported by the fact that she engaged in both theoretical and laboratory research during her PhD.

Her commitment to continuous improvement was inspiring to others and helped to maintain a high team spirit.

Dalal has a pleasant personality and is exceptionally active. She works well both independently and in diverse cultural and group environments. This was evident when she spent several weeks in Poland at the University of Lodz and conducted research at BorsodChem-Wanhua (Hungary).

All the findings presented in Dalal's publications and doctoral dissertation are her own and serve as strong indicators of her independent scientific work.

Based on all of this, I am confident that Dalal Karad Thbayh is capable of conducting independent research, and I strongly recommend that she be awarded a PhD degree.

Miskolc, 13 February 2025 Dr. Béla Fiser

DOI: 10.14750/ME.2025.027

CONTENTS

DOI: 10.14750/ME.2025.027

DOI: 10.14750/ME.2025.027

DOI: 10.14750/ME.2025.027

ACKNOWLEDGMENT

Before all else, I offer my heartfelt praise and thanks to **God**, the Almighty, for His continuous guidance and countless blessings throughout my research and dissertation journey.

After thanking God, I would like to express my gratitude to **myself** for staying committed, pushing through hardships, and never giving up, all of which have allowed me to successfully earn my PhD. A PhD degree is not just a degree but a new journey full of challenges and difficulties that make you a different person, very different from who you were before this stage. Today, I take a moment to truly appreciate my journey, my growth, and the strength that brought me to this significant milestone. I do so with gratitude, pride, and a renewed sense of purpose for the future ahead.

I would like to express my gratitude and thanks to the person who words cannot do justice to, my supervisor **Dr. Béla Fiser**. He was not only a supervisor but also a friend, teacher, and mentor throughout my doctoral studies. He made me a diligent researcher and taught me many of the basics of scientific research, so I will always be your student, and I will follow your methods in the future with my students. He is a very respectful person, with refined and friendly dealings. He did not only share my academic journey but also went through many trips and challenges with me. He was an important part of my journey to discover this country and its kind people, among whom I never felt like a stranger. This is why I have always maintained that having a supervisor is not inherently difficult, but it becomes more challenging when that supervisor fully supports your decisions and has faith in your abilities. Really, without you, I would not have been able to accomplish this work with such mastery and success. I am deeply grateful for your unwavering support, and I thank you for the care and attention you have given me over the years and for celebrating our successes together. Finally, my graduation from my doctorate does not mean the end of work with you, but rather the beginning of a new journey in our academic journey by participating together and working as a team.

I wish to express my gratitude to **Prof. Dr. Béla Viskolcz** for his diligent mentorship and unwavering support of my PhD research.

I am grateful and lucky to have a chance to meet and learn from one of the great Hungarian minds **Prof. Imre G. Csizmadia**.

I would like to say thank you to **Dr Kálmán Marossy** for helping me as a reviewer throughout the study period. Thank you for your valuable time, knowledge and useful information that you generously share with me whenever I need it.

I would like to express my gratitude and appreciation to BorsodChem Zrt., company which nurtured me during my study and provided me with the opportunity to complete my work requirements. It was a valuable year full of success, energy, vitality, and fun to work. I stand with respect for PVC plant staff, **Farkas László, Boros Renáta Zsanett, Bagi Péter, Bartha-Lengyel Kitti, Csaba Kónya, Gabriella Szemere, and Krisztina Tózsa**, for their generous assistance and support throughout my work in BorsodChem.

I would like to say thanks to the **Stipendium Hungaricum Scholarship** for supporting my studies.

Thank you to the **University of Basrah/ Polymer Research Center** for giving me this opportunity to complete my doctoral studies.

I would like to thank the staff of the **University of Miskolc** and **Institute of Chemistry** for welcoming me and creating a cheerful and kind atmosphere throughout my whole PhD study. Thanks to them, I was able to work in a wonderful environment, surrounded by kind, smart, and friendly people. Thanks for everything you gave me; I will not forget all the joyful moments in this institute.

I would like to dedicate my success and work to the soul of **my father**; may God have mercy on him. I know that even if you are not in my life, your soul accompanies me.

My tongue is unable to express my thanks and appreciation to the woman who is the reason for my success, **my mother**; may God preserve her for the unlimited sacrifices she made, her love, her care and prayers, and for devoting her life to my success. I do not forget her tears every time she said goodbye to me and missed me. Your tears are the reason for my success. Therefore, I will always say to you, "Thank you, the greatest struggling person I have ever seen," and "Thank you for being the reason for what I have achieved now." I hope that I will be able to repay some of your sacrifices for me, and I hope that I will never disappoint you.

Many thanks to all my family members, especially my brothers (**Ali and Murtada**) and sisters (**Kifaya, Ibtisam and Nidal**) for the care, support and encouragement they have given me all the time. I ask God Almighty to protect them and grant them success in their lives.

I will not forget to thank all of my **nieces and nephews** for playing such an important role in my life and making it more beautiful and joyful. I adore you all.

I would like to say thanks a lot, **Dr. Rachid** for being part of my PhD journey. Thanks for being good support and good friend.

Last but not least, I would like to thank all my best friends and tell them how lucky I am to have you as part of my journey. We have travelled, eaten, been happy, celebrated and even cried when we were at our worst. These days will always be etched in my memory, and I thank God that I met friends like you and I hope I was the best friend to you. I love you all.

This research was supported by the National Research, Development and Innovation Fund (Hungary) within the TKP2021-NVA-14 project. The GITDA (Governmental Information-Technology Development Agency, Hungary) is gratefully acknowledged for allocating computing resources used in this work. Further calculations have been carried out using resources provided by the Wroclaw Centre for Networking and Supercomputing. This research was funded in part by the National Science Centre, Poland under the MINIATURA 7 call within the project reg. No: 2023/07/X/ST4/01433.

DOI: 10.14750/ME.2025.027

Ethical Use of Artificial Intelligence in Dissertation Preparation

"I declare that during the preparation of the thesis, I did not use the services of artificial intelligence, except for grammatical and stylistic corrections".

Dalal Karad

TABLE OF FIGURES

DOI: 10.14750/ME.2025.027

TABLE OF TABLES

TABLE OF ABBREVIATION

Asc	L-Ascorbic acid
Asc. Pal.	Ascorbic Palmitate
AO	Antioxidants
B3LYP	Becke, 3 parameter, Lee-Yang-Parr
BLYP	Becke, Lee–Yang–Parr
BHA	butylated hydroxyanisole
BHT	butylated hydroxytoluene
BDE	Bond dissociation enthalpy
B88	Becke88
B.L	Bond lengths
BO	Born-Oppenheimer
Cur.	Curcumin
CC	coupled cluster
CB.A	chain- breaking acceptor
CB.D	chain - breaking donar
CFD	compression force deflection
DOP	dioctylphthalate
DFT	density functional theory
DI	delocalisation index
EDTA	Ethylenediaminetetraacetic acid
ETE	electron transfer enthalpies
ED	electron density
Eq	Equation
FPUF	Flexible Polyurethane Foam
G	Gibbs Free Energy
HAT	hydrogen atom transfer
HCl	hydrogen chloride
HF	Hartree–Fock
H	Enthalpy
Irg	Irganox
IP	ionization potential
LSDA	local spin density approximation
MCP	multicomponent polymerization
MD	Metal deactivator
NCO	Isocyanate
OG	octyl gallate
PMMA	poly (methyl methacrylate)
PVDF	polyvinylidene fluoride
PPhb	Parts per hundred of base

PBAT	polybutylene adipate terephthalate
PVC	Polyvinyl chloride
PES	Potential Energy Surface
PEC	Potential Energy Curve
PDE	proton dissociation enthalpy
PAs	proton affinities
PUR	polyurethane
PET	poly (ethylene terephthalate)
PTT	polytrimethylene terephthalate
PLA	polylactic acid
PHA	polyhydroxyalkanoates
PBS	polybutylene succinate
PCL	polycaprolactone.
PE	polyethylene
PP	polypropylene
PA	polyamide
PZ	Perdew-Zunger
PW	Perdew-Wang
PU	Polyurethane
PA	proton affinity
PG	propyl gallate
PD	Preroxide decomposes
P	Pressure
RS	radical scavenging
SET-PT	single electron transfer-proton transfer
SPLET	sequential proton loss electron transfer
SMD	Solvation Model based on Density
SPWL	Slater Perdew-Wang local
S	Entropy
TBHQ	tert-butylhydroquinone
TCP	tricresyl phosphate
TS	thermal stability
T	Temperature
UVA	UV absorber
VWN	Vosko-Wilk-Nusair
2D	Two Dimensional

DOI: 10.14750/ME.2025.027

1. Introduction

1.1. Polymers

Synthetic polymers are essential to the life of modern man, as they are used in industrial and agricultural fields, and despite their numerous advantages, most are not environmentally friendly, as they cannot integrate into natural recycling processes [1]. These polymers have a great effect on human life, because they are involved in many areas, including air, and water supply [2, 3], and medical devices which enhance the quality of life [4, 5]. Energy generation and storage [6], communications and electronic devices [7], and other applications of synthetic polymers are also important. Natural polymers are macromolecular materials which are essential for living organisms. Hermann Staudinger, who won the Nobel Prize in 1953 years, came to the conclusion that natural polymers follow the same scheme in terms of production: where monomers of small molecular weight are joined with each other and this will led to large macromolecules with high molecular weight [8]. Green polymers have been first mentioned in 1998 [2, 3], and in the next year, it was extended to some special polymer technology as well [4]. From that time, many green chemistry paths included into modern polymer technology. Green chemistry is the process of producing environmentally friendly materials using specific chemical processes [9]. Thus, green polymer technology is established, where the word “green” is not just refer to something similar to biomaterials and biotechnology. The production of green polymers has become inevitable, because of environmental concerns and not only the final materials, but their preparation needs to be environmentally friendly including all the applied chemicals such as solvents and additives as well. Therefore, organic solvents has to be replaced by water or other suitable nontoxic alternatives [10]. Green technology initiated dramatic change in various areas of polymer chemistry, including the use of catalysts, degradability of polymers, waste minimization, energy generation, application of benign solvents, *etc*. (***Table 1***) [9].

Table 1. Major changes initiated by the involvement of green technology in polymer chemistry [9].

Major Changes	Examples
Greener Catalysts	*e.g.* Biocatalysts such as, enzymes and whole cells.
Diverse feedstock base	Bio-based building blocks and agricultural feedstock (sugars, peptides, triglycerides, and lignin). Natural fillers in composites. CO_2 as monomer.
Degradable polymers and waste minimization	Natural renewable materials. Some polyesters and amides.
Recycling of polymer products and catalysts	Many degradable polymers can potentially be recycled. Immobilized enzymes can be reused.
Energy generation or minimization of use	Biofuels. Reactive extrusion method. Microwave-assisted synthesis.
Optimal molecular design and activity	Improved enzymes. Metabolic engineering. Protein synthesis.
Benign solvents	Water. Ionic liquids, or reactions without solvents
Improved syntheses and processes	Atom economy, reaction efficiency, toxicity reduction

There is a wide variety of polymers and several polymerization routes to satisfy the criteria of green chemistry and keep up with the demands of the society. Some of these green approaches will be mentioned and partially discussed in the following sections.

1.2. Green monomers

A monomer is the smallest basic unit of polymer synthesis. The monomers linked together by covalent bonds during the polymerization process to form a macromolecule which includes a series of repeating units. Monomers can be natural or synthetic according to their source [11]. Green monomers have become of great importance and are used daily in our life due to their many desirable qualities such as cheap, nontoxic, renewable, and sustainable. They can be converted into green polymers and as such used in many fields [12]. Among the

green monomers, which have been used in the multicomponent polymerization (MCP) processes to produce the functional materials, oxygen (O_2), water (H_2O), and carbon dioxide (CO_2) are especially important [13]. They can also be used to produce polycarbonates, polyesters, and polyurethanes, and other polymers as well even by using facile MCP processes [14, 15]. There are countless MCPs take place in living organisms to synthesize biomacromolecules such as DNA, RNA, and proteins. To mimic nature, various efficient organic reactions like Mannich, Passerini, Ugi, *etc.* have been developed and later transformed to MCPs [16]. By using multicomponent polymerization of green monomers, different polymers can be produced, similarly like it occurs in plants, and some bacteria which could easily transform CO_2 and H_2O into polysaccharides by photosynthesis.

1.3. Applications and a Little Bit of History of Plastics

The term of plastic is derived from the Greek word πλαστικός (*plastikos*) which mean "capable of being shaped or moulded" and originates from πλαστός (*plastos*), "moulded" [17]. In 1909, Dr. Leo Hendrick Baekeland developed the first phenol-formaldehyde resin (phenolics), which was the first man-made polymer or plastic [18]. It gained countless applications and expedited the development of synthetic polymer chemistry. The manufacturing of plastics have been developed significantly over time (***Table 2)*** [11].

Table 2. Plastic materials along with the date of their invention, and applications [1].

Materials	Date	Application
Cellulose nitrate	1868	Eyeglass frames
Phenol-formaldehyde	1909	Telephone handsets, knobs, handles
Casein	1919	Knitting needles
Alkyds	1926	Electrical insulators
Poly(vinyl chloride)	1927	Raincoats, flooring
Urea–formaldehyde	1929	Lighting fixtures, electrical switches
Polyethylene(low density)	1932	Squeezable bottles
Ethyl cellulose	1935	Flashlight cases
Polyacrylonitrile	1936	Brush backs, displays.
Poly(vinyl acetate)	1936	Flashbulb lining, adhesives
Polyurethane	1937	Foam cushions
Cellulose acetate butyrate	1938	Irrigation pipe
Polystyrene	1938	Kitchen wares, toys
Nylon (polyamide)	1938	Gears, fibers, films
Poly (vinyl acetal)	1938	Safety glass interlayer
Poly (vinylidene chloride)	1939	Auto seat covers, films, paper.
Melamine–formaldehyde	1939	Tableware
Silicone	1943	Rubber goods

Cellulose propionate	1945	Automatic pens and pencils
Epoxies	1947	Tools and Adhesives
Allylic	1949	Electrical connectors
Acetal resin	1956	Automotive parts
Polypropylene	1957	Safety helmets, carpet fiber
Chlorinated polyether	1959	Valves and fittings
Phenoxy resin	1962	Adhesives, coatings
Ionomer resins	1964	Skin packages, moldings
Polyphenylene oxide	1964	Battery cases, high temperature moldings
Ethylene–vinyl acetate	1964	Wire and Cable Insulation, flexible sheeting
Polybutene	1965	Films
Polysulfone	1965	Electrical/electronic parts
Thermoplastic polyester	1970	Electrical/electronic parts
Hydroxy acrylates	1971	Contact lenses.
Polybutylene	1973	Piping
Aromatic polyamides	1974	High-strength tire cord, Bulletproof vest
Nitrile barrier resins	1975	Containers

These materials were originally produced by using natural compounds, but now there are thousands of plastics formulated from a wide range of bio- and synthetic chemicals [19]. Recent developments focus on to make the production of plastics greener by improving recyclability [20]. Plastics can also be synthesized based on organic polymers such as lignin, which is an important material and the final products can be applied in agriculture or as dye dispersants, emulsifiers, cement additives, pelleting aids, battery expanders, binder, *etc*. [21]. However, lignin has to be purified before applications, because it contains large amounts of sulfur, which causes unpleasant odors and dark colour [22].

Regardless of their features green or not so, synthetic polymers are everywhere, in buildings, vehicles, sport equipment, and medical devices [11]. Biocompatible materials are especially important in medical applications as those are designed for interfacing with biological systems for the evaluation, treatment, enlargement, or substitution of one of the tissues or any other functions of the body [23]. Various polymers are used in this field such as polyvinylidene fluoride (PVDF), polyethylene (PE), polypropylene (PP), and poly(methyl methacrylate) (PMMA), *etc.* [24]. Moreover, there is a wide range of polymer properties that make them preferred for medical applications such as their mechanical, electrical, chemical, and thermal behaviour. If these can be combined with ease of synthesis, flexibility of packaging, and green properties almost ideal polymeric materials are established [25].

DOI: 10.14750/ME.2025.027

1.4. Green Composites

Composite materials have been classified into several types, such as (1) fiber-reinforced composites, (2) particle reinforced composites, and (3) structural composites [26]. Green composites are composite materials comprising of one or multiple-phase materials which could consist of both fibers and polymers originating from natural resources or from recycled materials [27]. The process used in the preparation of green composites is responsible for many of the properties of the resulting product (***Figure 1***) [28].

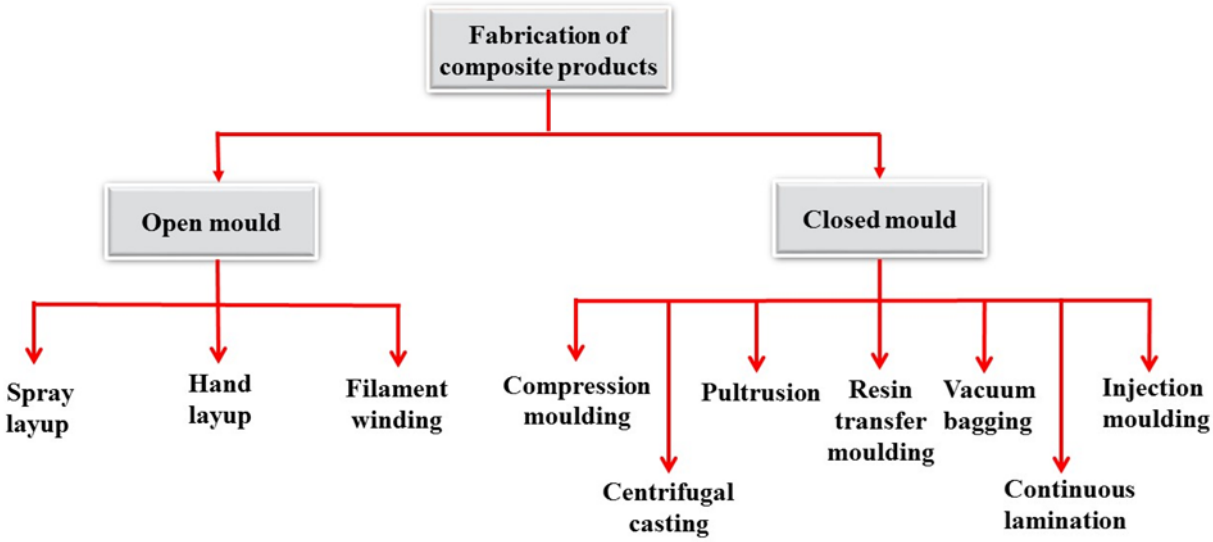

Figure 1. The classifications of fabrication processes of green composite products [28].

In order to pick the most appropriate biofiber or biopolymer for the composite, precise material design process has to be carried out. There are several factors which are essential to be fulfilled by the composite, such as its ability to withstand working conditions (*e.g.,* radiation, thermal stability, humidity, tensile stiffness, strength, fiber treatments), as well as to not increase processing costs [29-31]. Recently, several applications of natural fiber-reinforced polymer composites have appeared in various fields (

***Table* 3**) [28] .

Table 3. Common applications of natural fiber-reinforced polymer composites in various industrial fields [28].

Field	Applications
Sports	Ball, snowboard, bicycle frame, seat post, and boats

Transportation	Door panel, engine rubber insulation, engine cover, floor mat, dashboard, car spoiler, handbrake, steering, pedal components, parcel shelves, interior carpet, and body panels
Building and construction	Bridge, railing, false ceiling, partition boards, windows, doorframes, mobile structure, wall, and floor
Household	Mug pad, chairs, coffee table, shoe rack, suitcases, food tray, safety helmet, ropes, fencing elements, showers, and bath units, pipes
Materials handling and storage	Post-boxes, biogas containers, fuel container, and storage silos

1.5. Bio-based polymers

Polymers can also be classified according to the respective sources of their base materials, and the ones prepared from petroleum are called fossil-based, while the ones which are based on renewable materials are called bio-based polymers ***(Figure 2)*** [28].

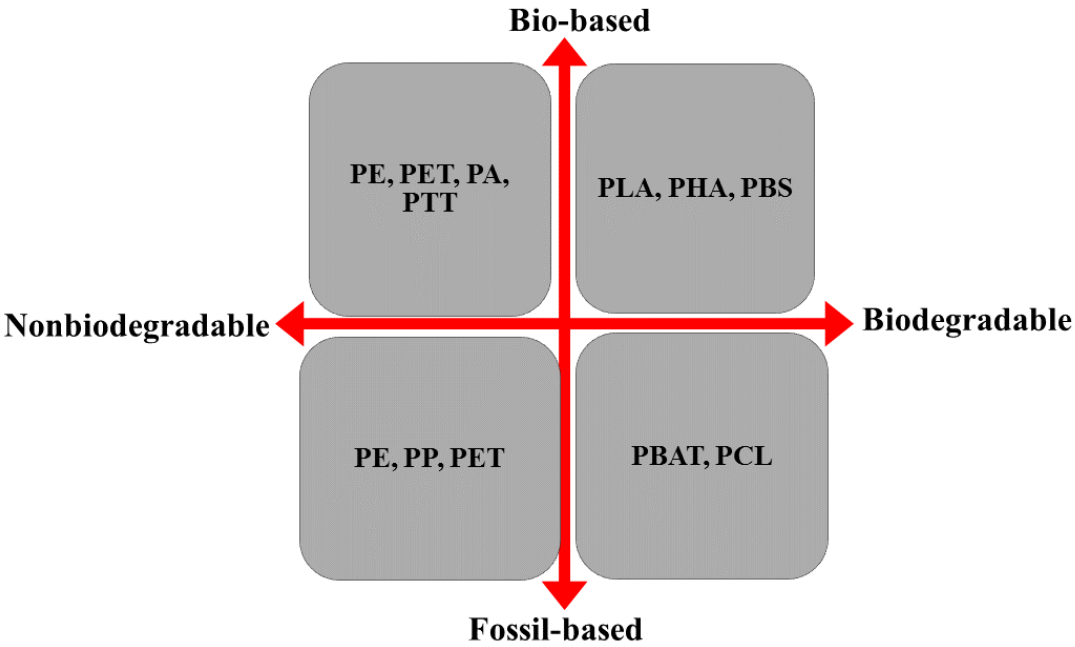

Figure 2. Classification of polymers based on the respective sources of their base materials with examples. PE - polyethylene, PET – poly (ethylene terephthalate), PA - polyamide, PTT - polytrimethylene terephthalate, PLA - polylactic acid, PHA - polyhydroxyalkanoates, PBS - polybutylene succinate, PP - polypropylene, PBAT - polybutylene adipate terephthalate, and PCL - polycaprolactone.

Another special group of bio-based polymers are biopolymers which are the main components of living organisms. Three different classes can be identified based on their monomers and their structure. There are polynucleotides (RNA or DNA), polypeptides (which are shorter or longer polymers of amino acids), and polysaccharides, which are often linear polymeric carbohydrate structures. Bio-based polymers have received a lot of attention in various fields [32]. Especially due to the increase in environmental pollution resulting from the excessive use of fossil fuel resources. Great efforts have been made to replace the traditional petroleum-based polymers with bio-based materials [33]. Biopolymers are used as raw materials for several applications, because of their safety, non-toxicity, low cost, high efficiency, biodegradability, biocompatibility, and reproducibility. These properties have led to the widespread use of biopolymers as thickeners, emulsifiers, suspending agents, and moisturizers in the food, cosmetics, pharmaceuticals, and paint industries [34]. Furthermore, bio-based packaging is considered one of the best candidate for replacing millions of tons of petrochemical-derived materials [35].

According to an additional classification of bio-based polymers there are 'bio-replacement' polymers, and 'bio-advantaged' polymers.

'Bio-replacement' polymers, where the applied monomers are produced from petroleum, but their structure is identical to bio-based compounds, but free of contamination. The 'replacement' technique improves quality of sugar, lignin, and cellulose present in trees, plants, and also in animals by using synthetic biology methods and catalysis to synthesize the monomers from fossil fuels [36]. 'Bio-advantaged' polymers, where the used monomers are coming from bio-sources (vegetable oils, cellulose, proteins, sugar, starch chitosan, alginates, *etc*.) and they are not or only minimally modified [37].

Bio-based polymers or bio-based plastics are synthesized by using renewable and natural resources and can be prepared through a two-step process from biomass (*e.g.,* lignin, cellulose, starch, plant oils) [38-40]. Bioplastics, such as bio-polyethylene (bio-PE), bio-poly (ethylene terephthalate) (bio-PET), poly (lactic acid) (PLA), and poly (ethylene 2,5-furandicarboxylate) (PEF), are produced by polymerizing various types of monomers such as ethylene, 1,2-ethanediol, terephthalic acid, or novel monomers like lactide, 2,5-furan dicarboxylic acid, 1,4-cyclohexane dicarboxylic acid, furfuryl alcohol, or isosorbide which is obtained by chemical or biochemical conversion of the biomass [8, 36].

DOI: 10.14750/ME.2025.027

1.6. Polyvinyl chloride (PVC)

Polyvinyl chloride (PVC) was first discovered in 1912 (***Scheme 1***). It is a white powder that results from the polymerization of vinyl chloride monomer (VCM). Its commercial production began in the late 1920s, following the addition of additives to generate novel polymeric materials [41]. There are two types of PVC: unplasticized (rigid PVC or PVC-U) and plasticized (flexible PVC or PVC-P) [42, 43].

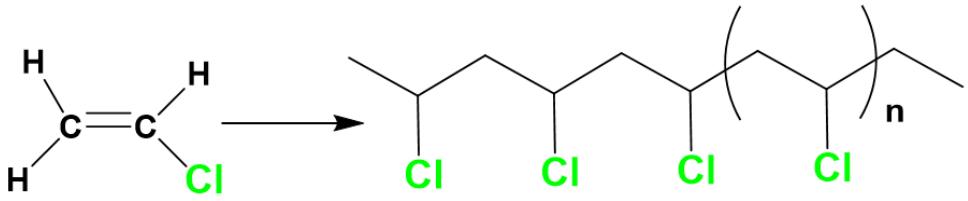

Scheme 1. 2D chemical structure of polyvinyl chloride (PVC).

In terms of production volume, it ranks as the third most-produced plastic, following polyethylene and polypropylene [44]. There are numerous cost-effective and versatile materials and products made from rigid and semi-flexible PVC (plasticized). These are extensively utilized in various construction applications, including water and sewer pipes, piping and siding, wire and cable insulation, windshield system components, and more [45]. It is established that PVC undergoes degradation at higher temperatures, resulting in the release of hydrogen chloride (HCl), which further speeds up the degradation process. The essential processes involved in PVC thermal degradation consist of two main stages. In the first stage, the primary reaction is dehydrochlorination, which results in the release of HCl and the formation of conjugated polyene (***Scheme 2***) [46]. In the second stage, the conjugated polyene undergoes cyclization reactions that produce aromatic hydrocarbons and small-molecule hydrocarbons [46, 47]. The colour of the substance varies according to the quantity of conjugated double bonds present, ranging from yellow, orange, and red to brown, and ultimately black [44, 48]. Although there is some debate in the literature on the precise mechanism, it is widely acknowledged that the heat induced breakdown of PVC occurs by the release of HCl using a chain mechanism known as "zipper elimination" or "unzipping" [49].

DOI: 10.14750/ME.2025.027

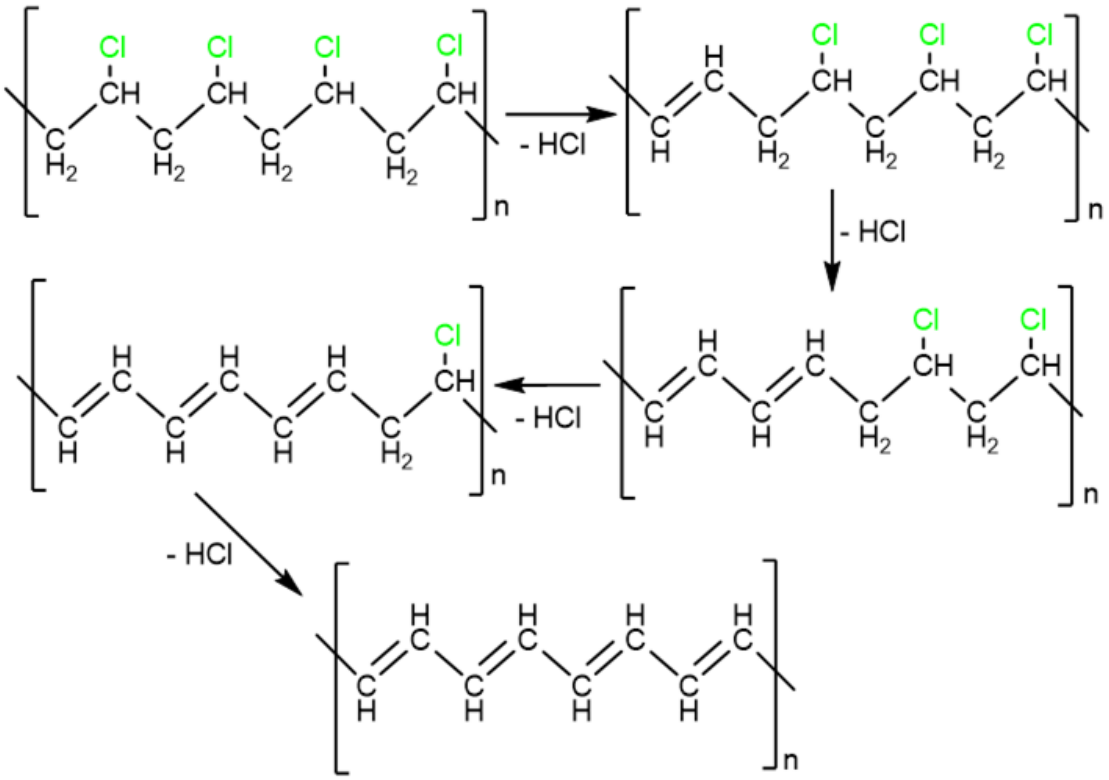

Scheme 2. Thermal decomposition path for the removal of HCl from PVC.

Thus, one of the main challenges is to prevent the deterioration of PVC caused by the release of HCl. Pure PVC incorporates additives to prevent dehydrochlorination, enhance its stability, and modify its final characteristics and product performance. These additives play a significant role in processing and improving the properties of polymers used in many applications, including automotive, medical, packaging, construction, and electronics. The biggest markets are window profiles and pipes, followed by rigid films and cables (***Figure 3)*** [48, 49][47].

DOI: 10.14750/ME.2025.027

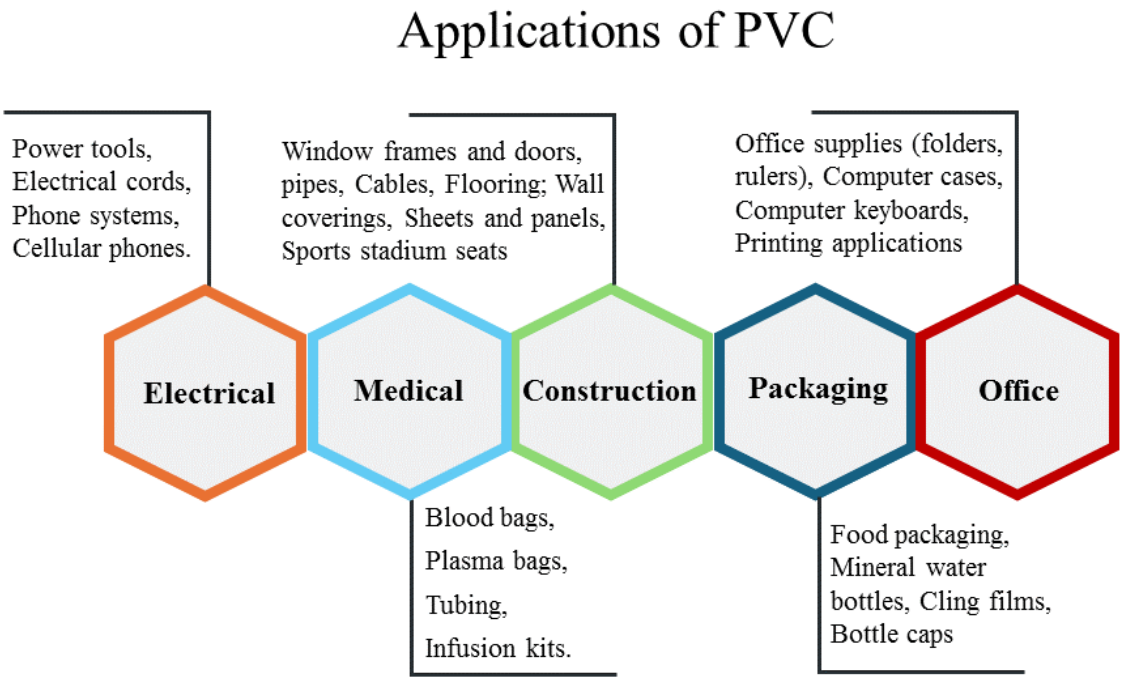

Figure 3. Overview of the applications of PVC.

There is a wide variety of additives available, such as plasticizers, lubricants, fillers, flame retardants, lubricants, stabilizers, colourants, and antimicrobial agents. Each of them improves the properties of the polymeric materials in some way [50].

1.7. Additives

Polymer products are competing with metal and ceramic based materials and their properties have to be satisfactory compared to the competition. There are several factors that impact the shelf life of polymers which has to be handled. The resistance of the polymeric materials to surrounding atmospheric conditions such as, exposure to sunlight, day/night, UV light, the seasonal change in the temperature, humidity, and air pollution by highly corrosive elements is a fundamental issue which have to be taken into consideration during applications [50]. These factors do not only cause aesthetic degradation in the product like discoloration, but also leads to potential deterioration of mechanical properties [51]. To overcome many of the problems facing polymeric materials, including stability and durability, additives have been used [50]. Pure polymeric materials are frequently found to have inferior properties, which would lead to their commercial failure. In the absence of additives, polypropylene (PP) and other polyolefins most probably would not be one of the most used polymers [52]. Due to its weak thermal oxidative stability, PP would decay in just a few weeks [53]. Additives are chemicals added to the base polymer to enhance processability, prolong lifespan, and enhance physical and chemical behaviour of the final

product. An excellent example of the use of additives is rubber, which is in its natural state, despite of many good properties such as flexibility, strength, durability, lack of electrical conductivity, and good resistance to water, also possess many undesirable qualities, including hardening in winter and increased adhesion in summer as well as its bad smell. Additives are used to improve all these disadvantages and thus, rubber became the versatile material it is known for today [54]. There are many types of additives that are used to improve specific characteristics of the final polymeric product. Polymer additives have been used as plasticizers (*e.g.,* dioctylphthalate (DOP) and tricresyl phosphate (TCP)) [55], flame retardants (*e.g.,* polybrominated diphenylethers (PBDES) and tris(chloropropyl) phosphate (TCPP)) [52], colorants (*e.g.,* anthraquinone and carbon blacks) [56], stabilizers (*e.g.,* barium-zinc and calcium-zinc) [57], antimicrobial agents (*e.g.,* 5-chloro-2-(2,4-dichlorophenoxy) phenol and 4,5-dichloro-2-noctylisothiazolinone) [56], antioxidants (*e.g.,* butylated hydroxytoluene (BHT), tert-butylhydroquinone (TBHQ), ascorbic acid (Asc) [58], curcumin [59, 60], vitamin E, and santowhite) [61]. Although, additives are typically just a small portion of the final product, their impact on the polymer properties and stability is considerable. In addition to alter physical-chemical properties, additives (plasticizers, lubricants, impact modifiers, antistatic agents, pigments, dyes, *etc*.) employed to decrease costs, and get better aesthetic qualities [11]. The additives can also be made from renewable resources (bio-based additives) which provide a good alternative to their synthetic counterparts [56]. There are many polymer additives that are commonly used in different forms, such as in solid-state (powders, flakes, beads, granulate, spheres, emulsions) or, in liquid state. The use of liquid additives is less common, because they require special methods of treatment, especially the ones that are of high concentrations, sticky, or sensitive to temperature [62]. The final form of the additive depends on the method of preparation (extrusion, pelletizing, grinding, spraying, or flaking) [52]. Once additives are added, the polymer mixture is referred to as a master blend and is processed accordingly [63].

1.7.1. Types of Polymer Additives

There are several options when it comes to additives and each one offers a specific improvement to the polymer's functionality, stability or improves its properties. The most common categories of polymer additives are the following:

a) Plasticizers
b) Colorants
c) Biocides/antimicrobial agents

d) Antistatic agents and antifogging agents
e) Lubricants
f) Flame-retardants/smoke suppressants
g) Antioxidants
h) Reinforcing agents
i) Heat stabilizers

1.7.1.1. Antioxidants

Antioxidants (AO) are compounds which are used to shield polymers and plastics from the thermal and photo-oxidative effects of aging [54]. Oxidative stress effects living organisms along with food and other commodities' [64] and thus, the importance of antioxidants exceeds the range of polymers. Oxidative stress is a process which involves the attack of free radicals, which are characterized by having an unpaired electron in their outer shell, making them unstable and highly reactive [8]. Free radicals in the body have the capability to damage DNA, cells, and tissues through the oxidative stress, because they can react swiftly with non-radical species to produce new radicals and propagate free-radical chain reactions [65]. Similar processes can occur in the case of polymeric materials. These harmful reactions can be prevented by antioxidant species which can donate an electron to free radicals and consequently, stabilize and detoxify them. There are various factors that must be considered to choose the best possible antioxidant compounds for a given system. The most important factors are the following: (1) radicals - the antioxidant should be capable of scavenging the appropriate radicals, (2) timing - the radical scavenging should occur at a specific location during the most suitable time, (3) activity - the antioxidants must remain active and not degrade as long as possible [66]. Chain-breaking (chain terminators, chain scavengers) and preventive antioxidants have also existed. In the first case, an alkyl peroxyl radical is stopped (acceptor or donor process). In the second one, hydroperoxides are either broken down more slowly (metal deactivators, UV absorbers) [66] or in a way that doesn't involve radicals (***Figure 4***) [67].

DOI: 10.14750/ME.2025.027

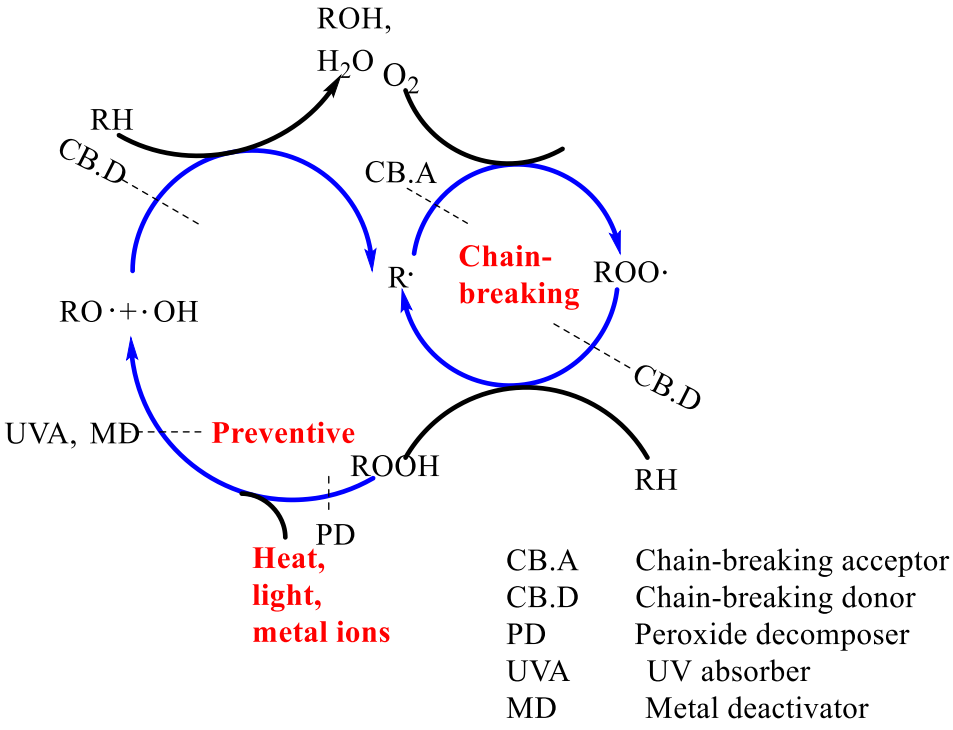

Figure 4. Types of antioxidants and their mode of action.

Significant environmental concerns have pushed manufacturers to investigate natural alternatives alongside regularly used synthetic materials. Thus, in terms of their origin, there are two main types of antioxidants, synthetic and natural species [68]. Several synthetic antioxidants are used in the chemical and food industry including butylated hydroxytoluene (BHT), octyl gallate (OG), butylated hydroxyanisole (BHA), propyl gallate (PG), *tert*-butylhydroquinone (TBHQ), and others (***Figure 5***) [69].

DOI: 10.14750/ME.2025.027

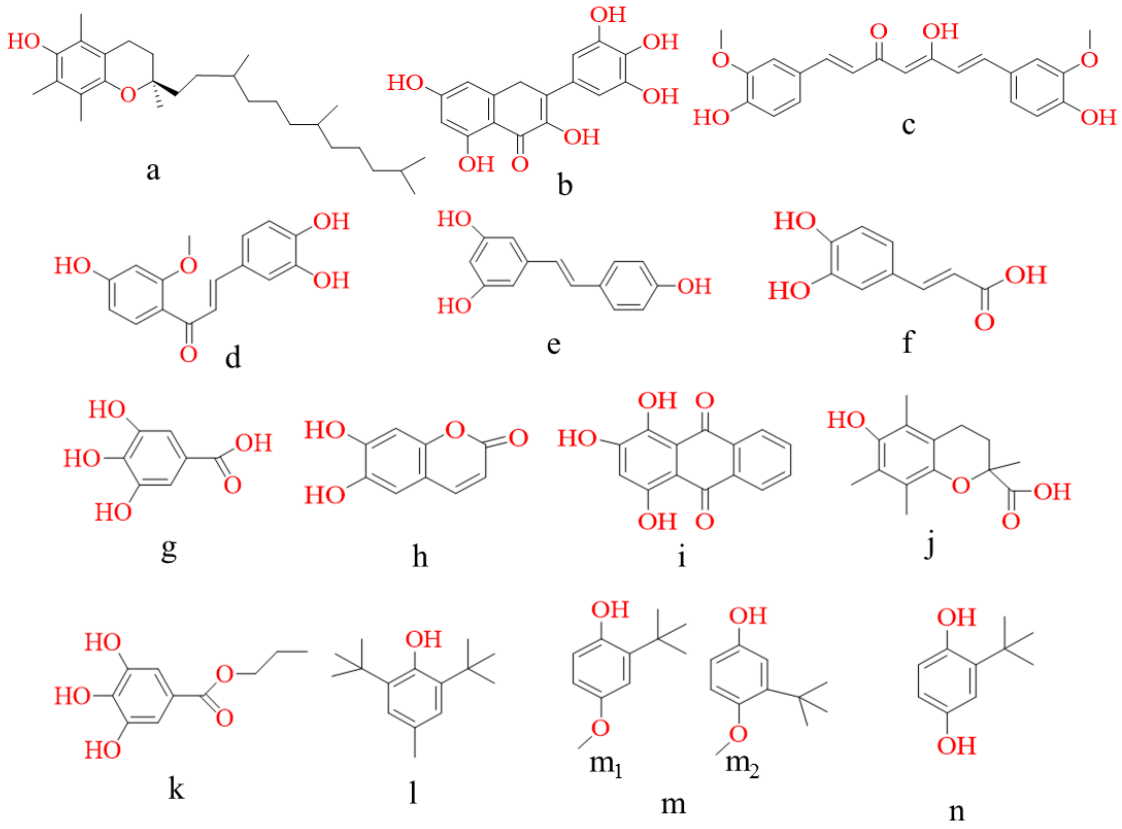

Figure 5. Schematic structures of some natural (a − i) and synthetic phenolic (j − n) antioxidant additives. a – α-tocopherol, b – myricetin, c – curcumin, d – sappanchalcone, e – resveratrol, f – caffeic acid, g – gallic acid, h − esculetin, i – purpurin, j – trolox, k – propyl gallate, l – butylated hydroxytoluene (BHT), m – butylated hydroxyanisole (m1 – 2-BHA and m2 – 3-BHA), n – tert-butylhydroquinone (TBHQ).

1.7.1.2. Stabilizers

Stabilizers are compounds incorporated into materials to inhibit or significantly reduce the rate of degradation the material experiences over time. They can be employed for a variety of reasons, including thermal and UV stabilization [70] . Heat stabilizers inhibit the degradation of plastics caused by high temperatures, particularly during the manufacturing process and in many other applications. One of the most popular polymers used stabilizer is PVC. PVC uses stabilizers as the most prominent class of additives to prevent degradation from heat, light, or oxygen. The classification includes lead-based stabilizers (lead stearate, lead phosphite, and lead sulfate), mixed metal stabilizers (such as Ca/Zn, Ba/Zn, and so on) [41], tin-based stabilizers (dibutyltin maleate, dioctyltin mercaptide, and tin maleates and tin thioglycolates), and organic stabilizers (organophosphites, beta-diketones, and organic tin mercaptides) [70]. Due to its composition, PVC is highly susceptible to heat. Heat stabilizers function by inhibiting thermal oxidation or focusing on decomposed oxidation products [48].

1.8. The common definitions of antioxidants and stabilizers

Antioxidant additives and stabilizers are chemical substances frequently employed in many industries, such as food and polymer processing. Despite their distinct goals, we can identify some convergence in their functions, particularly in the realm of polymers and specific materials [56]. Polymers and plastics frequently add antioxidants to prevent or slow down polymer degradation due to oxidation processes. This aids in the preservation of the material's physical and mechanical qualities throughout time [52]. One of the degradation processes that stabilizers try to combat is oxidation, which is why antioxidants might be considered a subgroup of stabilizers [70]. One thing they all have in common is that antioxidants can act as stabilizers, particularly when preventing oxidation-induced degradation. In this sense, antioxidants are a type of stabilizer that specifically addresses the oxidative degradation of materials. Some stabilizers may have antioxidant properties, and some antioxidants may offer stability against factors beyond oxidation [70]. The specific requirements of the material and the conditions it will encounter determine the choice of additives. For instance, heat, oxidative conditions, and ultraviolet radiation may require stabilizers and antioxidants for a plastic material like PVC to ensure long-term stability [71]. So, we can see that the antioxidants and stabilizers serve distinct purposes, but they do similar work, particularly in the context of protecting materials like polymers from degradation. The choice of additives depends on the types of degradation the material is likely to experience during its use and storage.

1.9. Studied antioxidant additives

1.9.1. Natural antioxidant additives

Environmental issues significantly becoming more prevalent due to the increasing number of synthetic materials, and the replacement of synthetic additives with environmentally friendly (*e.g.*, natural) substances is desired. Thus, finding ecologically safe and effective alternatives to commonly used additives is a top priority for the major players of the chemical industry, on the other hand, it is difficult and may lead to a significant increase in production costs [71]. Natural antioxidants can be found in a wide variety of natural products such as plant components (fruits, leaves, and flowers) [72], as well as in cow milk and honey [73, 74].

DOI: 10.14750/ME.2025.027

1.9.1.1. Curcumin

Curcumin [1,7-bis(4-hydroxy-3-methoxyphenyl)-1,6-heptadiene-3,5-dione] (***Figure 6)*** is a widespread natural antioxidant and a commonly used spice with a yellow color, and it has two isomers, curcumin A (enol) and D (diketone) [59, 60, 75]. Curcumin has several functional groups which plays a critical role in its beneficial characteristics [76]. It is a phenolic compound, extracted from the dried rhizomes of turmeric (*curcuma longa*) [77], and it has been utilized in various cosmetics and drugs as well. Besides its antioxidant effect [78, 79], it has good influence on various biological and cellular conditions, and thus, used as an anti-inflammatory [80, 81], anticancer and antimutagenic [82], wound healing, and hypocholesterolemic agent [59].

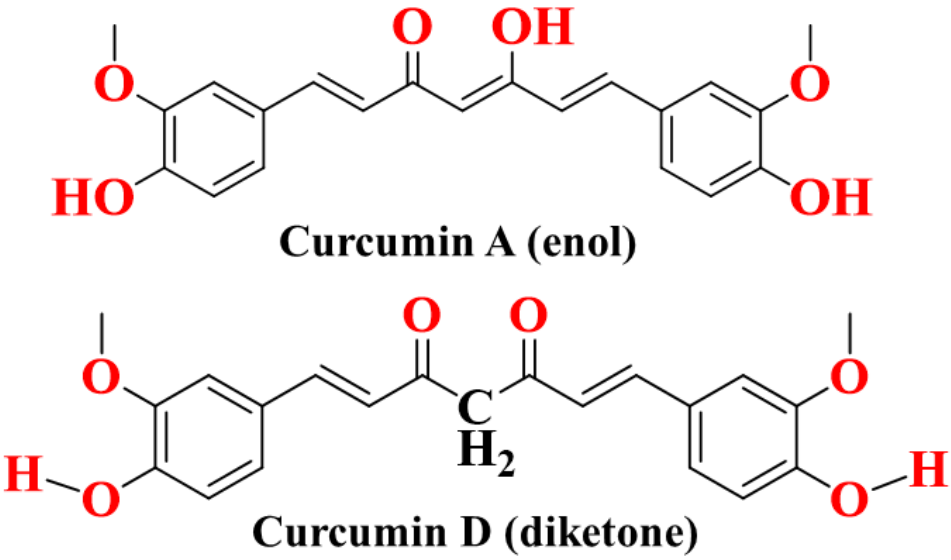

Figure 6. 2D structure of curcumin isomers.

1.9.1.2. Vitamin C, or L-ascorbic acid (Asc)

Vitamin C or L-ascorbic acid (Asc) is one of the most well-known natural antioxidants of all time. Asc has gained widespread recognition as a powerful antioxidant and free-radical scavenger since its discovery by Albert Szent-Györgyi and Walter Norman Haworth(***Figure*** **7**) [83, 84]. It can be oxidized via losing two protons and two electrons, but it usually only loses one electron at a time [85]. Asc is present mainly in fresh fruits including, citrus fruits, kiwifruit, strawberries, papaya, blackcurrant, and vegetables such as tomato, carrot, coriander, broccoli, cauliflower, cabbage, and others [58] [86].

DOI: 10.14750/ME.2025.027

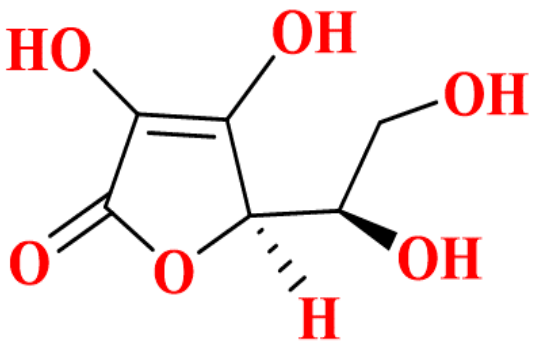

Figure 7. 2D structure of L-ascorbic acid (Asc).

1.9.1.3. Vitamin E (α-tocopherol)

Tocopherols are considered one of the most important, safe, and harmless groups of additives [87]. Vitamin E is a mixture of four tocopherols (alpha, beta, gamma, and delta) and four corresponding tocotrienols. Vitamin E activity is required for life because it protects human cells from oxidation and assists in the absorption of vitamin K. These compounds are naturally found in many foodstuffs, mainly fruits, oils, fats, and vegetables [88]. Tocopherols are classified into several categories based on the number and location of methyl groups bound to their cyclic unit. α-Tocopherol has three methyl groups bound to the aromatic ring, while in β- and γ-tocopherol there are two, while δ-tocopherol has only one (

Figure 8) [87, 89].

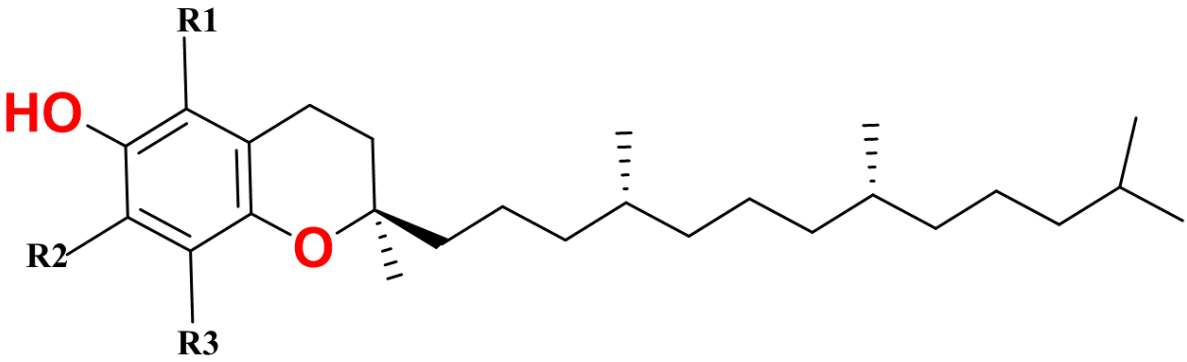

α-Tocopherol: R1 = R2 = R3 = CH_3
β-Tocopherol: R1 = R3 = CH_3 ; R2 = H
γ-Tocopherol: R1 = H ; R2 = R3 = CH_3
δ-Tocopherol: R1 = R2 = H ; R3 = CH_3

Figure 8. 2D structures of tocopherols.

1.9.1.4. Trolox

Trolox (6-hydroxy-2,5,7,8-tetramethylchroman-2-carboxylic acid) is a water-soluble tocopherol derivative that has numerous medicinal and industrial applications (***Figure 9***). Trolox is also capable of decreasing oxidation; therefore, it would be worth considering using it as an antioxidant additive to prevent oxidation and free radical intracellular formation [58, 90]. Trolox is well known for its antioxidant action in a variety of systems and under varied circumstances, and it works well as a food preservative. It has the ability to prevent the loss of serotonin and dopamine receptor binding sites in animal brain membranes, as well as the radical chain oxidation of proteins and enzymes [91]. Trolox has a chromanol structure that contributes to its antioxidant activity, as well as a carboxyl group, which influences water solubility [90, 91]. Although trolox and α-tocopherol are both important antioxidants and have been extensively studied with polymers, there is still a need for further understanding of their modes of action and their applicability in polymeric formulations [92, 93].

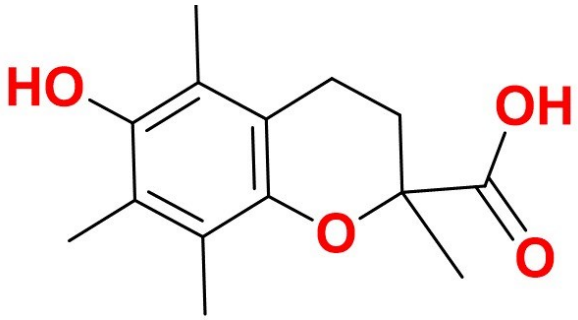

Figure 9. 2D structure of trolox.

1.9.2. Synthetic antioxidant additives

Several synthetic antioxidants are used in the chemical and food industry including butylated hydroxytoluene (BHT), butylated hydroxyanisole (BHA), *tert*-butylhydroquinone (TBHQ) [94], santowhite (SW) [95], ethylenediaminetetraacetic acid (EDTA) [96], Irganox 1010, Irganox 1035, Irganox 1076 [96], and others [71]. The antioxidant potential of all of these compounds has been investigated.

1.9.2.1. Butylated hydroxyanisole (BHA), Butylated hydroxytoluene (BHT), and Tert-butylhydroquinone (TBHQ)

Butylated hydroxyanisole (BHA), butylated hydroxytoluene (BHT), and *tert*-butylhydroquinone (TBHQ) are extensively used as additives in the food industry and have been utilized in a variety of food applications [58]. BHT is commonly used as a positive

control in the measurement of antioxidant activity due to its AO capabilities and simple structure [97, 98]. Thus, these additives are a good starting point for AO design and can serve as model compounds for many studies. From a structural point of view, many of these species are phenolic compounds (***Figure 10***).

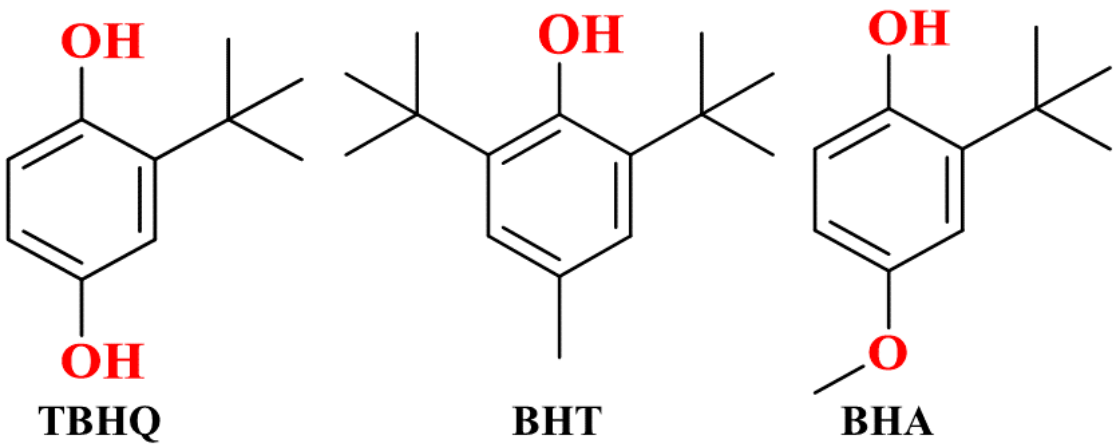

Figure 10. 2D structures of common synthetic antioxidants, *tert*-butylhydroquinone (TBHQ), butylated hydroxytoluene (BHT), and butylated hydroxyanisole (BHA).

1.9.2.2. Santowhite (SW)

Santowhite is a hindered phenolic antioxidant with two phenolic groups per molecule (***Figure 11***). Santowhite has the ability to inhibit the oxidation of polymers through donating a labile hydrogen atom to the radical ($ROO^{\bullet}$ or $R^{\bullet}$), resulting in the formation of a stable phenoxy radical [61]. SW is considered a highly effective antioxidant due to its stable phenoxy radical forms and its ability to end multiple chains [99]. Whilst the raw polymer is easily oxidized, efficient antioxidants like SW have proved that they are well suited to improving durability when employed in the polymer formulation. The molecular structure for the antioxidant and the dose of exposure have a considerable influence on the efficacy of stabilization [100].

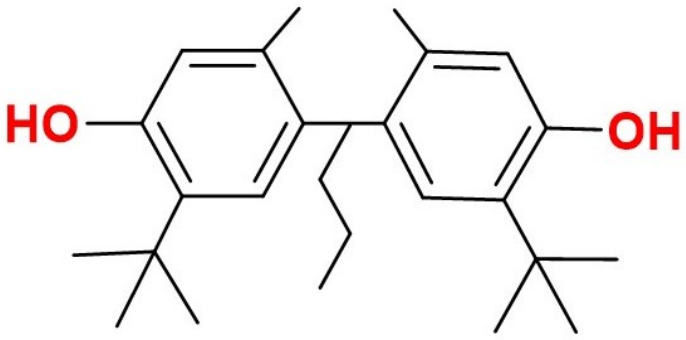

Figure 11. 2D structure of santowhite (SW).

DOI: 10.14750/ME.2025.027

1.9.2.3. Ethylenediaminetetraacetic acid (EDTA)

Ethylenediaminetetraacetic acid (EDTA) is an efficient metal chelating compound (***Figure 12***). It is also considered an efficient antioxidant and it can improve the oxidative stability, and some studies indicate that EDTA has the ability to protect against oxidation during storage [101]. Preservatives and packaging are both applied in food preservation. EDTA as synthetic antioxidant compound [96] is important in both areas because it is applied as additive for various pre-processed food products and for polymeric packaging materials [70, 102].

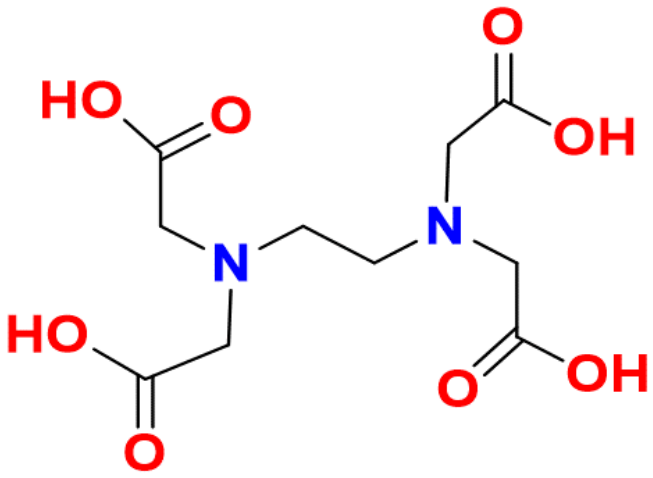

Figure 12. 2D structure of ethylenediaminetetraacetic acid (EDTA).

1.9.2.4. Irganox

Irganox is a family of compounds that are commercially available phenolic antioxidant additives (***Figure 13***). There are many types, such as 1330, 1010, 1035, 1076, MD1024, 3114, E201, PS 800, 1081, and PS 802 [94, 102, 103]. These synthetic additives used in many applications, including pre-processed food products and polymeric packaging materials [104, 105].

DOI: 10.14750/ME.2025.027

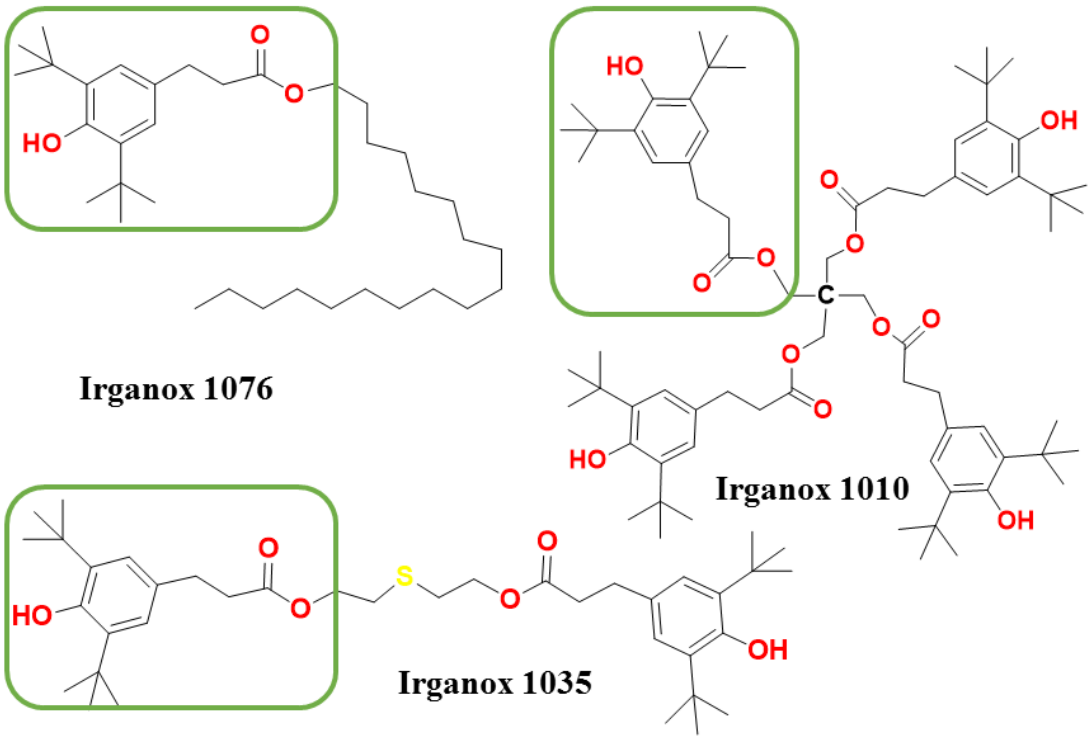

Figure 13. 2D structures of various Irganox types which have the same base unit (highlighted in green frame) studied in the present work.

1.10. The aim of this work

The goals of the current dissertation have been determined by considering the importance of additives, particularly the antioxidant and stabilizer additives in polymers, which affect the physical and chemical characteristics of the final polymeric products. The following goals were pursued:

1. The main aim was to achieve polymeric formulations that are more environmentally friendly by selecting the best antioxidant additives and using natural alternatives if it is possible. There were several steps involved in achieving this goal, as outlined below:

1.1. Selection of Eco-friendly Antioxidant Additives:

- First and foremost, investigating the use of natural antioxidants to replace synthetic ones in polymeric formulations.
- Evaluating the capability of different natural and synthetic antioxidants in preserving polymer stability and prolonging product lifespan.

1.2. Understand the Mechanism of the Antioxidant Additives.

- It is necessary to understand the mechanism of the antioxidant additives and calculate the molecules' antioxidant potential.
- To compare the antioxidant potential of different groups (X-H, where X = O and C), three major free radical scavenging (RS) mechanisms (HAT, SETPT, and SPLET) have been considered, and the corresponding bond dissociation enthalpy (BDE), ionization potential (IP), proton dissociation enthalpy (PDE), proton affinity (PA), and electron transfer enthalpy (ETE) values have been calculated for each potential hydrogen donor site of the studied species.
- The antioxidant properties of natural and synthetic antioxidant additives have been compared.

1.3. Incorporation of the antioxidant additives with polymers.

- Investigating the incorporation of antioxidant additives into polymers has been studied to improve the sustainability of the formulation and the chemical and physical properties of the final product, aiming to produce environmentally friendly polymers.
- We have tested our additives with PVC as stabilizers because they can act as antioxidants by studying their antioxidant properties and can also act as stabilizers

DOI: 10.14750/ME.2025.027

where the stabilizers serve distinct purposes; they perform similar functions, particularly in protecting materials like polymers from degradation. The choice of additives depends on the types of degradation the material is likely to experience during its use and storage.

2. Methods

2.1. Overview of Computational Chemistry

Computational chemistry is a field of study in chemistry that uses computer simulation to solve chemical problems. The field employs theoretical chemistry methodologies in conjunction with computational tools to determine the structures and characteristics of molecules and materials. Improvements in algorithms, software, and hardware, together with a deeper integration of computational methods with experimental methodologies, ensure that computational chemistry is ever evolving. Thus, more and more chemists will use theoretical methods as an indispensable tool for a deeper understanding of the molecular world [103]. Theoretical chemistry tries to determine the structure of stable and unstable species, their relative energies, dipole moment, polarizability, NMR coupling constants, and others. Reaction properties, such as how fast one stable molecule can change into another, how molecular structures and properties change over time, and how different molecules interact with each other also studied by using theoretical chemistry methods [104].

There are many advantages and disadvantages to computational chemistry. The first advantage is its predictive power, which allows computational chemistry to predict the structure, stability, reactivity, and properties of molecules and materials, often prior to their synthesis. Additionally, it can elucidate complex reaction mechanisms and offer insights into transition states and intermediates. The second benefit is cost: computational studies can reduce the need for extensive experimental trials, saving both time and resources. The third advantage is safety, where the computational methods allow the study of hazardous or unstable systems without the risk associated with physical experiments. Another primary benefit is speed, as computational methods swiftly test hypotheses and generate data, thereby accelerating the research process. Despite all these advantages, there are still some disadvantages inherent to any system. The first disadvantage is the high computational cost; high-accuracy methods require significant computational resources, including powerful hardware and extensive processing time. As system size increases, the computational cost often increases exponentially, limiting the study of larger systems. The second is the level of complexity and expertise involved; Master of Computational Chemistry necessitates significant expertise in both theoretical chemistry and computational techniques, and the use of advanced software tools can be complex, requiring detailed understanding to prevent misinterpretation of results. The third is validation and verification. Computational results

frequently require validation with experimental data, which can reveal discrepancies, and small changes in computational parameters can sometimes lead to significantly different results, complicating interpretation [104, 105].

The Born-Oppenheimer approximation, which separates electronic and nuclear movements, is a fundamental concept in computational chemistry. By solving the electronic Schrödinger equation, one can determine the potential energy surface (PES) for various geometries. The potential energy surface (PES) has a dimension of 3N, where N is the number of nuclei. This implies that the system's geometry is defined by 3N nuclear coordinates. Out of these coordinates, three represent the overall displacement of the molecule, while the other three represent the total rotation of the molecule in relation to the three axes. Only two coordinates can fully describe the rotation of a linear molecule. For tiny displacements, we might select 3N–6 remaining coordinates as "vibrational normal coordinates" to describe the internal movement of the nuclei [106]. By employing the PES concept, it becomes possible to introduce the fundamental notion of a molecule's spatial arrangement. This refers to the specific nuclei placements that guarantee a minimal PES value. Hund's work in 1927 might be the origin of this concept. It also matches a certain ground-state electron density distribution that shows atomic cores, atom-atom bonds, and atomic lone pairs [103].

A computational chemistry calculation commences with the process of geometry optimization, wherein the initial molecule geometry is selected as the first step. Various software programs can accomplish this work by utilizing established molecular structure properties, such as bond length, dihedral angles, and other properties [107]. Optimization algorithms are commonly employed to locate stationary points on a potential energy surface, namely local and global minima as well as saddle points. Prior to commencing a calculation, it is frequently advantageous to perform a geometry optimization, especially if the initial coordinates are expected to deviate significantly from their realistic values [103, 108].

In this investigation, we utilised the Gaussian 09 software package [109]. Gaussian 09 provides a variety of theoretical approaches for calculating the researched systems, which can accurately model chemical environments and molecular states. Once the optimization is complete, we can perform a frequency calculation using the optimized geometry of the projected structure. The analysis will consider the nuclear vibrations occurring in molecular systems when they are in a state of balance. The frequency calculation verifies that the structure is a true stationary point (either a minimum or a saddle point) and conforms to the investigated reaction pathway [110].

2.2. Thermodynamic Parameters

Calculating the antioxidant mechanisms of antioxidant additives involves determining the most important thermodynamic properties of the optimized molecules.

Thermodynamic functions relate to quantities that define the state and behaviour of a system in thermodynamics, including internal energy (**E**), entropy (**S**), Gibbs free energy (**G**), and enthalpy (***H***). These functions give vital information about the system's energy, work, and overall equilibrium conditions.

In our work, the most crucial parameter used to calculate the antioxidant potential is Enthalpy (***H***) which is a fundamental and highly valuable notion in the field of thermodynamics, especially when studying chemical processes and phase transitions. The term refers to a system's total energy, which includes both its internal energy (**E**) and the result of multiplying its pressure (**p**) and volume (**V**) ***(Eq. 1)*** [111, 112].

$$\boldsymbol{H(T) = E(T) + pV} \qquad \textit{Eq. 1}$$

And the enthalpy can be determined using the partition functions via the following ***(Eq. 2)***:

$$\boldsymbol{H - H(0) = \left(\frac{\partial \ln q}{\partial \beta}\right)_V + kTV \left(\frac{\partial \ln q}{\partial V}\right)_T} \qquad \textit{Eq. 2}$$

where q is the molecular partition function and β is the most likely population of the states of the system, strongly implying that it is temperature related.

The partition functions [q(V,T)] illustrates the distribution of probabilities among various microstates such as transition, rotation, vibration, and electronic state. We can then use the partition functions to find the thermodynamic state functions [*G*(T,p), *S*(T,p), *H*(T)] for each molecule involved in the mechanism. This lets us to get the thermodynamic properties of all species [113].

Entropy (*S*) is a fundamental concept in thermodynamics and statistical mechanics that quantifies the level of disorder or unpredictability in a system. Scientists devised this state function to elucidate why a fraction of the overall energy remains non-utilizable for productive work. The value is obtained by multiplying Boltzmann's constant ($k_B = 1.38 \times 10^{-23}$ J/K) by the natural logarithm of the total number of quantum states (W), as in the following (***Eq. 3***):

$$\boldsymbol{S = k_B \ln W} \qquad \textit{Eq. 3}$$

The entropy contribution can be determined using partition functions (***Eq. 4***).

$$s = Nk_B + Nk_B \ln\left(\frac{q(V,T)}{N}\right) + Nk_B T\left(\frac{\partial \ln q}{\partial T}\right)V \qquad \textit{Eq. 4}$$

where *N* represents the particle number of molecules as a dimensionless quantity.

Gibbs free energy (**G**) is a thermodynamic quantity that quantifies the greatest amount of reversible work that a system can perform under constant temperature (**T**) and pressure (**P**) conditions [114] (***Eq. 5***):

$$G(T,p) = H(T) - TS(T,p) \qquad \textit{Eq. 5}$$

Where ***H*** represents the enthalpy of the system (total heat content), and **S** is the entropy of the system. We obtain the Gibbs free energy by expressing the partition function as follows (***Eq. 6***):

$$G - G(0) = -nRT \ln\frac{q}{N} \qquad \textit{Eq. 6}$$

R represents the gas constant with a value equal to 8.314 J/K.mol, and **N** is the particle number of molecules as a dimensionless quantity.

After determining them the corresponding relative thermodynamic quantities were also computed such as the reaction enthalpy ($\Delta_r H°$), Gibbs free energy ($\Delta_r G°$), entropy ($\Delta_r S$), and other parameters.

2.3. Specific Computational Chemistry Methods

We employ a wide variety of theoretical and computational tools in computational chemistry methods to understand chemical structures, characteristics, and reactions. We frequently synergistically integrate and utilise these methodologies to address diverse chemical issues, ranging from predicting molecule structures to simulating intricate biochemical processes. The specific system under examination, the desired precision level, and the available computational resources all influence the methodology selection. Quantum chemistry and molecular mechanics are two of the main methodologies used in computational chemistry. Quantum chemistry entails explicitly considering electrons and uses the Born-Oppenheimer approximation to solve the time-independent electronic Schrödinger equation and determine the nature of the interactions between electrons and nuclei. Quantum chemistry methods can be classified into two significant categories: wavefunction and density functional theory (DFT) methods [115]. Computational chemistry uses these potent tools to provide detailed

and accurate descriptions of molecular systems based on first principles. Although they need significant processing power, they are indispensable for comprehending and forecasting chemical phenomena at the quantum level. The coupled-cluster (CC) methodology is widely regarded as the theoretical gold standard among wavefunction-based methods; nonetheless, the main drawback of this technique is that its computational cost escalates dramatically with system size. Even the largest computers and most effective algorithms in the world struggle to compute even a few tens of electrons at this level [116, 117]. Density Functional Theory (DFT) is a widely used quantum mechanical method employed in computational chemistry and physics to investigate the electronic structure of atoms, molecules, and solids. DFT, unlike methods that depend on wavefunctions, explicitly focusses on the electron density. This enables efficient computer calculations and is particularly suitable for analysing massive systems [118]. Although density functional theory is a potent and adaptable tool in computational chemistry, its limitations, such as convergence issues, must be carefully considered. DFT calculations during geometry optimizations can stuck in local minima, particularly for large and complex systems. This can lead to the wrong structures and energies. Additionally, the time required for simulation, particularly for large systems, can exceed available resources, limiting the effectiveness of computational studies.

We used four different DFT methods (B3LYP, M06, M05-2X, and M06-2X) in the current work to calculate the antioxidant potential of the studied additives. For all properties, there is no universally optimal function. Instead, the problem at hand determines the specific methodological approach to use. Nevertheless, many functionals are robust enough to give relatively reasonable results in a wide range of chemical properties [103]. However, all these methods performed exceptionally well in our tests. Occasionally, errors such as time limitations or configuration errors occur, especially in large structures, but overall, DFT proved to be an excellent choice for our application.

2.3.1. Density Functional Theory

The Hohenberg-Kohn theorem encapsulates the fundamental principle of Density Functional Theory, asserting that we can express the external potential as a mathematical function of the density of the system's ground state. The application of DFT in chemistry has had an exceptional influence on the use of quantum mechanics to solve complex and fascinating problems related to electronic structure. Each year, the number of applications experiences a rapid increase. Some notable recent studies include understanding and creating catalytic processes in enzymes and zeolites, electron transport, harnessing and converting solar

energy, drug design in medicine, and various other scientific and technological challenges [119].

There are two main theorems for DFT [120]: ***The first theorem*** represents that the electron density of a system with multiple electrons can exclusively determine the characteristics of its lowest energy state. Consequently, the electron density contains all the pertinent information regarding the system. According to ***the Second Theorem***, there is a universal function that depends on the electron density. Minimizing these functions yields the system's precise ground-state energy. Functionality is the sum of the kinetic energy of a system of non-interacting electrons with the same density, as well as the energy generated by electron-electron interactions. In DFT, the coulomb attraction between electrons and nuclei is the external potential. The Born-Oppenheimer approximation treats the nuclei as stationary entities that exert their Coulomb potential on the electrons [121]. Thus, the electronic Hamiltonian of the system can be written as follows (***Eq. 7***):

$$\widehat{\boldsymbol{H}}_{\boldsymbol{e}} = \widehat{\boldsymbol{V}}_{\boldsymbol{k}}(\boldsymbol{n}) + \widehat{\boldsymbol{V}}_{\boldsymbol{ee}}(\boldsymbol{n}) + \widehat{\boldsymbol{V}}_{\boldsymbol{ext}}(\boldsymbol{n}) \qquad \textit{Eq. 7}$$

where $\widehat{\mathbf{V}}_{\mathbf{k}}$ represents the kinetic interaction operators, $\widehat{\mathbf{V}}_{\mathbf{ee}}$ *is the* electron-electron interaction operators, and the external potential represented by $\widehat{\mathbf{V}}_{\mathbf{ext}}$. External potential is a functional of the ground-state density (***Eq. 8***).

$$\widehat{\boldsymbol{V}}_{\boldsymbol{ext}}(\boldsymbol{n}) = \int \boldsymbol{n}\,(\boldsymbol{r})\,\boldsymbol{\Psi}^{*}(\boldsymbol{r})\boldsymbol{\Psi}(\boldsymbol{r})\boldsymbol{dr} \qquad \textit{Eq. 8}$$

The electron density uniquely determines the Hamiltonian operator, suggesting that the total energy is a function of the electron density, leading to the following equation for energy (***Eq .9***)

$$\boldsymbol{E} = \int \widehat{\boldsymbol{V}}_{\boldsymbol{ext}}(\boldsymbol{n})\,\boldsymbol{n}(\boldsymbol{r}) + \boldsymbol{F}[\boldsymbol{n}(\boldsymbol{r})] \qquad \textit{Eq .9}$$

where **F** is the functional relation and consists of two terms including $\widehat{\mathbf{V}}_{\mathbf{k}}(\mathbf{n})$ and $\widehat{\mathbf{V}}_{\mathbf{ee}}(\mathbf{n})$

The Kohn-Sham equations use the energy of an idealized system with noninteracting electrons and a deviation parameter to determine the energy of a system. This theorem demonstrates that a set of equations involving a single electron can describe the electron density. They created a virtual non-interacting system, presuming that its ground state is the same as the density of the genuine interacting system [122].

The following expression defines the ground-state electron density at a location (***Eq. 10***):

$$\boldsymbol{n(r) = \sum_{i=1}^{n} \left|\varphi_i^{KS}(r)\right|^2} \qquad \textbf{\textit{Eq .10}}$$

where $\boldsymbol{\varphi_i^{KS}(r)}$ represent the Kohn-Sham orbitals. As a result, the ground state of the system can be defined as (***Eq. 11***):

$$\boldsymbol{\hat{h}^{KS}(i)\varphi_i^{KS} = \varepsilon_i^{KS}\varphi_i^{KS}} \qquad \textbf{\textit{Eq .11}}$$

where $\boldsymbol{\hat{h}^{KS}(i)}$ is the Kohn-Sham Hamiltonian, and $\boldsymbol{\varepsilon_i^{KS}}$ represents the corresponding energy of the Kohn-Sham orbital.

The sum of the kinetic energy term $\boldsymbol{\hat{V}_k[n(r)]}$, electron-electron repulsion term $\boldsymbol{\hat{V}_{ext}[n(r)]}$, external potential term $\boldsymbol{\hat{V}_{ext}[n(r)]}$, and exchange-correlation term $\boldsymbol{\hat{V}_{XC}[n(r)]}$ represents the Kohn-Sham Hamiltonian ($\boldsymbol{\hat{h}^{KS}(i)}$) of the real interacting system (***Eq. 12***):

$$\boldsymbol{\hat{h}^{KS}(i) = \hat{V}_k[n(r)] + \hat{V}_{ee}[n(r)] + \hat{V}_{ext}[n(r)] + \hat{V}_{XC}[n(r)]} \qquad \textbf{\textit{Eq .12}}$$

Where the exchange-correlation functional $\boldsymbol{\hat{V}_{XC}[n(r)]}$ represents the difference between the virtual and real system (***Eq. 13***):

$$\boldsymbol{\hat{V}_{XC}[n(r)] = \Delta_k^{corr}[n(r)] + \Delta_{ee}^{corr}[n(r)]} \qquad \textbf{\textit{Eq .13}}$$

The exchange-correlation functional is incorrectly named as it is not the same as exchange and correlation defined within wavefunction theory. However, this name serves as a weak analogy to the classic quantum mechanical concepts. Generally, we define the exchange-correlation functional as the sum of two parts: exchange and correlation. This is an assumption—an assumption that we have no way of knowing whether is true or not. Usually, we write these component functionals in terms of energy density [123]. $\boldsymbol{\hat{V}_{XC}[n(r)]}$ is corresponds to the exchange ($\boldsymbol{E^X[\mathbf{n}(\mathbf{r})]}$, where $\boldsymbol{E^X}$ is the interactions between electrons of the same spin), and correlation energy terms ($\boldsymbol{E^C[\mathbf{n}(\mathbf{r})]}$, where $\boldsymbol{E^C}$ is associated with the electron-electron interactions with opposite spin)[124].

Perdew has characterised "Jacob's Ladder"[125] as a hierarchical structure consisting of successive approximations of the exchange-correlation term. The ladder, firmly rooted in HF theory on Earth, extends to heaven, where the precise functional is located (***Figure 14***). During the process, there are five levels, each establishing a set of assumptions that are established while formulating an exchange-correlation expression [123, 126].

DOI: 10.14750/ME.2025.027

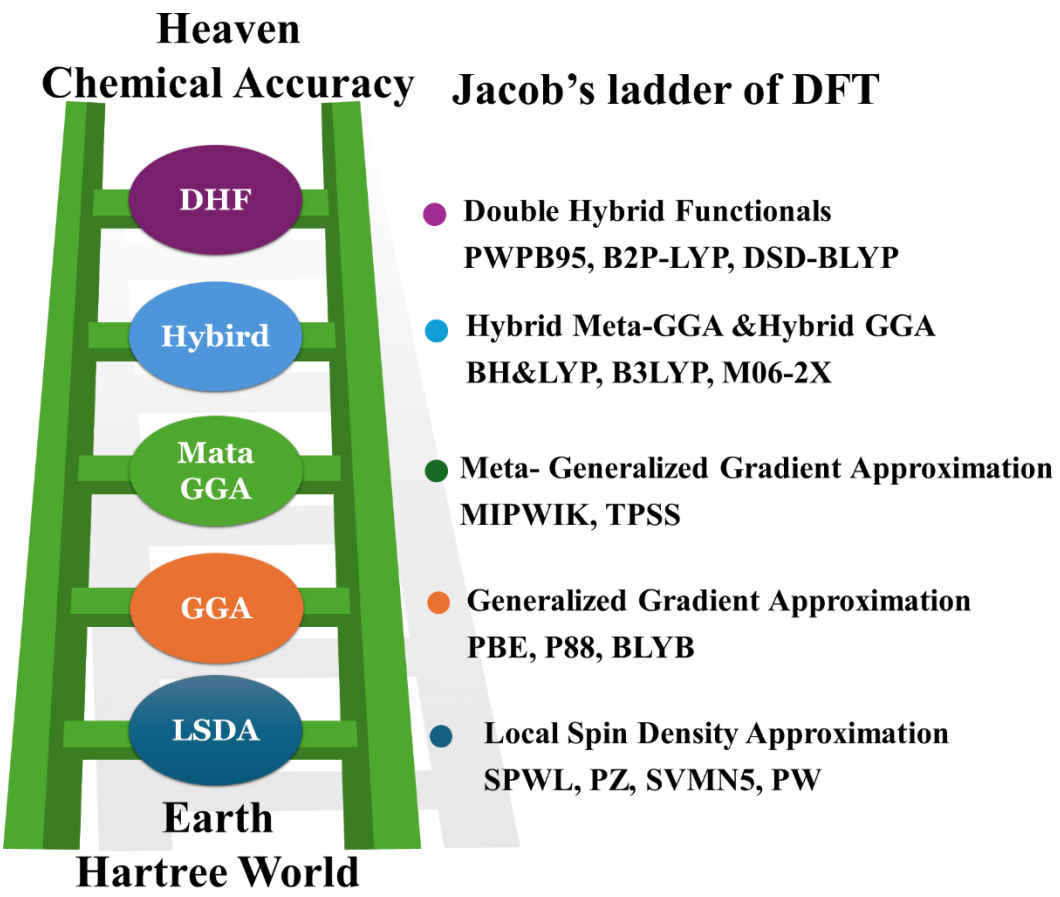

Figure 14. Jacob's ladder of density functional approximations.

Jacob's ladder consists of many functions; the first rung is the local spin density approximation (LSDA), and one must assume that the density is not uniform. The approach that has been taken is to develop functionals that are dependent on not only the electron density but also derivatives of the density. The most typical LSDA functionals are the SPWL (Slater Perdew-Wang local), PZ (Perdew-Zunger), VWN (Vosko-Wilk-Nusair), and the PW (Perdew-Wang) functionals [127]. The second rung on Jacob's ladder is the generalized gradient approximation (GGA), and it may lead to better results for the geometries and ground state energies than the first one, especially for weak and covalent systems. The PBE (Perdew-Burke-Ernzerhof), B88 (Becke88), and BLYP (Becke, Lee-Yang-Parr) are the most common gradient-corrected correlation functionals [128-131] (***Figure 14***). The third rung represents the meta-GGA functionals, which includes a dependence on the Laplacian of the density or on the orbital kinetic energy density. Some well-known meta-GGA functions are TPSS (Tao-Perdew-Staroverov-Scuseria) and MPW1K (a modified version of the Perdew-Wang gradient-corrected exchange functional, with one parameter optimised to give the best fit to the kinetic data) [117, 125, 132, 133]. The fourth row, the hybrid methods, combine the exchange-correlation functionals with some admixture of the HF exchange term. The most

well-known methods for this functionals are B3LYP, M06-L, and M06-2X. Several studies have used the B3LYP; B3 stands for Becke's 3 parameter exchange-correlation functional, and LYP is the Lee-Yang-Parr correlation functional [130, 134]. Many researchers in applied density functional theory have adopted this functional as a standard due to its versatility in various situations [135]. The most often used functionals are M06-L and M06-2X, with 0% and 54% HF exchange, respectively [136-139]. The last one includes the unoccupied Kohn-Sham orbitals. This is mostly achieved within the so-called double hybrid functionals. The most widely used methods for this function are: B2PLYP combines Becke's B88 exchange functional with the LYP correlation functionals; PWPB95 combines the Perdew-Wang exchange functional with Becke's 95 correlation functional, along with an MP2-like correction; and DSD-BLYP is a spin-component-scaled double hybrid functional combining Becke's B88 exchange with Lee-Yang-Parr correlation and including MP2 correction [123] (***Figure 14***).

2.3.2. Basis Sets

A basis set in chemistry is a set of functions used to estimate the molecular orbitals in quantum chemistry computations. Often, these functions centre on the atomic nuclei of the molecules under investigation, forming atomic orbitals. In computational chemistry, if we need to do some calculations using the previously mentioned methods, we must have a basis set. The term "levels of theory" refers to the combination of the method and basis set [123, 140].

For molecular systems, the nuclear-centred Slater (STO-nG) or Gaussian Type Orbital (GTO) functions have dominated [141]. Researchers prefer Gaussian functions due to their superior computational efficiency and analytical integrability, which makes them efficient and numerically stable. Many common basis sets use GTOs, such as STO-nG, a minimal basis set and part of the STO-nG family. In this case, STO represents a slater-type orbital, and n denotes the number of primitive Gaussian functions that make up one basis function. For instance, in STO-3G and STO-6G, the minimal basis set STO-3G treats each atomic orbital as a single slater type orbital (STO), approximating it with a linear combination of 3 Gaussian functions (3G) [142, 143]. The second one is split-valence basis sets, where the valence orbitals are split into multiple components to provide more flexibility and are typically used in calculations requiring a balance between accuracy and computational cost. The most common example basis sets of this type are 3-21G, 6-311G, and 6-31G. Split-valence double-zeta basis set (6-31G) where the core orbitals are created by using 6 primitive

Gaussian functions, and two basis functions (double-zeta) are used to describe the valence orbitals, each of them made from three Gaussians and one Gaussian. Adding polarization (*) to the basis sets, such as 6-31G*, and diffuse functions (+) to 6-31+G*, enhances their sensitivity in describing weak interactions or anionic systems [144-147]. The third type, known as polarized basis sets, includes additional functions to accommodate orbital polarization. This has the advantage of improving the description of molecular geometries and electronic distributions. The two most common examples are 6-31G(d) and 6-31G(d,p). The fourth type is called correlation consistent basis sets. Their goal is to improve electron correlation descriptions in a planned way and provide higher precision, especially in correlated wavefunction methods. Examples of this type are cc-pVDZ (correlation-consistent valence double zeta), cc-pVQZ (correlation-consistent valence quadruple zeta), and cc-pVTZ (correlation-consistent valence triple zeta)[142].

The goal of the basis set is to provide the most accurate representation of the unknown molecular orbitals (or electron density) while minimizing processing expenses. Due to variations in theoretical methods, molecular characterization, computer architectures, algorithms, efficiency requirements, and desired precision, it is not feasible to create a single "optimum" basis set [141].

2.4. Applied Levels of Theory

All calculations have been carried out by using the Gaussian 09 software package [109]. The studied additives and the corresponding radicals, radical cations, and anions were optimized by employing different global hybrid functionals including, B3LYP [129, 130, 148, 149] in combination with the 6-31G(d) basis set, M06 and M06-2X [150] in combination with the 6-311+G(d,p) basis set, and M05-2X [151], M06-2X [150] in combination with the 6-311++G(2d,2p) basis set applied to optimize all the molecules in gas phase and water (***Table 4***). Solvent effect of water was approximated by using the Solvation Model based on Density (SMD) method. All the applied methods have been effectively utilized before to study the thermochemistry, kinetics, and non-covalent interactions, particularly of free radical processes [152-155] and other similar systems [94, 152, 153, 156, 157]. Thus, the methods have been chosen to calculate the antioxidant potential of the studied species. Frequency calculations have also been carried out by using the previously optimized geometries.

DOI: 10.14750/ME.2025.027

Table 4. The applied level of theories to calculate the antioxidant potential of natural and synthetic antioxidant additives.

Molecules	B3LYP/ 6-31G(d)	M06/ 6-311+G(d,p)	M06-2X/ 6-311+G(d,p)	M05-2X/ 6-311++G(2d,2p)	M06-2X/ 6-311++G(2d,2p)
Natural Antioxidant Additives					
Curcumin	✓	✓	✓		
L-ascorbic acid				✓	✓
α-Tocopherol				✓	✓
Trolox				✓	✓
Synthetic Antioxidant Additives					
BHA	✓	✓	✓		
BHT	✓	✓	✓		
TBHQ	✓	✓	✓		
Santowhite				✓	✓
EDTA				✓	✓
Irganox				✓	✓

2.5. Antioxidant mechanisms

Three major free radical scavenging (RS) mechanisms were considered to examine $H^{\bullet}$ transfers from all unique X-H (X = C, or O) positions of the studied molecules: hydrogen atom transfer (HAT), single electron transfer-proton transfer (SET-PT), and sequential proton loss electron transfer (SPLET) [49, 107, 110-115] (***Figure 15***).

DOI: 10.14750/ME.2025.027

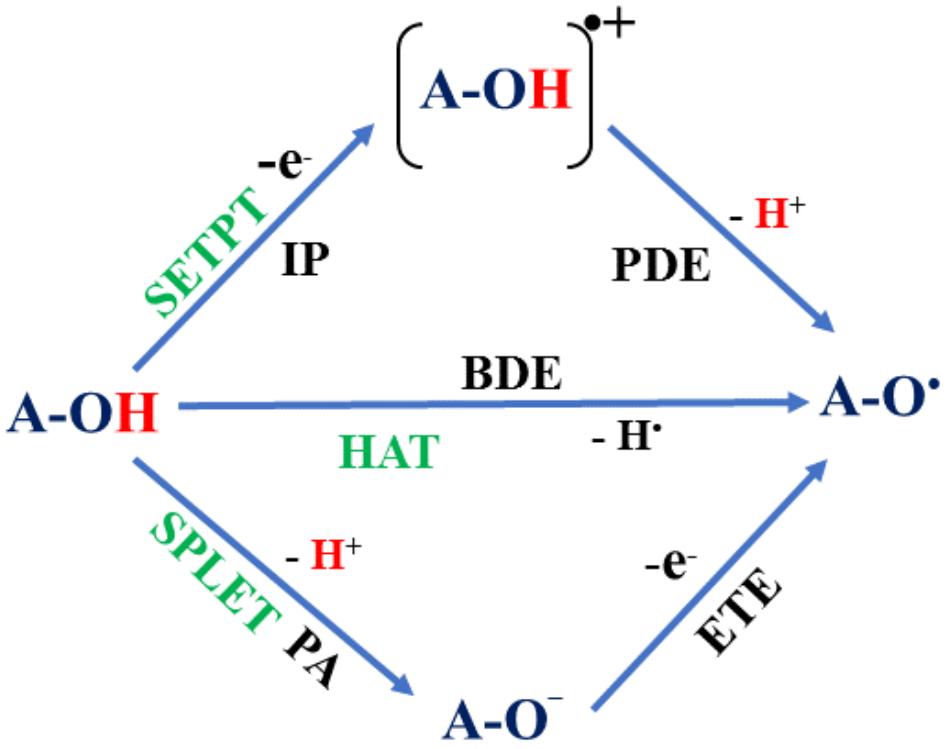

Figure 15. Schematic representation of the studied radical scavenging mechanisms through a hydroxyl group: hydrogen atom transfer (HAT), single electron transfer-proton transfer (SET-PT), and sequential proton loss electron transfer (SPLET). A – antioxidant, OH - hydroxyl group. BDE: bond dissociation enthalpy, IP: ionization potential, PDE: proton dissociation enthalpy, PA: proton affinity, and ETE: electron transfer enthalpy.

2.5.1. Hydrogen atom transfer (HAT) mechanism

The HAT mechanism involves a hydrogen atom ($H^{\bullet}$) transfer from hydrogen donor sites, such as methyl group, hydroxyl group and others, of the antioxidant compound to the free radical. From a thermodynamic point of view, the antioxidant potential can be measured by the bond dissociation enthalpy (BDE) of the corresponding X-H bond, where the lower the BDE the greater the antioxidant capacity of the compound [94, 95, 158-160]. The BDE values for all unique X-H bonds of antioxidant additives have been calculated and compared.

$$BDE = H(A^{\bullet}) + H(H^{\bullet}) - H(A) \qquad \textbf{Eq. 14}$$

Where H(A) is the enthalpy of antioxidant, while $H(A^{\bullet})$ and $H(H^{\bullet})$ are the enthalpies of the corresponding antioxidant radical and hydrogen atom, respectively, which are the free radicals formed after the dissociation of an X-H (X = C, or O) bond.

2.5.2. Single electron transfer proton transfer (SET-PT)

The second studied mechanism was SET-PT which includes two steps. First an electron is donated from the antioxidant to the radical which is followed by proton transfer [94, 95]. In this case, the antioxidant potential is determined by the ionization potential (IP), and proton dissociation enthalpy (PDE) values. The lower IP and PDE values are associated with higher antioxidant capability of the additives [58, 94, 95, 160, 161].

$$IP = H(A^{\bullet+}) + H(e^{-}) - H(A) \qquad \textit{Eq. 15}$$

$$PDE = H(A^{\bullet}) + H(H+) - H(A^{\bullet+}) \qquad \textit{Eq. 16}$$

where $H(A^{\bullet+})$ is the enthalpy of the radical cation formed after an electron transferred from the antioxidant, H(e−) and $H(H^{+})$ in gas phase are 3.1351 kJ/mol and 6.1398 kJ/mol, respectively [94, 162-164].

In this part, the solvent (water) was used in the calculation, and then the enthalpy of the proton $\Delta H_{H2O}(H^{+})$ and electron $\Delta H_{H2O}(e^{-})$ in the solvent phase had to be calculated to get the other parameters. This will create a charged particle H (S-H) $^{+}$sol or H (S-e)$^{-\bullet}$sol [111, 114–116].

S = water

H (S-H) $^{+}_{sol}$ = H_3O^{+}

H (S-e)$^{-\bullet}_{sol}$ = $H_2O^{-\bullet}$

$$H^{+}gas + H_2O \leftrightarrow H_3O^{+} \qquad \textit{Eq. 17}$$

$$e^{-}gas + H_2O \leftrightarrow H_2O^{-\bullet} \qquad \textit{Eq. 18}$$

After that, we can calculate the electron ΔH_{H2O} (e−) and proton ΔH_{H2O} (H^{+}) enthalpies:

$$\Delta H_{H2O}(H^{+}) = H(H_3O^{+}) - H(H_2O) - H(H^{+}gas) \qquad \textit{Eq. 19}$$

$$\Delta H_{H2O}(e^{-}) = H(H_2O^{-\cdot}) - H(H_2O) - H(e^{-}gas) \qquad \textit{Eq. 20}$$

The electron and proton enthalpies have been calculated using M05-2X and M06-2X, as well as the 6-311++G(2d,2p) basis set in the water phase (***Eq. 19, and Eq. 20***) [111]. In the M05-2X, $\Delta H(e^{-})$ and $\Delta H(H^{+})$ are -66.46 kJ/mol and -1053.32 kJ/mol, respectively, while in the M06-2X, the values are equal to -80.16 kJ/mol ($\Delta H(e^{-})$) and -1056.57 kJ/mol ($\Delta H(H^{+})$). These values are in good agreement with the literature for the same method, just different in the basis set [111].

2.5.3. Sequential proton loss electron transfer (SPLET)

The last antioxidant mechanism to consider is SPLET. It also includes two steps, a proton transfer followed by an electron transfer from the antioxidant to the radical [165]. The values of proton affinity (PA) and electron transfer enthalpy (ETE) define the antioxidant potential for the studied compounds, the lower PA and ETE the better antioxidant.

$$PA = H(A^-) + H(H^+) - H(A) \qquad \textit{Eq. 21}$$

$$ETE = H(A^\bullet) + H(e^-) - H(A^-) \qquad \textit{Eq. 22}$$

where $H(A^-)$ is the enthalpy of the anion which is formed after a proton loss has been occurred.

2.6. Experimental Details (Additives as stabilizer with PVC)

In the previous section, the theoretical aspects of the calculations of antioxidant properties of common synthetic additives like BHT, BHA, TBHQ, santowhite, Irganox, and EDTA, as well as natural antioxidants like curcumin, Asc, Trolox, and α-tocopherol have been described. Antioxidants selected based on the theoretical calculations have also been tested in the laboratory to enhance polyvinyl chloride's (PVC) properties, especially heat stability. Thus, the following section encompasses the materials utilized and their specifications, the methods employed to prepare the samples, the tests conducted on them, and the standards applied during the preparation and testing of these samples.

2.6.1. Materials

Polyvinyl chloride type S-5070 (under the trademark Ongrovil®) is produced and supplied by Wanhua-BorsodChem Zrt., Hungary [144]. S-5070 is a suspension-type homopolymer of medium molecular mass. It is a white powder with a porous particle structure, a narrow particle size range, a relatively high apparent density, and excellent pourability. As additives, Butylated hydroxyanisole (BHA), tert-butylhydroquinone (TBHQ), ascorbic acid, and curcumin from Sigma-Aldrich Company, ethylenediaminetetraacetic acid (EDTA) from Merck, and ascorbyl palmitate purchased from Thermo Scientific Company were used. All experiments were carried out at the Process Technology Support Laboratory of Wanhua-BorsodChem and further support was provided by the FIEK and the Institute of Chemistry, University of Miskolc.

2.6.2. Sample preparation for thermal stability tests using conductivity measurements

PVC samples for heat degradation were prepared by thoroughly mixing 0.5 g of PVC powder and different ratios of BHA, TBHQ, EDTA, Asc, ascorbyl palmitate, and curcumin (0.0, 0.1, 0.3, 0.5, 1.0, 3.0, 5.0, 10, 20) wt% (***Table 5***) as stabilizer in the reaction test tube for each experiment and transferring it into a degradation tube. All samples have been prepared according to ISO standards, and all preparation steps have been completed at Wanhua-BorsodChem Zrt., Hungary.

Table 5. Components of the prepared samples

Sample No.	Ratios wt%	Content (PVC +Additives)
Sample 1	0.0	Pure PVC
Sample 2	0.1	PVC + 0.1wt.% Add.
Sample 3	0.3	PVC + 0.3 wt.% Add.
Sample 4	0.5	PVC + 0.5 wt.% Add.
Sample 5	1.0	PVC + 1.0 wt.% Add.
Sample 6	3.0	PVC + 3.0 wt.% Add.
Sample 7	5.0	PVC + 5.0 wt.% Add.
Sample 8	10.0	PVC + 10 wt.% Add.
Sample 9	20.0	PVC + 20 wt.% Add.

2.6.3. Dehydrochlorination Test

The dehydrochlorination rates were calculated by using two different methods.

2.6.3.1. Standard Method

The dehydrochlorination rates were measured by using the 895 Professional PVC Thermomat in conjunction with StabNet software, a modern analytical system for automatic determination of the thermal stability (dehydrochlorination method) of PVC and other chlorine-containing polymers (***Figure 16***) located at Wanhua-BorsodChem Zrt., Hungary. Preparation of the reaction tube, weighing out of the sample and closing of the reaction tube are very simple and safe. The tube was connected to a source of nitrogen maintained at a flow rate of 7.0 L/h. The degradation tube was then immersed in electric heating unit, and the temperature was set to 180 °C [166-168]. Thereafter, the reaction test tube was connected to the measuring cell and ventilated with nitrogen gas for 1-2 minutes, during which the

DOI: 10.14750/ME.2025.027

connection and the gas flow was checked. After that, when the temperature and gas flow have stabilized, the test tube was inserted into the heating blocks. The measurement can be started individually in the software by clicking on the start button next to the information fields or by pressing the buttons next to the individual measurement positions. Using this method, the stability time (***Figure 16C)*** that is, the amount of time until poly(vinyl chloride) starts to release HCl—is measured by subjecting the samples of poly(vinyl chloride) inside the device to high temperatures [169]. The stability time was defined as the duration required to reach a conductivity of 50 µS/cm, indicating approximately 0.9% conversion of dehydrochlorination. The point at which the time axis intersects is referred to as the induction time.

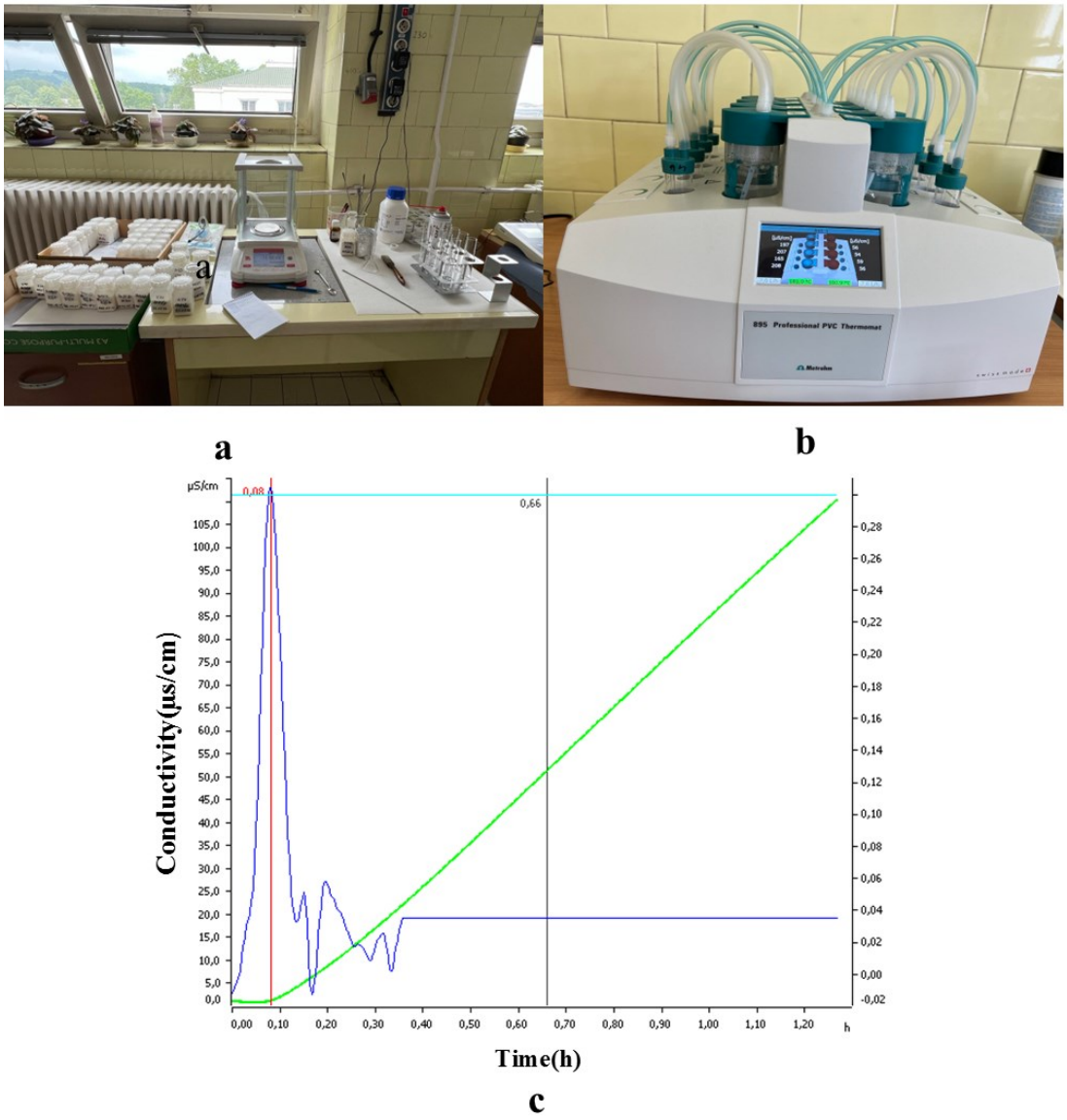

Figure 16. Preparation of PVC samples for conductivity and thermal stability measurements by using the 895 Professional PVC Thermomat: a) preparation of the samples; b) starting the measurement; c) the conductivity diagram of PVC from StabNet software.

2.6.3.2. Novel Evaluation Method

This method was employed to graphically represent the dehydrochlorination data. After each examination, the data was recorded in the device's database. Subsequently, a thorough analysis of the data was conducted in order to extract kinetic information.

- To determine the concentration of HCl, the measured conductivity was used. We can then convert the conductivity to HCl concentration. We determined the conversion function using the following (***Eq. 23***) [170, 171]:

$$lgc = -1.05788 + 0.9882 \times lg\,k + 0.003988 \times (lg\,k)^2 \quad \textbf{\textit{Eq. 23}}$$

where *c* is HCl concentration in mg/l, while *k* is specific conductivity in µS/cm.

Furthermore, the HCl concentration can be calculated from the absorbent water quantity, where the instrument is using 60 ml of water.

- The second piece of information that can be calculated is the conversion of degradation. We can convert the dehydrochlorination curve to the conversion of degradation if we know the exact mass of PVC in the sample. The total degradation process produces 58.4% HCl from pure PVC (***Eq. 24***) [170].

$$\boldsymbol{k = mHCl / 0.584 \times mPVC} \qquad \textbf{\textit{Eq. 24}}$$

where mHCl is the mass of HCl in mg, mPVC is the exact mass of PVC in the sample in mg.

2.7. Experimental Details (α-Tocopherol as an Effective Natural Antioxidant for Polyurethane Foams)

2.7.1. Preparation of Flexible Polyurethane Foam and α-tocopherol as additives (FPUF/ α-tocopherol)

Polyurethane flexible foam samples were produced using Ongronat TR4040 (a mixture of methylene-diphenyl-diisocyanate isomers from Wanhua-BorsodChem in Kazincbarcika, Hungary) and Ongropur FFP-303 (a polyether type polyol premix also from Wanhua-BorsodChem in Kazincbarcika, Hungary). In order to produce the applied polyol, catalysts and supplementary additives, including blowing agents and surfactants, have been combined into a base polyol (Alcupol F2831, Repsol, Madrid, Spain). FPUF foam samples with different raw material ratios and, thus, different hardness was prepared. The raw material ratios (isocyanate index, NCO) were 1.0 and 1.1 isocyanate to 1.0 polyol (**Table 6**). The isocyanate index is the ratio of the total number of NCO groups to the sum of the OH groups of the polyol premix, which includes additives (e.g., water) within the reaction mixture. The

DOI: 10.14750/ME.2025.027

hardness of the samples increased with increasing isocyanate index due to the greater proportion of hard segments. Different ratios (0.0, 0.25, 0.5, 0.75, 1.0) % wt from α-tocopherol as an additive were added to the polyol (***Table 7***). α-tocopherol was used as an additive to evaluate the mechanical properties of the final product of the prepared samples. The FPUF samples were cut out into a cylinder shape with a diameter of 30 mm and a total sample height of approximately 35 mm, and this FPUF foam was used for the mechanical tests.

Table 6. Formulation of Flexible Polyurethane Foam

Polyol Premix Ongropur FFP-303	Ratio pphb
Wanol F3160	100
Water	3.6
Alcupol F3231	1
Tegostab B4113	0.5
Tegoamin DEOA 85	0.5
DABCO 33LV	0.15
Jaffcat ZF-22	0.1

NCO-index	Polyol Premix Ongropur FFP-303 (%m/m)	Isocyanate Ongronat TR4040 (%m/m)
1.0	63.61%	36.39%
1.1	59.98%	40.02%

DOI: 10.14750/ME.2025.027

Table 7. Formulation of Flexible Polyurethane Foam and α-tocopherol as additives (FPUF/ α-tocopherol)

NCO- index-1.0			
Percentage of α-tocopherol (% wt)	**Weight of α-tocopherol [g]**	**Polyol premix Ongropur FFP-303 [g]**	**Isocyanate Ongronat TR4040 [g]**
0	0	38.16	21.83
0.25	0.15	38.16	21.83
0.5	0.3	38.16	21.83
0.75	0.45	38.16	21.83
1	0.6	38.16	21.83
NCO- index-1.1			
Percentage of α-tocopherol (% wt)	**Weight of α-tocopherol [g]**	**Polyol premix Ongropur FFP-303 [g]**	**Isocyanate Ongronat TR4040 [g]**
0	0	35.98	24.01
0.25	0.15	35.98	24.01
0.5	0.3	35.98	24.01
0.75	0.45	35.98	24.01
1	0.6	35.98	24.01

2.7.2. Mechanical Measurements

The mechanical properties of the prepared samples (FPUF/ α-tocopherol) have been carried out using the mechanical testing method C of ASTM D3574 (complex test standard for flexible polyurethanes) [161]. Samples were cut out into a cylinder shape with a diameter of 30 mm and the total sample height approximately 35 mm. To test and know the value of the compression force deflection (CFD), samples were pressured on their entire surface up to 50% of their height, held them for 1 min, and then measured the change in force.

DOI: 10.14750/ME.2025.027

3. Results and Discussion

3.1. Antioxidant potential of BHA, BHT, TBHQ, and Curcumin as synthetic and natural polymer additives [1]

The antioxidant potential of commonly used synthetic and natural antioxidant additives, including butylated hydroxytoluene (BHT), butylated hydroxyanisole (BHA), *tert*-butylhydroquinone (TBHQ), and natural additive, curcumin have been studied. The geometries of all the molecules and the corresponding ionic and radical species were calculated by using the Gaussian 09 program package [109]. Three different density functional theory (DFT) methods have been used, the B3LYP functional [129, 130, 148, 149] in combination with the 6-31G(d) basis set, and the M06 and M06-2X [150] in combination with the 6-311+G(d,p) basis set applied to optimize all the molecules in gas phase. These methods have been chosen to calculate the antioxidant potential of the studied species, because they have been successfully applied for similar systems [152, 153, 156, 157]. Frequency calculations have also been carried out by using the previously optimized geometries. To explore the antioxidant activity of the studied species three different free radical scavenging (RS) mechanisms have been considered: hydrogen atom transfer (HAT), single electron transfer proton transfer (SETPT), and sequential proton loss electron transfer (SPLET) [58, 161, 172-176] (***Figure 15***).

To compare the antioxidant activity of the compounds, the bond dissociation enthalpy (BDE), ionization potential (IP), proton dissociation enthalpy (PDE), proton affinity (PA), and electron transfer enthalpy (ETE) have been computed for each structure as in the questions ***(Eq. 14, Eq. 15, Eq. 16, Eq. 21, Eq. 22).***

3.1.1. Validation of the selected methods

The antioxidant potential of BHA, BHT, TBHQ and curcumin (enol and diketone forms) have been studied by using three different levels of theory. Experimental O-H bond dissociation enthalpy values for BHA and BHT were used to validate the calculations and to select the best combination of method and basis set for the discussion. In each case, gas phase data were used in the comparison, and the computed values underestimated the measured BDEs (***Table 8***).

[1]The following subchapter is based on: Dalal K. Thbayh, Béla Fiser, Polymer Degradation and Stability, *201*, p.109979, 2022. https://doi.org/10.1016/j.polymdegradstab.2022.109979

Table 8. Bond dissociation enthalpy (BDE) values (in kJ/mol) of O-H bonds in butylated hydroxytoluene (BHT), and butylated hydroxyanisole (BHA) in gas phase calculated at the B3LYP/6-31G(d), M06//6-311+G(d,p), and M06-2X/6-311+G(d,p) levels of theory.

Compound	BDE(O-H) (kJ/mol)			
	B3LYP/6-31G(d)	M06/6-311+G(d,p)	M06-2X/6-311+G(d,p)	Exp. value [177]
BHA 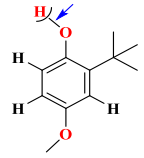	298.0	319.3	335.9	343.4
BHT 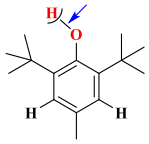	290.3	307.9	327.0	333.0

The least favourable choice of method would be B3LYP in combination with the 6-31G(d) basis set, as the computed BDEs are lower by >40 kJ/mol than the experimental values. By using the M06/6-311+G(d,p) level of theory, the computed BDEs improved, but the differences were still >20 kJ/mol compared to the measured values. The best method – basis set combination is the M06-2X/6-311+G(d,p) level of theory which is able to predict the BDEs with good accuracy as the difference between the calculated and experimentally measured values were only 7.5 kJ/mol and 6.0 kJ/mol for the O-H bond in BHA and BHT, respectively (***Table 8***). Therefore, M06-2X/6-311+G(d,p) is selected and used in the discussion to study the antioxidants. All calculations were carried out in gas phase as the validation is based on gas phase data.

3.1.2. Theoretical evaluation of the antioxidant potential

3.1.2.1. Structural considerations

The geometries of the antioxidant additives have been optimized and it was found that the longest and shortest C-H bonds are located in BHA (C7-H) and curcumin A (C11-H), respectively (***Figure 17 and Figure 18)***. As for O-H bonds, the longest one is 0.999 Å for all structures and can be found in curcumin A (O3-H). The longest bond in BHA is C7-H with a bond length equal to 1.095 Å and it is located on the methyl group in the para position, while the shortest is a benzylic hydrogen C5-H (1.081Å). For BHT the situation is similar, and the longest C-H bond is C7-H with a bond length equal to 1.093 Å and it is located on the methyl group while the shortest bond belongs to a benzylic

DOI: 10.14750/ME.2025.027

hydrogen C5-H (1.082Å). In case of TBHQ, the longest C-H bond is C7-H again with a bond length equal to 1.093 Å and it is located on the methyl group, while the shortest is a benzylic hydrogen C5-H (1.085Å) again. All in all, the bond length in each studied synthetic species follow similar trend (***Figure 17***). As for the natural additive, the longest C-H bonds are located on the *o*-methoxy phenolic group on both sides of curcumin A, C1-H and C21-H, and these are equal to 1.094 Å, while the shortest bond is C11-H (1.080 Å). As for the diketone form, the longest C-H bonds are the same, C1-H and C21-H (1.094 Å), while the shortest C-H bond is located on the aromatic ring (1.083 Å).

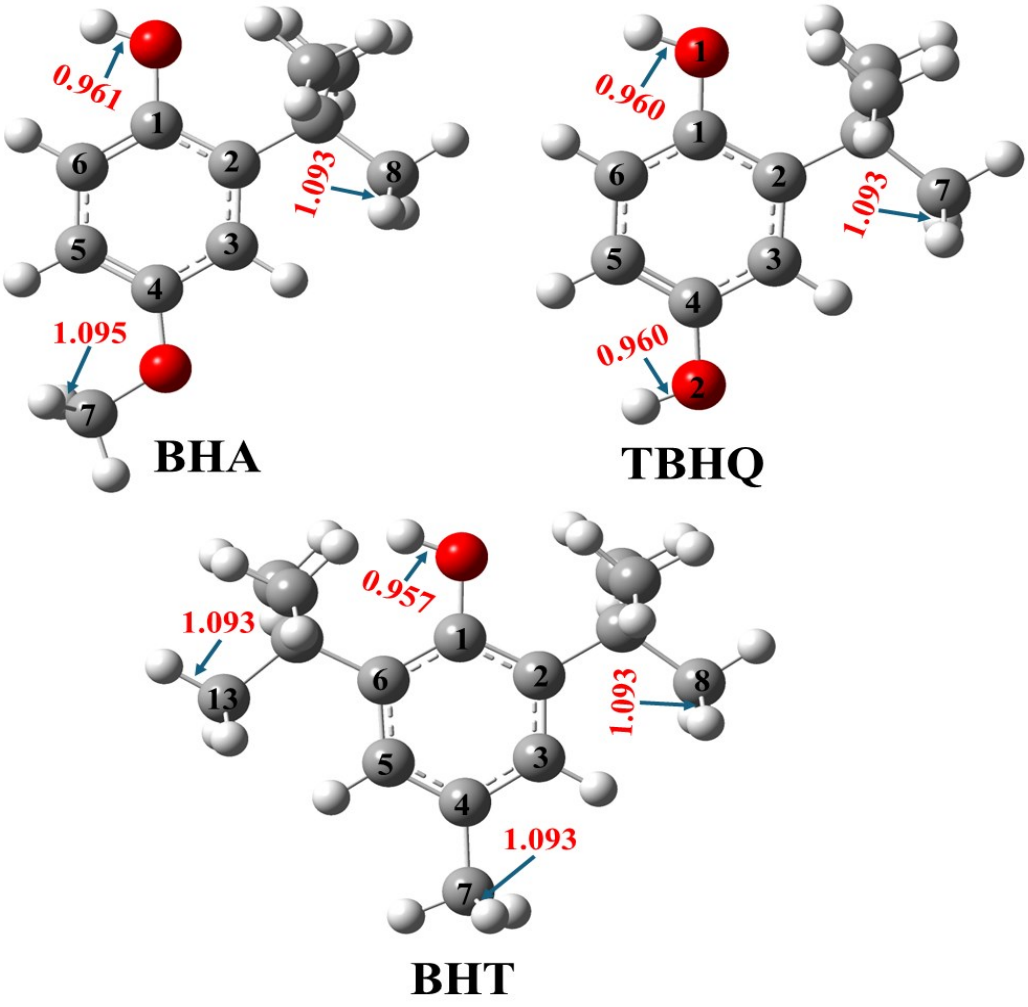

Figure 17. Optimized structures of the studied synthetic antioxidant additives: butylated hydroxytoluene – BHT, butylated hydroxyanisole – BHA, and tert-butylhydroquinone – TBHQ. The optimization have been carried out at the M06-2X/6-311+G(d,p) level of theory in gas phase. The corresponding bond lengths (in Å) are also shown.

DOI: 10.14750/ME.2025.027

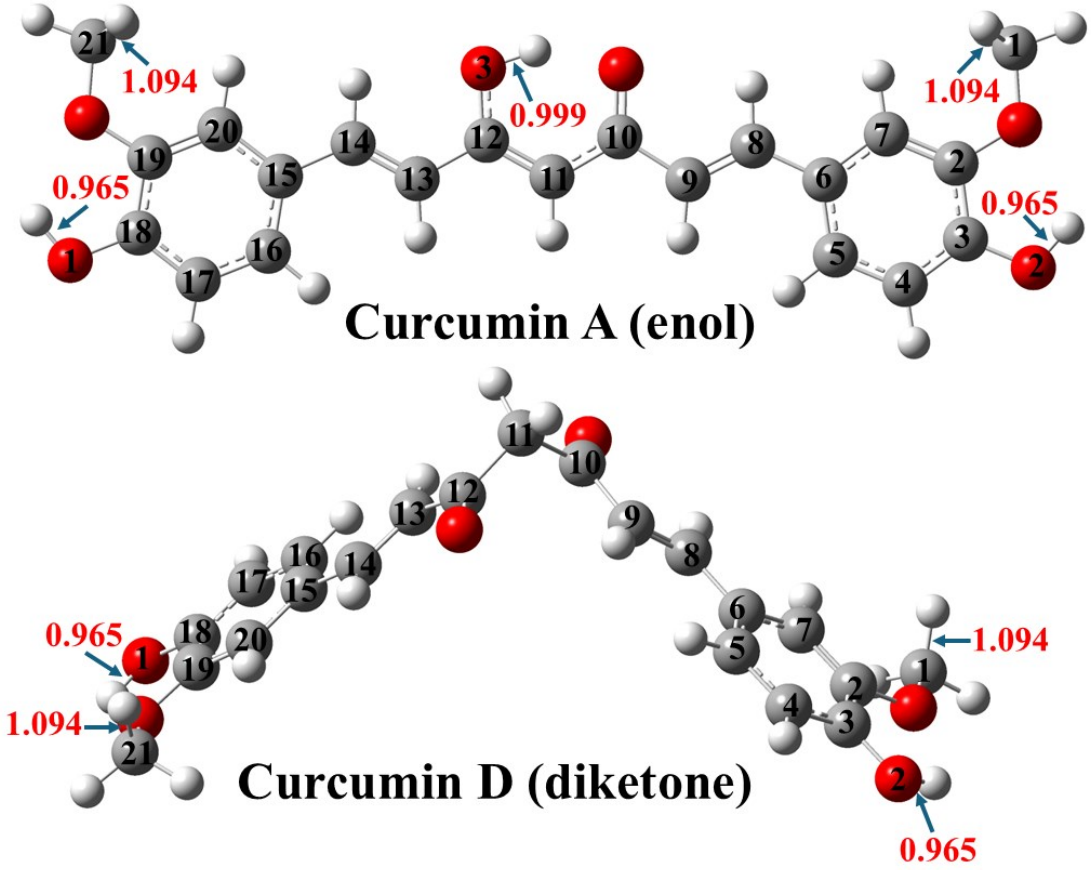

Figure 18. Optimized geometries of the studied natural antioxidant additive structures*:* curcumin A and D, enol and diketone forms, respectively. The optimization have been carried out at the M06-2X/6-311+G(d,p) level of theory in gas phase. The corresponding bond lengths (in Å) are also shown.

3.1.2.2. Antioxidant mechanisms

In the hydrogen atom transfer (HAT) mechanism, a hydrogen atom (H$^{\bullet}$) will be directly transferred to the free radical in a one-step process. To study the effectiveness of this process, and thus, to compare the antioxidant potential of the molecules, the bond dissociation enthalpies of each unique C-H and O-H bonds in BHA, BHT, TBHQ, curcumin A, and curcumin D have been computed (***Table 9***, ***Table 10***, ***Figure 19***).

DOI: 10.14750/ME.2025.027

Table 9. Bond dissociation enthalpy (BDE) values (in kJ/mol) of all unique C-H and O-H bonds in butylated hydroxytoluene - BHT, butylated hydroxyanisole - BHA, and tert-butylhydroquinone – TBHQ calculated at the M06-2X/6-311+G(d,p) level of theory in gas phase.

BHA	B. L (Å)	BDE	BHT	B. L (Å)	BDE	TBHQ	B. L (Å)	BDE
O-H	0.961	335. 9	O-H	0.957	327.0	O1-H	0.960	335.5
C3-H	1.081	454.4	C3-H	1.083	450.2	O2-H	0.960	345.5
C5-H	1.081	465.2	C5-H	1.082	450.1	C3-H	1.081	463.9
C6-H	1.086	464.6	C7-H	1.093	374.4	C5-H	1.085	469.3
C7-H	1.095	403.0	C8-H	1.093	417.2	C6-H	1.086	465.5
C8-H	1.093	421.3	C13-H	1.093	417.2	C7-H	1.093	420.9

Table 10. Bond dissociation enthalpy (BDE) values (in kJ/mol) of all unique C-H and O-H bonds in curcumin A and D calculated at the M06-2X/6-311+G(d,p) level of theory in gas phase.

Curcumin A	B. L (Å)	BDE	Curcumin D	B. L (Å)	BDE
O1-H	0.965	355.9	O1-H	0.965	359.1
O2-H	0.965	357.5	O2-H	0.965	359.1
O3-H	0.999	461.9	-		-
C1-H	1.094	408.0	C1-H	1.094	405.9
C4-H	1.083	474.5	C4-H	1.083	475.4
C5-H	1.083	464.0	C5-H	1.083	465.2
C7-H	1.083	466.8	C7-H	1.083	467.1
C8-H	1.088	438.3	C8-H	1.089	439.1
C9-H	1.084	458.8	C9-H	1.085	452.4
C11-H	1.080	482.2	C11-H	1.091	376.4
C13-H	1.083	460.2	C13-H	1.083	427.3
C14-H	1.087	439.3	C14-H	1.089	436.1
C16-H	1.083	463.4	C16-H	1.083	465.2
C17-H	1.083	474.7	C17-H	1.083	475.4
C20-H	1.083	466.6	C20-H	1.083	467.1
C21-H	1.094	407.9	C21-H	1.094	405.9

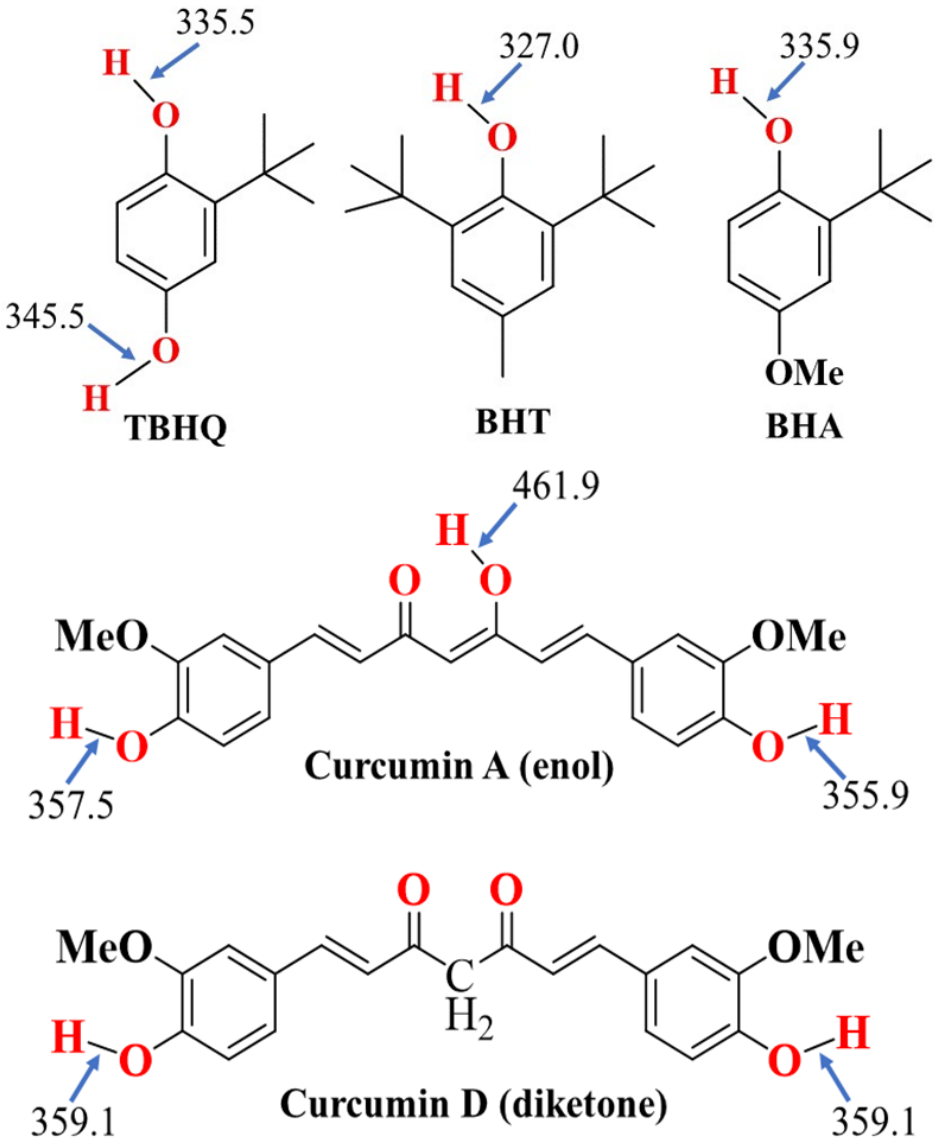

Figure 19. Bond dissociation enthalpies (BDEs, in kJ/mol) of the weakest X-H bonds within butylated hydroxytoluene – BHT, butylated hydroxyanisole – BHA, and tert-butylhydroquinone – TBHQ, and curcumin A and D calculated at the M062-X/6-311+G(d,p) level of theory in gas phase.

The lower the BDE value, the higher the antioxidant potential as it is easier to donate the corresponding hydrogen atom to free radicals [178]. The BDEs of the O-H bonds for synthetic additives are lower compared to the C-H bonds and cover a narrow range starting from 327.0 kJ/mol for BHT and reaching 345.5 kJ/mol in case of TBHQ (***Figure 20***). The C-H bonds are generally stronger as the corresponding BDEs are higher than their O-H counterparts. In case of BHA, BDE_{C-H} values are in a range between 403.0 and 465.2 kJ/mol. The weakest C-H bond in BHA is C7-H (1.095 Å) and it is located on the methyl group, which is in the para position, while the benzylic hydrogen C5-H (1.081 Å) is the strongest

bond with a BDE = 465.2 kJ/mol (***Figure 20*** and ***Figure 15)***. The BDE values of the C-H bonds in BHT covers a range between 374.4 to 450.2 kJ/mol. C7-H (1.092 Å) has the lowest BDE_{C-H} (374.4 kJ/mol) and it is located on the methyl group in the para position while the strongest one not surprisingly is a benzylic hydrogen, C3-H (1.083 Å) with BDE_{C-H} = 450.2 kJ/mol. For TBHQ, the BDE_{C-H} values cover a range between 420.9 to 469.3 kJ/mol. The smallest BDE_{C-H} (420.9 kJ/mol) belongs to C7-H (1.093 Å) which is located on the methyl in the meta position, while a benzylic hydrogen (C5-H, 1.085 Å) is attached to its respective carbon via the strongest bond.

All in all, the BDE values indicate that the O-H bonds are weaker than the C-H bonds for all synthetic species and thus, the most potent functional groups within them are the hydroxyl groups (***Figure 19***). Furthermore, it is not surprisingly easier to remove hydrogen atoms which are part of methyl groups than their benzylic counterparts. Based on the computed BDE values of the C-H and O-H bonds of the synthetic additives, BHT has the highest antioxidant potential. The studied natural antioxidant, curcumin has two isomers, the enol (curcumin A) and diketone (curcumin D) forms, where β-diketones are used in the PVC industry as co-stabilizer, namely Rhodiastab 50. (Stearoylbenzoylmethane). There are three O-H bonds in curcumin A and only two in curcumin D. Four of these are very similar in terms of the computed BDEO-H values as these are around 355.9 and 359.1 kJ/mol. However, in the case of the enol form, O3-H has an exceptionally high BDE value (461.9 kJ/mol) as it is participating in a hydrogen bond (***Figure 18*** and ***Figure 20***). For C-H bonds, the BDE values in the case of the enol form start from 407.9 kJ/mol and reach up to 482.2 kJ/mol. The weakest C-H bond within curcumin A is C21-H and it is located on the o-methoxy phenolic group while the strongest one is C11-H, and it has a quite high BDE value of 482.2 kJ/mol. As for the diketone form, the BDEC-H values cover a similar range starting from 405.9 to 475.4 kJ/mol. The weakest C-H bond in curcumin D is at the same position, C21-H whereas the strongest bond is C4-H. All in all, with one exception the O-H bonds in curcumin are weaker than the C-H bonds which follows the trend of the synthetic structures (***Figure 19***). By comparing the computed BDE values of curcumin, A and D, and the other studied species, the molecules can be ranked based on their antioxidant potential as follows: BHT > BHA ≈ TBHQ > curcumin A > curcumin D.

DOI: 10.14750/ME.2025.027

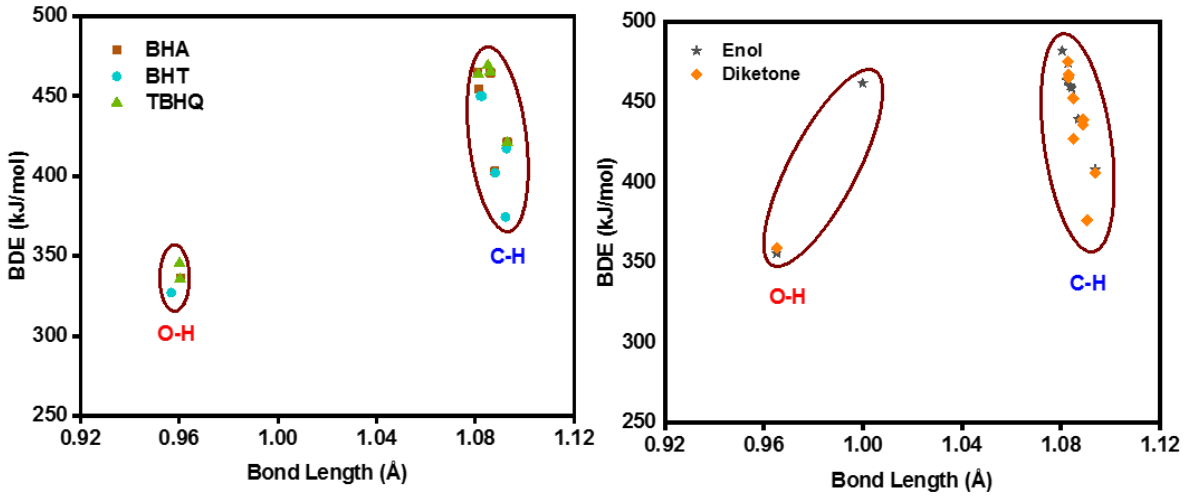

Figure 20. Bond dissociation enthalpies (BDEs) vs bond length in case of butylated hydroxytoluene - BHT, butylated hydroxyanisole - BHA, tert-butylhydroquinone – TBHQ (left panel), and curcumin A and D (right panel) antioxidant additives. All compounds have been computed at the M06-2X/6-311+G(d,p) level of theory in gas phase.

The experimental BDEs of a few commonly used polymers were collected from the literature (***Table 11***) and it was found that they are in a range of 393.7 and 406.2 kJ/mol [179]. In each studied antioxidant additive, there is at least one X-H bond which has a lower BDE than the polymers. Thus, the additives can be applied to protect the polymers and prevent the oxidative stress induced deterioration of the materials.

Table 11. Lowest bond dissociation enthalpy (BDE) values (in kJ/mol) of the studied antioxidants, butylated hydroxyanisole (BHA), butylated hydroxytoluene (BHT), tert-butylhydroquinone (TBHQ) calculated at the M06-2X/6-311+G(d,p) level of theory in gas phase along with experimental BDEs of commonly used polymers such as polyethylene (PE), polysulfone (PS), polycarbonate (PC), and polypropylene (PP).

Compound	BDE (kJ/mol)
Synthetic additives	
BHA	335.9
BHT	327.0
TBHQ	335.5
Natural additives	
Curcumin A	355.9
Curcumin D	359.1
Polymers[179]	
PE	393.7
PP	403.7

PC	405.0
PS	406.2

The second studied antioxidant mechanism is the single electron transfer proton transfer (SETPT), which involves two steps, an electron transfer which is followed by a proton transfer (***Figure 15***). To describe the process, the ionization potential (IP) of the antioxidants was calculated (first step – electron transfer to a free radical), which resulted in the formation of a radical cation, and then, the proton dissociation enthalpy (PDE) was calculated (second step – proton transfer from the radical cation). The value of IP relates to the energy necessary to remove an electron from the neutral antioxidant compound, whereas the PDE value shows the enthalpy of deprotonation of the antioxidant radical cation. The lower the IP and PDE values, the greater the antioxidant potential of the molecule [180]. The computed ionization potentials (***Table 12)*** indicate that curcumin A requires the lowest energy (699.2 kJ/mol) to donate an electron, so it has the highest potential to participate in such reaction among all additives followed by BHA, BHT, curcumin D, and TBHQ.

Table 12. Ionization potential (IP) and lowest proton dissociation enthalpy (PDE) values (in kJ/mol) of butylated hydroxytoluene (BHT), butylated hydroxyanisole (BHA), tert-butylhydroquinone (TBHQ), curcumin A, and D calculated at the M06-2X/6-311+G(d,p) level of theory in gas phase.

Compound	IP	PDE	IP+PDE
BHA	726.0		
O-H		920.9	1646.9
C7-H		988.0	1714.0
BHT	728.9		
O-H		909.0	1637.9
C7-H		956.5	1685.4
TBHQ	741.3		
O1-H		905.1	1646.4
O2-H		915.1	1656.4
C7-H		990.5	1731.8
Curcumin A	699.2		
O1-H		967.5	1666.7
O2-H		969.2	1668.4
O3-H		1033.7	1732.9

C21-H		1019.6	1718.8
Curcumin D	738.4		
O1-H		931.6	1670.0
O2-H		931.6	1670.0
C11-H		948.9	1687.3

The computed PDE values show that the O-H bonds are preferred over the C-H bonds for deprotonation in all additives, which means that proton donation is preferable from an O-H of the antioxidant radical cation than from a C-H. The PDE values of O-H bonds for the compounds range from 905.1 to 1033.7 kJ/mol. The lowest value is 905.1 kJ/mol for TBHQ and the highest is 1033.7 kJ/mol for curcumin A and located at the center of the structure (O3-H). The molecules can be ranked based on their PDEs of O-H bonds as follows: curcumin A > curcumin D > BHA> BHT> TBHQ.

The third studied mechanism is the sequential proton loss electron transfer (SPLET), which also includes two steps (***Figure 15***). First, a proton from the antioxidant molecules transferred and thus, an anion is formed, then, the electron transfer occurs from the antioxidant anion to the free radical. The antioxidant potential of the species in this mechanism has been characterized by computing the proton affinities (PAs) and the electron transfer enthalpy (ETE) values (***Table 13***).

Table 13. Lowest proton affinities (PA) and electron transfer enthalpy (ETE) values in kJ/mol for butylated hydroxytoluene (BHT), butylated hydroxyanisole (BHA), tert-butylhydroquinone (TBHQ), and curcumin A, and D calculated at the M06-2X/6-311+G(d,p) level of theory in gas phase.

Compound	**PA**	**ETE**	**PA+ETE**
BHA			
O-H	1447.5	199.3	1646.8
C7-H	1676.7	37.3	1714.0
BHT			
O-H	1417.3	220.7	1638.0
C7-H	1594.7	96.2	1690.9
TBHQ			
O1-H	1446.2	200.3	1646.5
O2-H	1458.8	197.7	1656.5

C7-H	1686.5	54.0	1740.5
Curcumin A (enol)			
O1-H	1380.7	286.0	1666.7
O2-H	1384.4	284.1	1668.5
O3-H	1436.8	296.2	1733.0
C21-H	1609.5	109.3	1718.8
Curcumin D (diketone)			
O1-H	1382.6	287.4	1670.0
O2-H	1383.1	287.0	1670.1
C11-H	1413.7	296.2	1709.9

The PA values for the natural compounds are smaller than for the synthetic antioxidant additives for each of the studied O-H and C-H bonds. The PA values of O-H bonds for the studied compounds range from 1380.7 to 1458.8 kJ/mol. The lowest value is 1380.7 kJ/mol belongs to curcumin A (O1-H) and the largest one is 1458.8 kJ/mol and the corresponding hydrogen can be found in TBHQ (O2-H). While for C-H bonds, the results indicated that the lowest value is associated with C11-H (1413.7 kJ/mol) in curcumin D and the strongest one is C7-H (1686.5 kJ/mol) and located in TBHQ. Based on their proton affinities the molecules can be ranked as follows curcumin < BHT< BHA< TBHQ. Thus, curcumin requires less energy for proton dissociation compared to the other species studied. As for the results of the ETE values, the synthetic antioxidant additives require less energy to donate an electron than curcumin. The ETE values are smaller than the IP values for all studied compounds, because the single electron transfer from the anionic structure is more favored than from the neutral molecule, which is in good agreement with previous findings [58, 174, 180-183]. The IP and PA values are much larger than the corresponding BDE values. Thus, the HAT can be considered as the predominant mechanism, which is in good agreement with previous theoretical studies about BHA and BHT [58] and also with experimental result [177]. All in all, BHT is a great choice as radical scavenger additive in case of the HAT, and SPLET mechanisms, but SETPT curcumin could also be suitable.

DOI: 10.14750/ME.2025.027

3.2. Antioxidant potential of santowhite as synthetic and ascorbic acid as natural polymer additives[2]

A wide variety of additives are used to improve specific characteristics of the final polymeric product. Antioxidant additives (AAs) can prevent oxidative stress and thus, the damage of polymeric materials. In this work, the antioxidant potential and thus, the applicability of santowhite (SW) as a synthetic and ascorbic acid (Asc) as a natural AA were explored using computational tools. All calculations have been carried out by using the Gaussian 09 software package [109]. The studied species, SW, Asc, and the corresponding radicals, radical cations, and anions were optimized by employing two global hybrid functionals M05-2X [151], and M06-2X [150] in combination with the 6-311++G(2d,2p) basis set in the gas phase. Both applied methods have been effectively utilized before to study the thermochemistry, kinetics, and non-covalent interactions, particularly of free radical processes [152-155]. However, the M06-2X/6-311++G(2d,2p) level of theory has been chosen to use during the discussion as it was successfully utilized in the study of similar systems and processes before [94]. Three antioxidant mechanisms have been considered as presented in the previous chapter.

3.2.1. Structural properties

The structure of santowhite has been optimized by employing two global hybrid functionals M05-2X and M06-2X (***Figure 21***). The X-H bonds of SW optimized at the M05-2X//6-311++G(2d,2p) level of theory is shorter compared to the M06-2X results, but the trends are the same. O1-H and O2-H are equal to 0.960 Å at the M06-2X//6-311++G(2d,2p) level of theory. As for C-H bonds, the longest is C3-H (1.093 Å) whilst the shortest is a benzylic carbon – hydrogen bond, C4-H with 1.077 Å (***Figure 21***).

[2] The following subchapter is based on: Dalal K. Thbayh et al. Polymers, 14(17), 3518, 2022 https://doi.org/10.3390/polym14173518

DOI: 10.14750/ME.2025.027

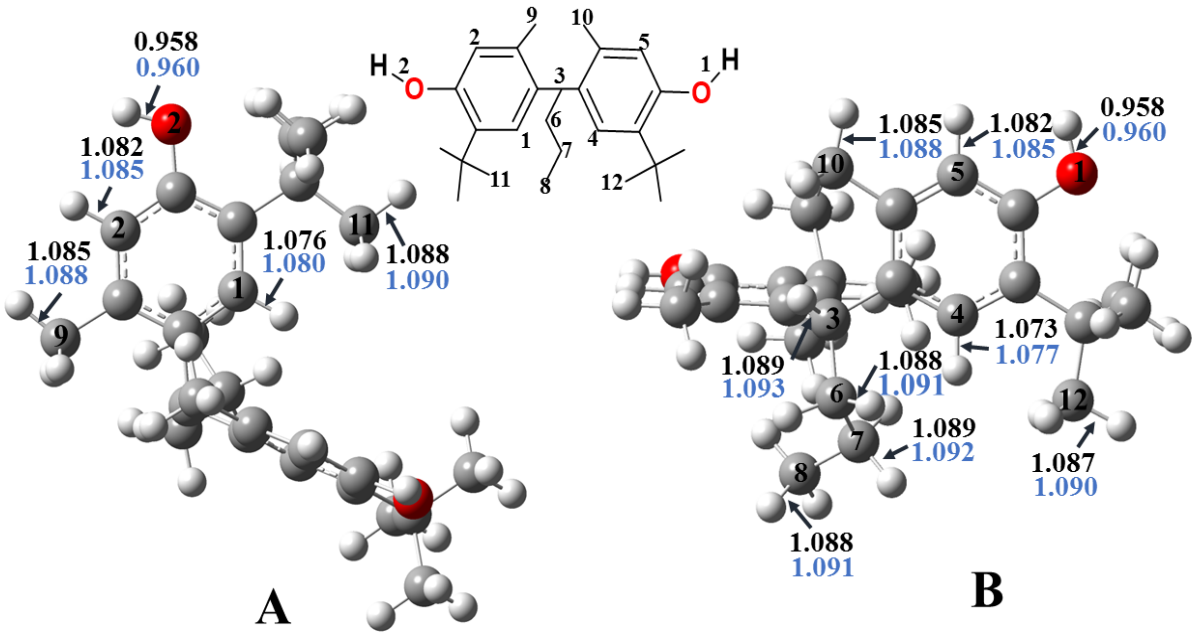

Figure 21. 2D and 3D structures of the studied synthetic antioxidant additive, santowhite. A and B have the same 3D structure from different points of view. Geometry optimizations have been carried out at the M05-2X/6-311++G(2d,2p) and M06-2X/6-311++G(2d,2p) levels of theory in gas phase, and the corresponding bond lengths (in Å) are also shown in black and blue, respectively.

In the case of Asc, the structure includes four hydroxyl groups and three unique C-H positions (***Figure 22***).

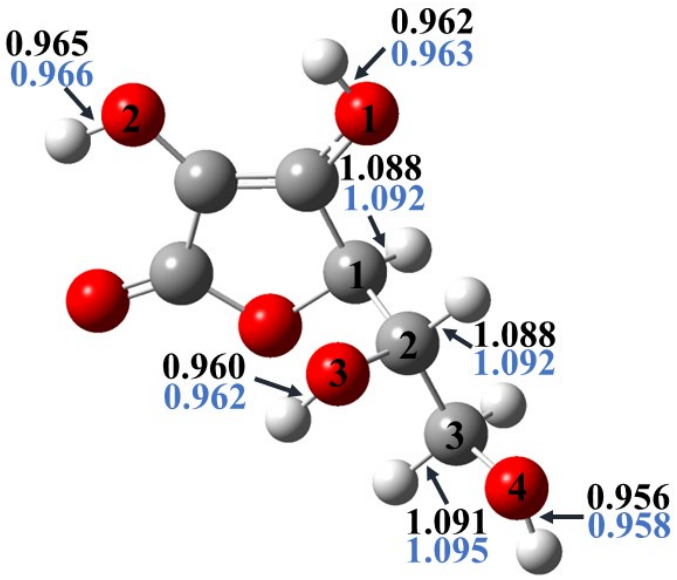

Figure 22. 3D structure of the studied natural antioxidant additive, ascorbic acid (Asc). Geometry optimizations have been carried out at the M05-2X/6-311++G(2d,2p) and M06-2X/6-311++G(2d,2p) levels of theory in gas phase, and the corresponding bond lengths (in Å) are also shown in black and blue, respectively.

The shortest O-H bond is O4-H with a length equal to 0.958 Å, while the longest value belongs to O2-H with a length equal to 0.966 Å at the M06-2X//6-311++G(2d,2p) level of theory (***Figure 22)***. The C-H bonds cover a range from 1.092 to 1.095 Å, where the longest is C3-H with whereas the shortest value belongs to C1-H and C2-H with a length equal to 1.092 Å (Figure 4). All in all, the trend is the same, but the bonds are longer compared to the results obtained at the M05-2X//6-311++G(2d,2p) level of theory (***Figure 22)***.

3.2.2. Antioxidant mechanisms

3.2.2.1. Hydrogen atom transfer (HAT)

In the case of the HAT mechanism, the most active bonds are those with the lowest BDE value [184]. The higher the antioxidant potential, the lower the BDE value, since it is easier to donate the hydrogen atom to free radicals [94, 159, 178]. BDE values of O-H and C-H bonds for SW have been computed and compared to determine the most potent antioxidant sites and also verify the applicability of the studied additives in polymer formulations (***Table 14*** and ***Figure 23***). SW has two O-H bonds, O1-H and O2-H, which have lower BDE values compare to C-H bonds and their BDE values cover a narrow range of 350.0 to 351.5 kJ/mol at both theoretical levels M05-2X and M06-2X (***Table 14*** and ***Figure 23***). The BDE of O2-H was found to be slightly lower than O1-H, but both are smaller compared to the bond dissociation enthalpy of the C-H bonds within the structure determined by using both functionals (***Table 14***).

As for the BDE values of the C-H bonds of SW at M06-2X/6-311++G(2d,2p), these cover a range between 357.0 to 465.3 kJ/mol (***Figure 23***). The weakest bond is C3-H with a BDE=357.0 kJ/mol and it is located between the two phenolic groups while the strongest one is a benzylic hydrogen (C2-H, BDE=465.3 kJ/mol). Similar results were obtained at the M05-2X/6-311++G(2d,2p) level of theory (***Table 14***). The C-H bonds are mostly stronger as the corresponding BDE values are higher than their O-H counterparts, but we noticed that some C-H bonds are close to the O-H bonds in terms of their antioxidant potential, including C3-H, C6-H, C7-H, C9-H, and C10-H, where C3-H is between the two phenolic groups in the molecule, whilst C6-H and C7-H are located on the propyl group in the middle, whereas C9-H and C10-H are located on methyl groups (***Figure 23***). The BDE values of these C-H bonds can be arranged in the following order: C3-H < C9-H < C10-H < C6-H < C7-H with BDE values equal to 357.0 < 375.9 < 377.9 < 395.4 < 398.4 kJ/mol. All in all, based on the results, the O-H bonds are more potent antioxidant sites in SW, and to donate a H atom from

DOI: 10.14750/ME.2025.027

these to a free radical is easier than from their C-H counterparts. However, there are some potentially good free radical scavengers within the C-H sites as well.

Table 14. Bond dissociation enthalpy (BDE) (in kJ/mol) for all unique C-H and O-H bonds in santowhite (SW) calculated at the M05-2X/6-311++G(2d,2p) and M06-2X/6-311++G(2d,2p) level of theory in gas phase.

X-H positions	**BDE (kJ/mol)**	
SW	**M05-2X/ 6-311++G(2d,2p)**	**M06-2X/ 6-311++G(2d,2p)**
O1-H	351.5	351.3
O2-H	351.2	350.0
C1-H	461.2	450.7
C2-H	474.8	465.3
C3-H	356.2	357.0
C4-H	456.8	444.3
C5-H	472.2	465.2
C6-H	395.7	395.4
C7-H	397.2	398.4
C8-H	418.2	417.6
C9-H	372.0	375.9
C10-H	369.2	377.9
C11-H	425.6	421.8
C12-H	420.1	422.7

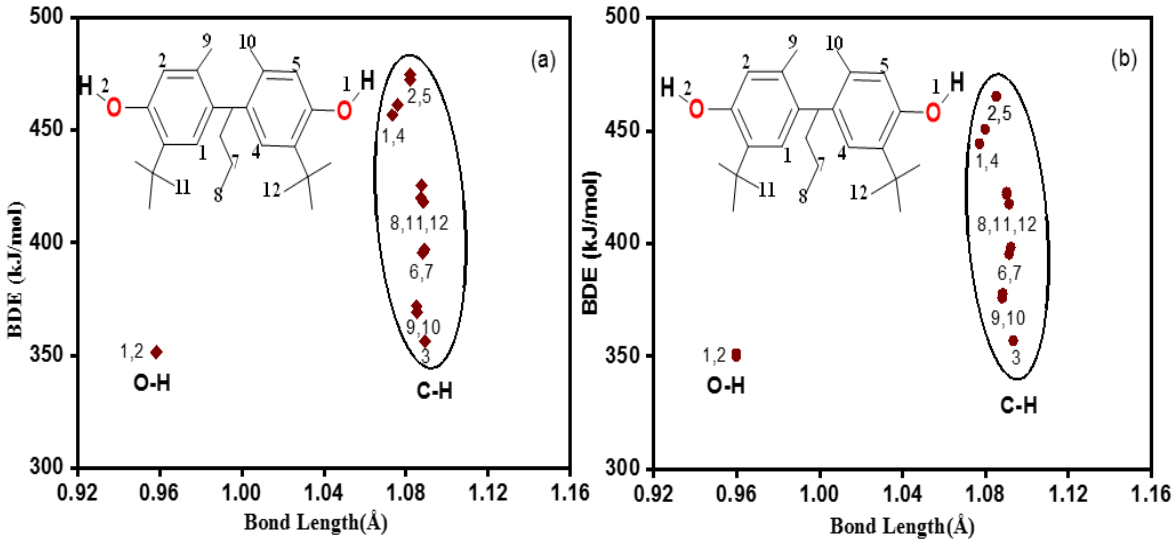

Figure 23. Bond dissociation enthalpy (BDE) vs. bond length plot for santowhite (SW). Calculations have been carried out at (a) M05-2X/6-311++G(2d,2p) and (b) M06-2X/6-311++G(2d,2p) levels of theory in the gas phase. The numbers represent the X-H (X = C, H) bonds in the structure.

In the case of Asc, there are four O-H and three C-H bonds for which the bond dissociation enthalpies have been computed (***Table 15***, and **Figure 24**).

Table 15. Bond dissociation enthalpy (BDE) values (in kJ/mol) for all C-H and O-H bonds of ascorbic acid (Asc) at the M05-2X/6-311++G(2d,2p) and M06-2X/6-311++G(2d,2p) level of theory in gas phase.

X-H positions	**BDE (kJ/mol)**	
Ascorbic Acid	M05-2X/ 6-311++G(2d,2p)	**M06-2X/ 6-311++G(2d,2p)**
O1-H	318.7	319.5
O2-H	349.1	348.5
O3-H	433.2	434.7
O4-H	433.3	434.8
C1-H	351.2	353.4
C2-H	381.7	383.6
C3-H	387.7	391.0

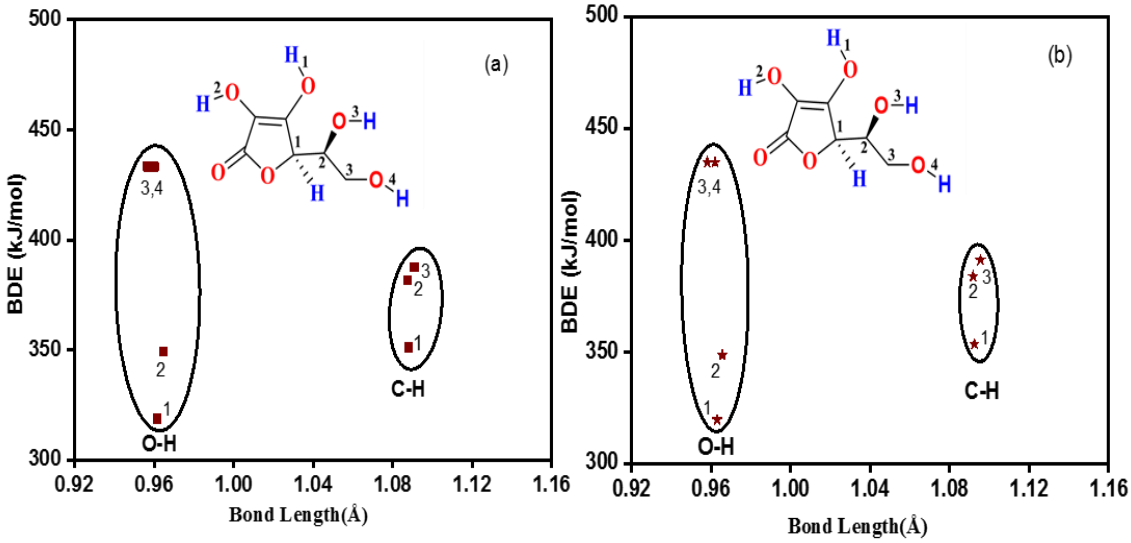

Figure 24. Bond dissociation enthalpy (BDE) vs bond length plot for L-ascorbic acid (Asc) as natural antioxidant additive. The calculations have been carried out at (a) M05-2X/6-311++G(2d,2p) and (b) M06-2X/6-311++G(2d,2p) levels of theory in the gas phase.

The corresponding computed X-H bond dissociation enthalpy values of Asc are similar in case of both M05-2X and M06-2X functionals (***Table 15***). According to the calculations, O1-H has the highest antioxidant potential within Asc and its BDE is lower by 30 kJ/mol and 114.5 kJ/mol, than that of O2-H, and O3-H≈O4-H, respectively in the M05-2X. Whist for M06-2X, its BDE is lower by 29 kJ/mol and 115.3 kJ/mol, than that of O2-H, and O3-H≈O4-H, respectively (***Table 15*** and **Figure 24**).

These results are in good agreement with previous studies [58, 184-186]. The BDEs of the C-H bonds are higher than O1-H and O2-H, but lower than O3-H and O4-H and cover a range from 353.4 to 391.0 kJ/mol where the weakest bond is C1-H, while the strongest one is C3-H (***Table 15***). Thus, it can be concluded that the O1-H followed by O2-H has the highest contribution to the antioxidant activity of Asc in the case of the HAT mechanism.

By comparing Asc with SW, the natural antioxidant has a higher antioxidant potential than its synthetic counterpart. To test the applicability of the studied antioxidant additives, BDE values of commonly used polymers including polyethylene (PE), polysulfone (PS), polycarbonate (PC), and polypropylene (PP) have been collected from the literature and compared to the calculated data (***Table 16***). It was found that the BDE values of commonly used polymers cover a range between 393.7 and 406.2 kJ/mol [179] (***Table 16***).

Table 16. Bond dissociation enthalpy (BDE) values of commonly used polymers such as polyethylene (PE), polysulfone (PS), polycarbonate (PC), and polypropylene (PP) along with the lowest BDE values (in kJ/mol) of the studied antioxidants, santowhite (SW) and L-ascorbic acid (Asc) computed at the M06-2X/6-311++G(2d,2p) level of theory in the gas phase.

Compound	BDE (kJ/mol)	Ref.
Synthetic additive		*
SW	350.0	
Natural additive		
Asc	319.5	
Polymers		
PE	393.7	[179]**
PP	403.7	
PC	405.0	
PS	406.2	

** This work*

*** Literature value*

It can be seen that the lowest BDE value of both studied structures is well below the corresponding bond dissociation enthalpies of commonly used polymers. This indicates that the studied molecules are applicable to prevent oxidative stress induced deterioration of polymeric products.

3.2.2.2. Single electron transfer-proton transfer (SET-PT)

In the SET-PT mechanism, the first step is an electron transfer from an antioxidant (A) to the radical. The A then becomes a radical cation ($A^{\bullet+}$), which in turn deprotonates through the

second step to form a radical (A•) [58, 94, 175]. To measure the antioxidant activity of the corresponding X-H site, first the ionization potential (IP) is calculated and then the proton dissociation enthalpy (PDE) has to be determined (***Figure 15***) [58, 94, 180] . The IP for SW was found to be 717.7 kJ/mol at the M05-2X/6-311++G(2d,2p) and 715.8 kJ/mol at the M06-2X/6-311++G(2d,2p) levels of theory (***Table 17***). PDEs indicate that O-H bonds are more prone to deprotonation in the case of the second step of the SET-PT mechanism of SW than C-H bonds, but C3-H is a close competitor of O-H groups. Similar results were obtained at the M05-2X/6-311++G(2d,2p) level of theory (***Table 17***).

Table 17. Calculated ionization potential (IP) and lowest proton dissociation enthalpy (PDE) values in kJ/mol for santowhite (SW) determined at the M05-2X/6-311++G(2d,2p) and M06-2X/6-311++G(2d,2p) levels of theory in gas phase.

	M05-2X/6-311++G(2d,2p)			M06-2X/6-311++G(2d,2p)		
Compound	**IP**	**PDE**	**IP+PDE**	**IP**	**PDE**	**IP+PDE**
SW	717.7			715.8		
O1-H		947.8	1665.5		946.6	1662.4
O2-H		947.5	1665.2		945.3	1661.1
C3-H		952.4	1670.1		952.3	1668.1

In the case of Asc, IP was found to be 818.6 and 816.7 kJ/mol in M05-2X and M06-2X, respectively (Table 18). The PDEs for all C-H and O-H sites cover a range between 814.0 and 928.6 kJ/mol at M05-2X and 813.9 to 929.2 kJ/mol at M06-2X, where the weakest one is O1-H and the strongest one is O3-H. The PDEs of these C-H and O-H bonds can be arranged in the following order: O1-H < O2-H < C1-H < C2-H < C3-H < O4-H < O3-H with PDE values equal to 814.0 < 834.2 < 836.6 < 877.1 < 884.8 < 921.6 < 928.6 kJ/mol at M05-2X and 813.9 < 833.0 < 838.3 < 878.1 < 892.0 < 921.8 < 929.2 kJ/mol, at M06-2X (***Table 18***). The results corresponding to O-H bonds are in good agreement with previous studies [58, 186].

Table 18. Calculated ionization potential (IP) and proton dissociation enthalpy (PDE) values in kJ/mol for ascorbic acid (Asc) determined at the M05-2X/6-311++G(2d,2p) and M06-2X/6-311++G(2d,2p) levels of theory in gas phase.

	M05-2X/6-311++G(2d,2p)			M06-2X/6-311++G(2d,2p)		
Compound	**IP**	**PDE**	**IP+PDE**	**IP**	**PDE**	**IP+PDE**
Asc	818.6			816.7		
O1-H		814.0	1632.6		813.9	1630.6
O2-H		834.2	1652.7		833.0	1649.7

O3-H		928.6	1747.2		929.2	1745.9
O4-H		921.6	1740.2		921.8	1738.5
C1-H		836.6	1655.2		838.3	1655.0
C2-H		877.1	1695.7		878.1	1694.8
C3-H		884.8	1703.4		892.0	1708.7

All in all, the IP+PDE values of both SW and Asc indicate that the antioxidant activity of ascorbic acid is higher than santowhite which is in agreement with the findings of the HAT mechanism.

3.2.2.3. Sequential proton loss electron transfer (SPLET)

In the case of the SPLET mechanism, the first step includes the dissociation of a proton from the antioxidant (A) which led to the formation of an anion (A^-). Thereafter, the (A^-) anion transfers an electron to the scavenged radical and became a radical ($A^{\bullet}$) itself. To determine the antioxidant potential in the case of the SPLET mechanism, PA and ETE values have been computed for SW (***Table 19***).

Table 19. Lowest proton affinities (PAs) and electron transfer enthalpies (ETE) in kJ/mol for santowhite (SW) calculated at the M05-2X/6-311++G(2d,2p) and M06-2X/6-311++G(2d,2p) levels of theory in gas phase.

M05-2X/6-311++G(2d,2p)				**M06-2X/6-311++G(2d,2p)**		
SW	**PA**	**ETE**	**PA+ETE**	**PA**	**ETE**	**PA+ETE**
O1-H	1438.4	227.1	1665.5	1434.4	228.0	1662.4
O2-H	1431.6	233.6	1665.2	1427.2	233.9	1661.1
C3-H	1563.6	106.6	1670.1	1554.1	114.0	1668.1

The proton affinities of SW indicates that proton transfer is more probable from the hydroxyl groups than from the C-H sites. The best proton transfer ability corresponds to the O2-H site with a PA equal to 1431.6 kJ/mol and it is lower by about 6.8 kJ/mol than O1-H (1438.4 kJ/mol) according to the M05-2X, while for M06-2X it was equal to 1427.2 kJ/mol and it is lower by about 7.2 kJ/mol than the corresponding value of O1-H (1434.4 kJ/mol). The antioxidant potential of the different X-H bonds of SW in the case of the SPLET mechanism was determined by calculating the sum of PA and ETE and the best O-H and C-H sites were ranked as follows: O2-H > O1-H > C3-H (***Table 19***). Similar trends were obtained at both levels of theory (***Table 19***).

As for Asc, the values of PA and ETE have been computed only for four sites (O1-H, O2-H, C1-H, and C3-H) in case of both M05-2X and M06-2X functional (***Table 20***), nubecause in

the case of the other three X-H sites (O3-H, O4-H, and C2-H) intramolecular rear-rangement is occurred after the proton transfer and thus, the SPLET was not comparable (***Figure 25***).

Table 20. Proton affinities (PAs) and electron transfer enthalpies (ETEs) in kJ/mol for ascorbic acid (Asc) calculated at the M05-2X/6-311++G(2d,2p) and M06-2X/6-311++G(2d,2p) levels of theory in the gas phase.

	M05-2X/6-311++G(2d,2p)			M06-2X/6-311++G(2d,2p)		
Asc	**PA**	**ETE**	**PA+ETE**	**PA**	**ETE**	**PA+ETE**
O1-H	1329.3	304.0	1633.3	1336.1	295.8	1631.9
O2-H	1382.3	276.6	1658.9	1388.6	267.2	1655.8
O3-H	-*	-*	-*	-*	-*	-*
O4-H	-*	-*	-*	-*	-*	-*
C1-H	1450.5	199.4	1650.0	1455.6	194.1	1649.7
C2-H	-*	-*	-*	-*	-*	-*
C3-H	1624.9	69.4	1694.3	1624.0	69.7	1693.7

-* intramolecular rearrangement after proton transfer

Similarly, in case of Asc, proton transfer is more probable from the hydroxyl groups compared to the C-H sites. The best proton donor is O1-H with a proton affinity equal to 1336.1 kJ/mol and it is lower by about 52.5 kJ/mol than O2-H (1388.6 kJ/mol) (***Table 20***). Regarding the C-H sites, it can be noticed that the PA of C1-H (1455.6 kJ/mol) is lower by about 168.4 kJ/mol than that of C3-H (1624.0 kJ/mol). The antioxidant potential was determined as in case of SW and the ranking of the X-H sites within Asc is the following, O1-H > C1-H > O2-H > C3-H with PA+ETE values of 1631.9 > 1649.7 > 1655.8 > 1693.7 kJ/mol, respectively (***Table 20***). The order is the same in case of the M05-2X functional with slight deviations in the values (***Table 20***). All in all, the antioxidant activity of ascorbic acid is higher considering the SPLET mechanism as well compared to santowhite.

In case of the above mentioned three X-H sites, O3-H, O4-H, and C2-H, intramolecular rearrangement is experienced after the proton transfer step (***Figure 25***). The O3-H and O4-H sites are gaining back the proton from nearby positions such as O1-H and O3-H, respectively (***Figure 25***). In case of C2-H, the proton loss initiates the opening of the ring and leads to an acyclic compound. Although the rearrangements prevent us from comparing these sites with the others in the case of the SPLET mechanism, it does not mean that O3-H, O4-H, and C2-H do not contribute to the antioxidant activity of ascorbic acid.

DOI: 10.14750/ME.2025.027

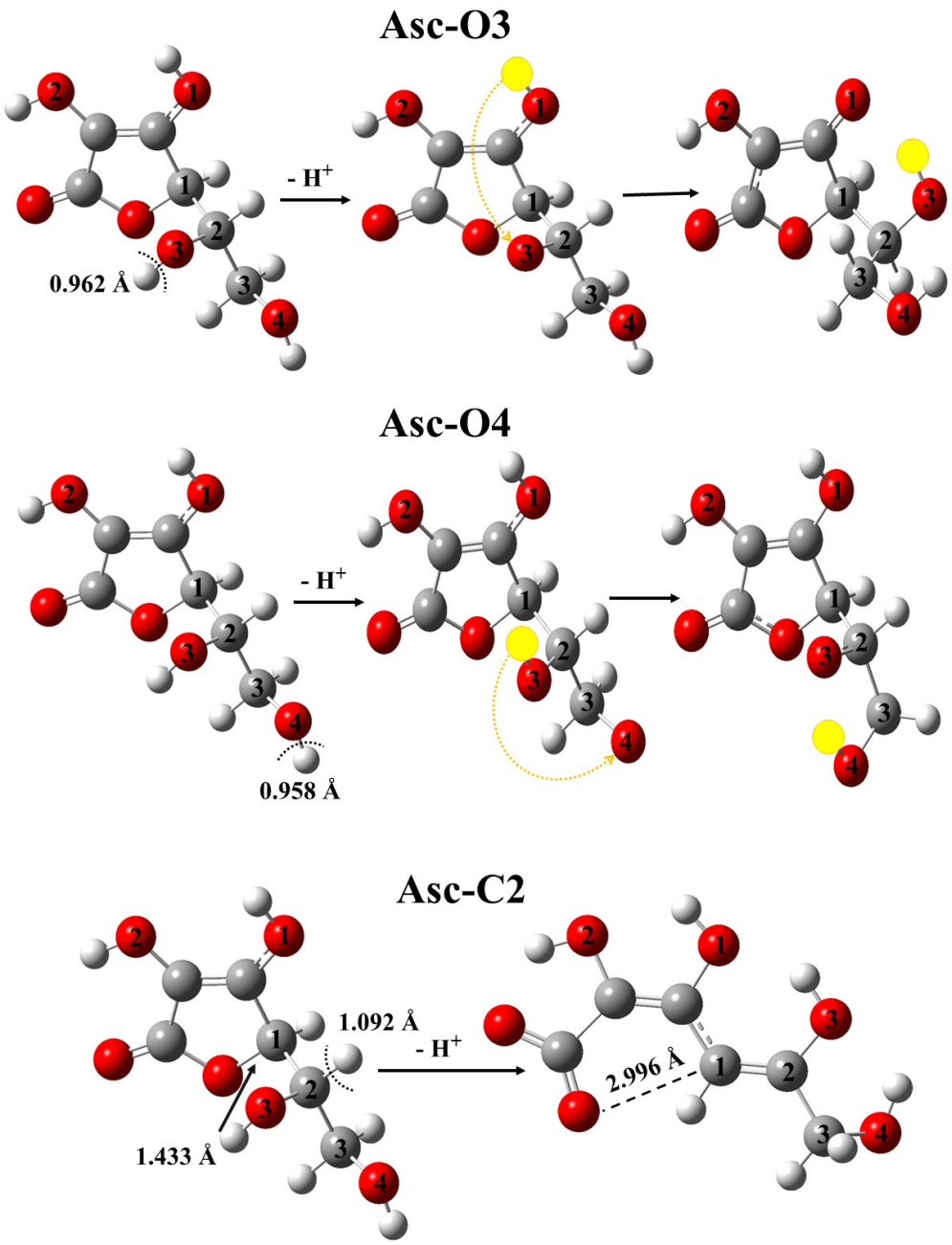

Figure 25. Optimized structures of ascorbic acid (Asc) and the corresponding anionic species after proton loss in the case of the O3-H, O4-H, and C2-H sites. The species have been computed at the M06-2X/6-311++G(2d,2p) level of theory in the gas phase and the corresponding bond lengths and distances (in Å) are also shown. Intramolecular proton transfers are indicated with orange arrows and the transferred protons are highlighted as yellow spheres.

All in all, the antioxidant potential of Asc and SW have been studied and compared. To the best of our knowledge santowhite has not been studied before and thus, the current results are important and novel contributions to the field. Furthermore, there are some C-H sites

which are almost as important as the O-H sites in terms of antioxidant potential. This information could also be important in synthetic antioxidant additive design.

3.3. Comparative Study of the Antioxidant Capability of EDTA and Irganox[3]

Oxidative stress makes it difficult to preserve food and negatively affect the applicability of polymeric packaging. It is typically caused by an excess of free radicals, and it is dangerous to human health, resulting in the onset and development of diseases. The antioxidant ability and activity of ethylenediaminetetraacetic acid (EDTA) and Irganox (Irg) as synthetic antioxidant additives were also studied. To calculate the antioxidant potential of these molecules, three antioxidant mechanisms have been considered as presented before (***Figure 15***) and used the following equations (Eq. 1-5) [158, 161, 178, 187]. To do all these calculation, we have been used Gaussian 09 software package for the studied molecules [109] and two density functionals, M05-2X [151] and M06-2X [150] in combination with the 6-311++G(2d,2p) basis set in gas phase. The applied methodologies were previously validated in similar studies including thermochemistry, kinetics, and non-covalent interactions, especially those involving free radical reactions. Furthermore, because it has previously been utilized successfully in the study of similar systems and processes, the M06-2X/6-311++G(2d,2p) level of theory was chosen to be employed throughout the discussion in this article [94, 95, 152, 153, 155, 187-190].

Both additives can be used to protect pre-processed food products and polymeric packaging from oxidative stress related material deterioration. By comparing the two studied compounds, it was found that EDTA has a higher antioxidant potential than Irganox. To the best of our knowledge several studies have been carried out to understand the antioxidant potential of various natural and synthetic species, but EDTA and Irganox were not compared and investigated before. These additives can be used to protect pre-processed food products and polymeric packaging and prevent material deterioration caused by oxidative stress.

3.3.1. Geometrical considerations

EDTA has four carboxyl groups which have very similar O-H bonds, in terms of their length which are between 0.965 to 0.970 Å where the shortest one is O1-H and the longest one is O2-H while O3-H and O4-H are both equal to 0.966 Å (***Figure 26***). The carbon atoms which

[3] The following subchapter is based on: Dalal K. Thbayh, *et al.*, Heliyon 9 (2023) e16064 https://doi.org/10.1016/j.heliyon.2023.e16064

DOI: 10.14750/ME.2025.027

carry hydrogens in the structure are all directly linked to nitrogen atoms. The lengths of the bonds cover a narrow range from 1.087 to 1.092 Å where the longest is C6-H whilst the shortest is C2-H (***Figure 26***). As for the Irganox model, the structure contains only one hydroxyl group with a bond length equal to 0.956 Å while the C-H bonds cover a range from 1.080 to 1.091 Å at the M06-2X/6-311++G(2d,2p) level of theory (***Figure 26***). The shortest C-H bonds are C1-H and C2-H with 1.080 Å and these are located on the benzene ring whereas the longest one belongs to C6-H.

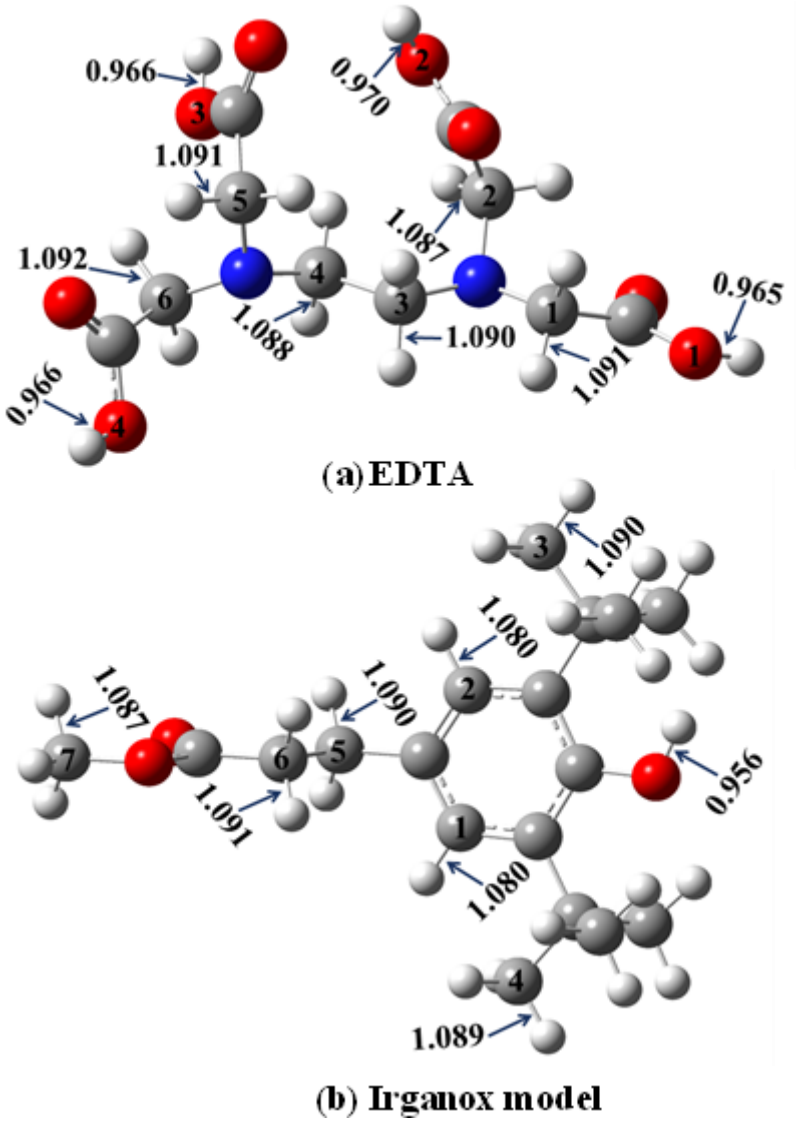

Figure 26. Optimized geometries of the studied synthetic antioxidant additives (a) ethylenediaminetetraacetic acid (EDTA) and (b) Irganox model. Geometry optimizations have been carried out at the M06-2X/6-311++G(2d,2p) level of theory in gas phase, and the corresponding bond lengths (in Å) are also shown.

DOI: 10.14750/ME.2025.027

3.3.2. Antioxidant mechanisms

The antioxidant properties of the two synthetic antioxidant additives including EDTA and the Irganox model have been studied by using two global hybrid functionals M05-2X and M06-2X in combination with the 6-311++G(2d,2p) basis set in gas phase. The antioxidant potential has been measured by comparing the two species in HAT, SET-PT and SPLET mechanisms.

3.3.2.1. Hydrogen atom transfer (HAT) mechanism

The HAT mechanism involves a hydrogen atom transfer from hydrogen donor sites, such as methyl group, hydroxyl group and others, of the antioxidant compound to the free radical. From a thermodynamic point of view, the antioxidant potential can be measured by the bond dissociation enthalpy of the corresponding X-H bond, where the lower the BDE the greater the antioxidant capacity of the compound [94, 95, 158-160]. The BDE values for all unique X-H bonds of EDTA have been calculated and compared (***Table 21*** and ***Figure 28***).

Table 21. Bond dissociation enthalpy (BDE) (in kJ/mol) for all unique C-H and O-H bonds in ethylenediaminetetraacetic acid (EDTA) at the M05-2X/6-311++G(2d,2p) and M06-2X/6-311++G(2d,2p) levels of theory in gas phase.

EDTA	**BDE (kJ/mol)**	
X-H positions	**M05-2X/ 6-311++G(2d,2p)**	**M06-2X/ 6-311++G(2d,2p)**
O1-H	362.0	354.0
O2-H	361.1	351.8
O3-H	345.4	340.4
O4-H	342.9	338.5
C1-H	328.0	330.3
C2-H	321.4	323.6
C3-H	368.4	367.2
C4-H	365.7	364.8
C5-H	317.5	316.7
C6-H	313.1	317.3

BDE values of the C-H bonds of EDTA computed at the M06-2X/6-311++G(2d,2p) level of theory, which cover a range between 316.7 to 367.2 kJ/mol. The weakest bond is C5-H while the strongest one is C3-H. In the case of the M05-2X (***Table 21***), the weakest C-H bond is C6-H with a BDE equal to 313.1 kJ/mol, whilst the strongest is C3-H.

As for BDE values of O-H bonds, special situations arise in case of the carboxyl groups of EDTA. When the hydrogens were removed from the carboxyl groups large structural changes occurred (***Figure 27*** and ***Figure A1)*** as it induced a homolytic bond dissociation. The hydrogen atom abstraction from the carboxyl groups of EDTA initiated a successive C-C bond break, resulting in decarboxylation, a similar situation experienced before in the literature [191]. However, BDE values can be computed for O-H bonds, and these can be compared with the corresponding values of C-H bonds, but any conclusion must take into account the effect of the mentioned structural changes. The BDE of O-H bonds cover a range between 338.5 to 354.0 kJ/mol where the weakest bond is O4-H whilst the strongest is O1-H (***Table 21***) determined at the M06-2X/6-311++G(2d,2p) level of theory. Thus, O4-H has the highest antioxidant potential within the O-H bonds. The results with the other density functional are similar with only small deviations. But this is just an artefact of the position of the released carbon dioxide, as the four O-H groups should have identical bond dissociation values. As for the BDE values of the C-H bonds of EDTA computed at the M06-2X/6-311++G(2d,2p) level of theory, these cover a range between 316.7 to 367.2 kJ/mol. The weakest bond is C5-H while the strongest one is C3-H. In the case of the M05-2X (***Table 21***), the weakest C-H bond is C6-H with a BDE equal to 313.1 kJ/mol, whilst the strongest is C3-H.

Therefore, by comparing the X-H bonds within EDTA, the order of antioxidant potential is the following: C3-H < C4-H < O1-H < O2-H < O3-H < O4-H < C1-H < C2-H < C6-H < C5-H. Thus, C-H bonds have higher antioxidant potential than O-H bonds within EDTA. At the same time, C3-H and C4-H have lower antioxidant potential and these bonds are located between two nitrogen atoms.

DOI: 10.14750/ME.2025.027

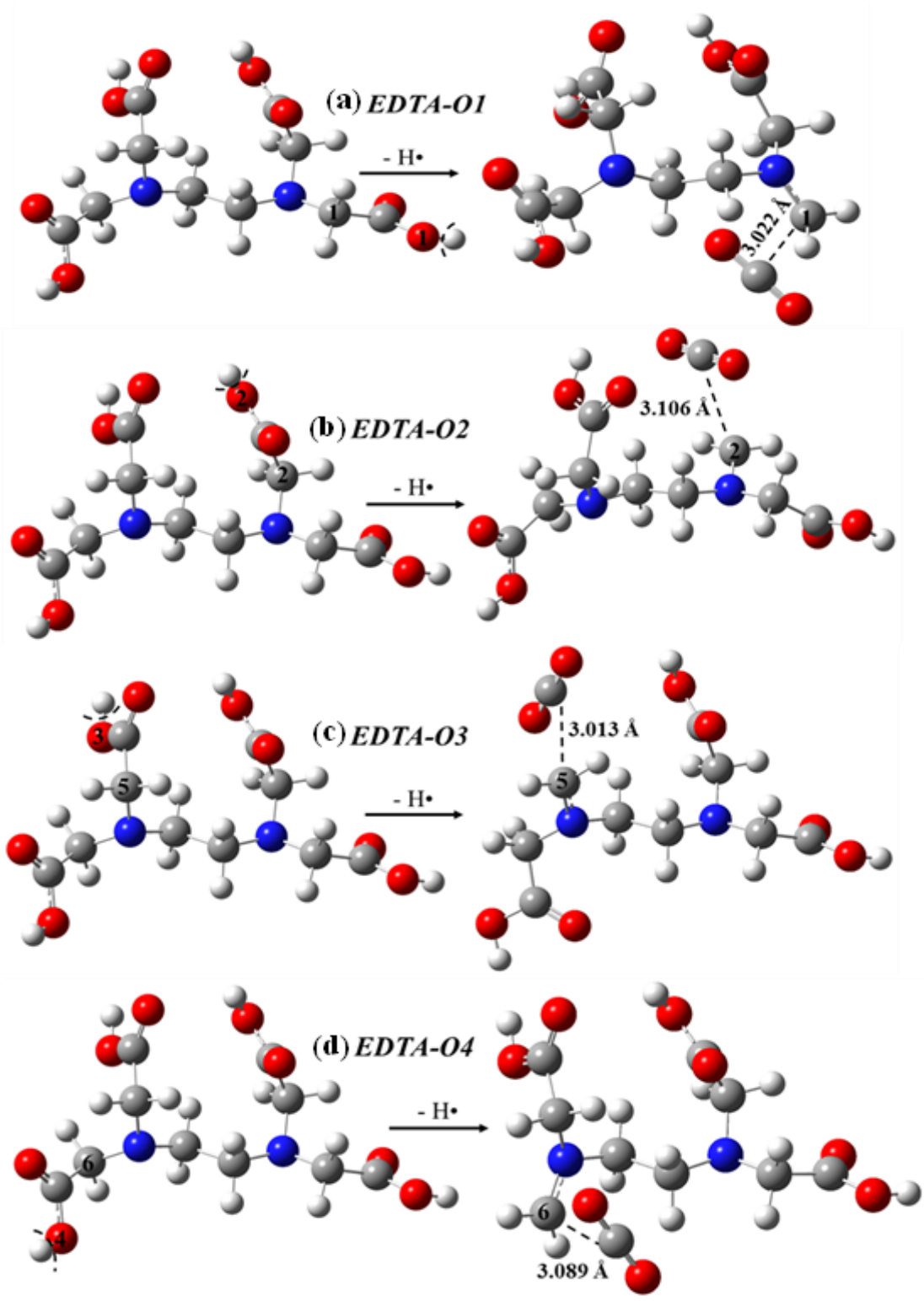

Figure 27. Optimized structures of ethylenediaminetetraacetic acid (EDTA) and the corresponding radical species after H-atom transfer in the hydrogen atom transfer (HAT) mechanism in case of the (a) O1-H (EDTA-O1), (b) O2-H (EDTA-O2), (c) O3-H (EDTA-O3), and (d) O4-H (EDTA-O4) sites. The species have been computed at the M06-2X/6-311++G(2d,2p) level of theory in the gas phase and specific geometrical parameters are also shown (in Å).

In the case of the Irganox model, the BDE values of the studied X-H bonds have also been calculated and compared (

Table* 22** and ***Figure 28). There is only one hydroxyl group in this structure and the corresponding BDE is 331.7 and 333.8 kJ/mol calculated with M05-2X and M06-2X, respectively. BDEs of the C-H bonds cover a range from 364.8 to 454.0 kJ/mol (

***Table* 22**), and the weakest C-H bond is C5-H whilst the strongest one is C1-H, a benzylic hydrogen. The O-H and C5-H are the most potent antioxidant sites within the model compound.

Table 22. Bond dissociation enthalpy (BDE) (in kJ/mol) for all unique C-H and O-H bonds in the studied Irganox model at the M05-2X/6-311++G(2d,2p) and M06-2X/6-311++G(2d,2p) levels of theory in gas phase.

Irganox	**BDE (kJ/mol)**	
X-H positions	**M05-2X/ 6-311++G(2d,2p)**	**M06-2X/ 6-311++G(2d,2p)**
O-H	331.7	333.8
C1-H	458.5	454.0
C2-H	459.9	450.6
C3-H	423.0	423.4
C4-H	422.2	422.5
C5-H	358.3	364.8
C6-H	383.3	385.2
C7-H	412.3	413.1

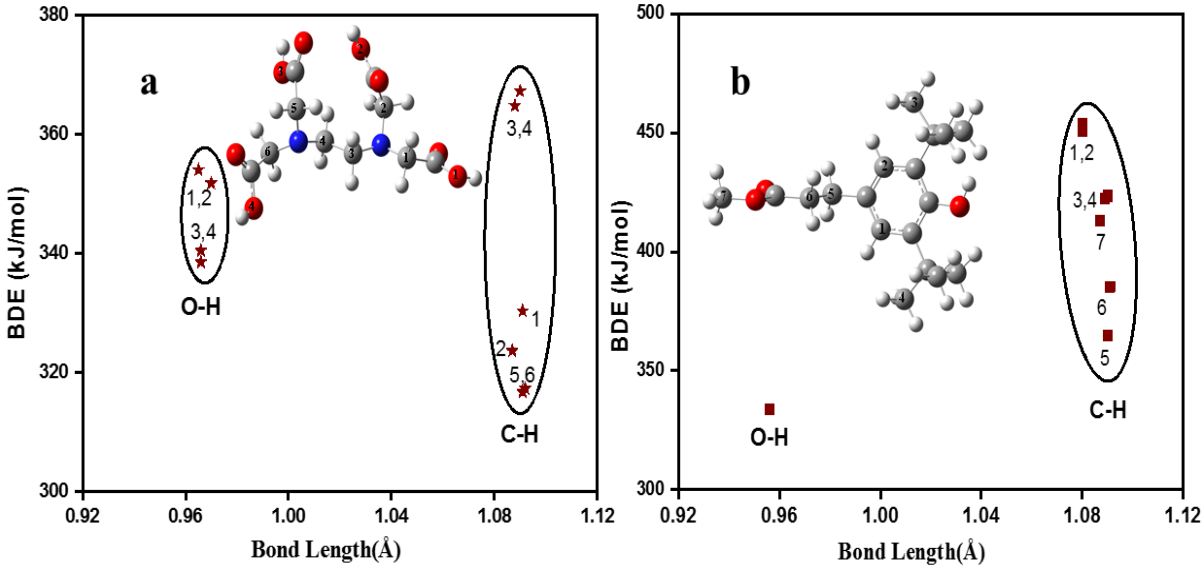

Figure 28. Bond dissociation enthalpy (BDE) *vs* bond length plot for two studied synthetic antioxidant additives (a) ethylenediaminetetraaceticacid (EDTA) and (b) Irganox model. The calculations have been carried out at the M06-2X/6-311++G(2d,2p) level of theory in gas

phase. It has to be noted that the hydrogen atom abstraction from the carboxyl groups (O1-H, O2-H, O3-H, and O4-H) of EDTA initiated a successive C-C bond break, resulting in decarboxylation.

By comparing the results of the two synthetic antioxidant additives, it can be concluded that EDTA has a higher antioxidant potential than Irganox. To assess the applicability of these compounds as antioxidant additives, experimental BDE values of regularly used polymers (from 393.7 to 406.2 kJ/mol) [94, 95, 179] were compared to the lowest bond dissociation enthalpies (316.7 and 333.8 kJ/mol) of the studied species. It was found that both species can be used to protect polymers and prevent material deterioration caused by oxidative stress [94, 95, 179]. It must be noted somehow that some of the polymers compared applied in food packaging.

3.3.2.2. Single electron transfer proton transfer (SET-PT)

The second studied mechanism was SET-PT which includes two steps. First an electron is donated from the antioxidant to the radical which is followed by proton transfer [94, 95]. In this case, the antioxidant potential is determined by the ionization potential (IP) and proton dissociation enthalpy (PDE) values. The lower IP and PDE values are associated with higher antioxidant capability of the additives [58, 94, 95, 160, 161]. The IP for EDTA is slightly above 700 kJ/mol (***Table A1.*** and ***Table* 23**). PDEs indicates that C-H bonds in some positions in the structure are more prone to deprotonation in the second step of the SET-PT mechanism than O-H bonds except C3-H and C4-H. Thus, C-H bonds in EDTA have higher antioxidant potential than O-H bonds according to their IP+PDE values which is in good agreement with the results of the HAT mechanism.

The IP of the Irganox model is higher compared to EDTA and it is just above 730 kJ/mol (***Table* A1.** and ***Table* 23**). Furthermore, the PDE values cover a range between 911.7 and 1031.9 kJ/mol (calculated at the M06-2X/6-311++G(2d,2p) level of theory) where the lowest one belongs to the O-H bond and the strongest one is C1-H which is a benzylic hydrogen (**Table 23**). The most potent antioxidant site of the Irganox model is O-H followed by C5-H, C6-H, C7-H, C4-H, C3-H, C2-H, and C1-H. Thus, the strongest bonds are C1-H and C2-H which are benzylic hydrogens, while the weakest bonds are the O-H, C5-H, and C6-H. By comparing the ionization potentials of the compounds, it can be seen that EDTA has stronger electron donating ability than Irganox. Furthermore, the sum of the IP and PDE values further strengthen that EDTA has higher antioxidant potential compared to Irganox, and this also is in good agreement with the HAT results.

3.3.2.3. Sequential proton loss electron transfer (SPLET)

The last antioxidant mechanism to consider is SPLET. It also includes two steps, a proton transfer followed by an electron transfer from the antioxidant to the radical. The values of proton affinity (PA) and electron transfer enthalpy (ETE) define the antioxidant potential for the studied compounds, the lower PA and ETE the better antioxidant. The computed PA and ETE values of the X-H (X=O or C) bonds of EDTA has been collected and compared (***Table A1.*** and ***Table 23***). In the case of EDTA, during the first step of SPL, in case of the deprotonation from O2-H and O3-H, the process leads to an interesting situation. Both deprotonated species rearrange in a way that the nearby proton holding carboxyl group will stabilize the system by forming a bridge with the group which just lost its proton (***Figure 29*** and ***Figure A2***) and thus, the remaining proton will be shared between the two groups. Nevertheless, the corresponding PA and ETA values have also been computed and compared to C-H bonds, but the conclusions drawn by using these two cases have to consider the specificity of the mechanism. According to the calculated proton affinities for all, from highest to lowest the X-H sites within EDTA are ranked in the following order: C4-H, C3-H, C1-H, C6-H, C2-H, O1-H, C5-H, O4-H, O2-H, and O3-H. Thus, O-H sites are more prone to deprotonation, but in terms of ETE results, the C-H bonds have lower values compared to O-H bonds.

Due to the special situation (O2 and O3 in SPL), the order of the antioxidant potential (PA+ETE) in this mechanism is different compared to the HAT and SET-PT mechanisms. The antioxidant potential of C3-H and C4-H were the lowest among all bonds in case of HAT and SET-PT, but in this mechanism O2-H and O3-H are the least potent antioxidant sites.

DOI: 10.14750/ME.2025.027

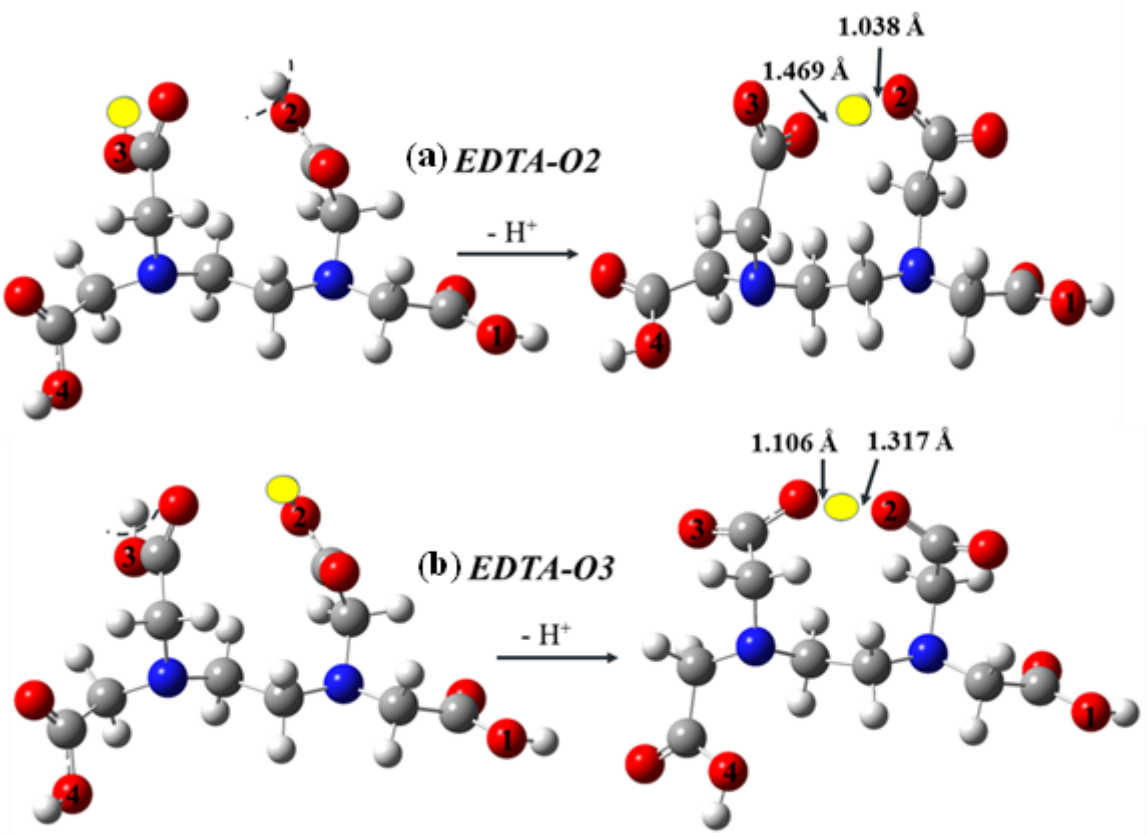

Figure 29. Optimized structures of ethylenediaminetetraacetic acid (EDTA) and the corresponding anionic species after proton loss in the first step of the SPLET mechanism in the cases of the (a) O2-H (EDTA-O2) and (b) O3-H (EDTA-O3) donor sites. The species have been computed at the M06-2X/6-311++G(2d,2p) level of theory in the gas phase and the corresponding specific geometric parameters are also shown (in Å).

In case of the Irganox model, PA values cover a range between 1406.9 (O-H) and 1701.7 (C4-H) kJ/mol calculated at the M06-2X/6-311++G(2d,2p) level of theory. As for ETE results of Irganox, the values start from 31.8 to 238.0 kJ/mol (***Table 23***). From the result, we can notice that the PA and ETE results indicate that the antioxidant potential of O-H is higher than C-H bonds which are in good agreement with the results of the HAT and SET-PT mechanisms.

Table 23. The ionization potential (IP), proton dissociation enthalpy (PDE), proton affinities (PAs) and electron transfer enthalpies (ETE) values in kJ/mol for ethylenediaminetetraacetic acid (EDTA) and Irganox model calculated at the M06-2X/6-311++G(2d,2p) level of theory in gas phase.

Compound	IP	PDE	IP+PDE	PA	ETE	PA+ETE
EDTA	700.1					
O1-H		956.0	1656.1	1410.0	255.1	1665.1
O2-H		947.5	1647.5	1325.2*	380.1*	1705.3*
O3-H		950.9	1651.0	1300.7*	395.5*	1696.3*
O4-H		953.1	1653.2	1393.2	256.4	1649.6
C1-H		923.3	1623.3	1497.7	145.6	1643.3
C2-H		921.4	1621.5	1462.6	168.5	1631.1
C3-H		959.0	1659.1	1617.5	60.8	1678.3
C4-H		959.0	1659.1	1618.3	57.6	1675.9
C5-H		921.4	1621.5	1407.2	241.7	1648.9
C6-H		924.7	1624.8	1486.5	141.9	1628.4
Irganox	733.1					
O-H		911.7	1644.9	1406.9	238.0	1644.9
C1-H		1031.9	1765.0	1632.5	132.6	1765.0
C2-H		1028.5	1761.7	1622.7	140.7	1763.5
C3-H		1001.4	1734.5	1666.2	68.3	1734.5
C4-H		1000.4	1733.6	1701.7	31.8	1733.6
C5-H		942.8	1675.9	1576.0	99.9	1675.9
C6-H		963.1	1696.3	1525.5	170.8	1696.3
C7-H		991.1	1724.2	1668.2	52.4	1720.6

*Rearrangement after deprotonation

All in all, the O-H bond is more prone to deprotonation compared to the C-H sites and both EDTA and Irganox are more prone to express their antioxidant effect through the HAT than SET-PT or SPLET mechanisms.

3.4. Potential of α-Tocopherol and Trolox as an Effective Natural Antioxidant for Polyurethane Foams: A DFT and Experimental Study[4]

The main source of this type of antioxidant is plants, and they often have substantial phenolic contents that serve to be used as antioxidants, like tocotrienols, tocopherols, chlorophylls, polyphenols, ascorbates, and carotenoids. In this work, α-tocopherol and trolox were studied as compounds that have the highest biological activity. α-tocopherol (Vitamin E) is considered a food additive because the refining process of vegetable oils causes the depletion of this vitamin, and thus, its inclusion is required to keep them from oxidizing. The antioxidant activity of these additives has been determined using computational tools. The

[4] The following subchapter is based on: Dalal K. Thbayh, *et al.*, Molecules 29, no. 24 (2024) 6037. https://doi.org/10.3390/molecules29246037

Gaussian 09 program was used to do all the calculations [109]. The structures of the studied species, α-tocopherol, trolox, and their corresponding species (radicals, radical cations, and anions), were optimized by using two density functional methods, M05-2X [151] and M06-2X [150], along with the 6-311++G(2d,2p) as the basis set in the gas and water phases. The applicability of these methods has been verified before [94, 95, 152, 153, 155, 187, 188, 192]. The experimental value of bond dissociation enthalpy (BDE) for a specific O–H bond determined in the case of α-tocopherol was used to validate the calculations and to select the most suitable combination of method and basis set for the subsequent analysis and discussion [177, 193-195]. The antioxidant activity for the examined geometries was calculated using three alternative mechanisms as mentioned in the previous chapter. To test the applicability of α-Tocopherol to enhance the mechanical properties of polyurethane (PUR) was studied with the aim of using a single additive material to achieve multiple effects.

3.4.1. Computational Results

3.4.1.1. Optimized Geometries

In this work, α-tocopherol and trolox have been optimised. The former has three methyl groups (CH_3) bound to the aromatic ring, and optimizations have been calculated by using M05-2X (***Figure B 1***) and M06-2X (***Figure 30***) in the gas and water phase. There is one hydroxyl group (OH) in α-tocopherol, and its corresponding bond length is equal to 0.958 Å in the gas phase and 0.963 Å in the water phase, whereas the C-H bonds start between 1.084 - 1.097 Å The shortest is C2-H, which is located in the methyl group, whilst the longest bonds are C11-H and C16-H, which are located on the isoprenoid side-chain in the gas phase (***Figure 30*** *and* ***Table 24***) and for the solvent phase, there are little differences in the values for the same position bonds (***Figure 30*** *and* ***Table 25***). Both methods, M05-2X and M06-2X, provide similar results with minor changes in the values in all of the gas and water phases (***Figure B 1****,* ***Table B1****, and* ***Table B 2***).

DOI: 10.14750/ME.2025.027

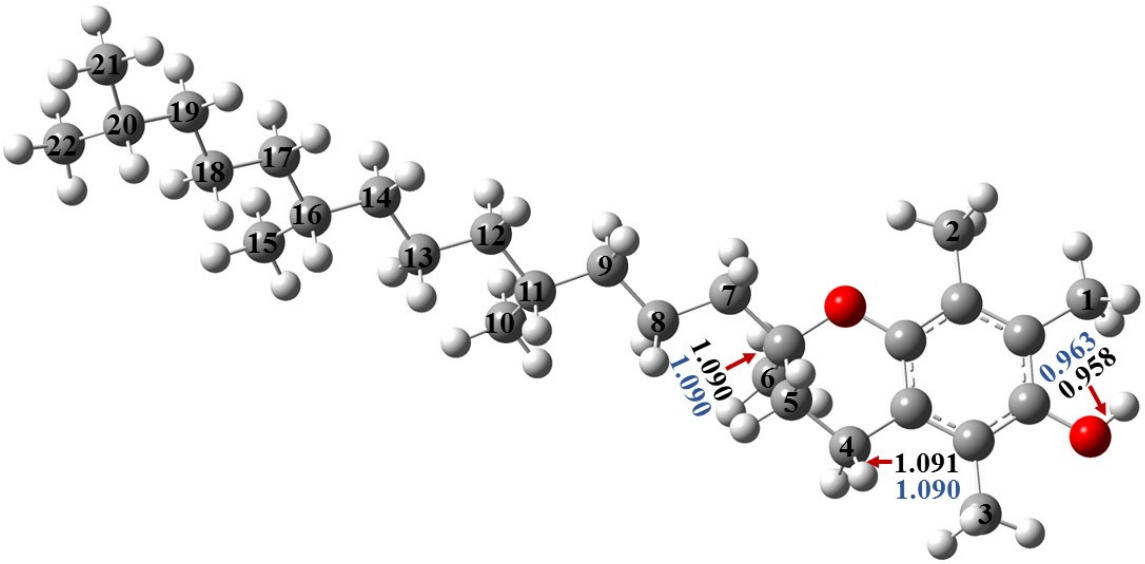

Figure 30. The investigated compound of a natural antioxidant additive (α-tocopherol). Geometry optimizations were performed in the gas and water phases at the M06-2X/6-311++G(2d,2p) level of theory, and the appropriate bond lengths (in Å) for the strongest and weakest X-H (X=O, C) bond are also displayed in the black (gas) and blue (water) phases.

Trolox is a smaller tocopherol derivative. As for trolox, the structure has two hydroxyl groups (OH), with the value of bond length equal to 0.959 Å (O1-H) and 0.966 Å (O2-H) in the gas phase while equal to 0.963 Å (O1-H) and 0.970 Å (O2-H) in the water phase, whereas the C-H bonds cover a range start from 1.084 (C1-H) to 1.095 Å (C4-H) as determined at the M06-2X/6-311++G(2d,2p) level of theory (***Figure 23 and Table 26***) in the gas phase and the bond lengths for C-H cover value from 1.085 (C1-H) to 1.095 Å (C4-H) in the water phase (***Figure 31 and Table 27)***. The shortest C-H bond is C1-H, and it's located on the methyl group, while the longest one is located on the heterocyclic ring. The behavior is similar for the M05-2X/6-311++G(2d,2p), with only a few differences in the values experienced (***Figure B2 , Table B 3*****, and** ***Table B4).***

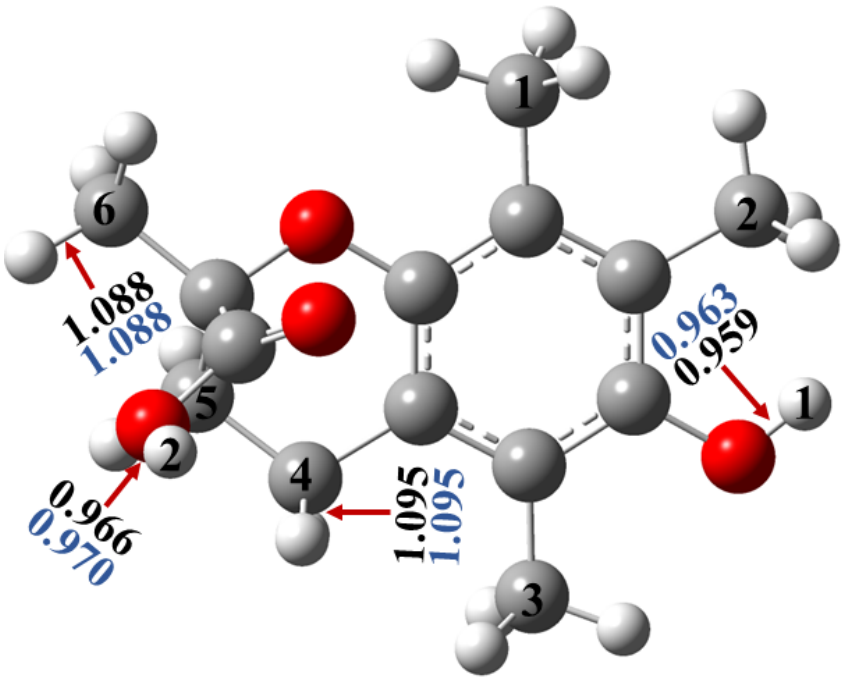

Figure 31. The investigated natural antioxidant additive of the studied tocopherol derivative trolox. The geometry optimizations were performed in the gas and water phase at the M06-2X/6-311++G(2d,2p) level of theory, and the appropriate bond lengths (in Å) for the strongest and weakest X-H (X=O, C) bond are also displayed in the black (gas) and blue (water) phases.

3.4.1.2. Antioxidant capability and scavenging mechanisms

The antioxidant efficacy of α-tocopherol and trolox has been evaluated, and three mechanisms, including hydrogen atom transfer (HAT), sequential proton loss electron transfer (SPLET), and single electron transfer proton transfer (SET-PT), in the gas and water phase have been studied. The most important parameters from these mechanisms have been calculated to compare the antioxidant ability of the studied molecules.

As for HAT, hydrogen atoms can be transferred from numerous hydrogen donor positions of the antioxidant additive, like the methyl group (CH_3), hydroxyl group (OH), benzene ring, and others, to the free radicals. Within the HAT mechanism, antioxidant compounds participate in a one-step process by donating a hydrogen atom, resulting in the formation of a radical. Simultaneously, the original free radical is neutralized. Thus, BDE values can be used to measure the antioxidant's ability to donate its hydrogen atom. Although there are numerous descriptors that can demonstrate antioxidant activity, BDE is currently the most trustworthy and is often used when taking the HAT mechanism into account [196]. The lower the value of BDE, that means the better the antioxidant properties of a compound [58, 94, 95, 158, 160, 192].

The values of BDE for all unique X-H bonds of α-tocopherol were computed in the gas and water phases by using two methods, including M05-2X and M06-2X (***Table 24***, ***Table 25***, ***Table B1***, ***Table B 2***,

Figure 32, *and* ***Figure B3***). As for M062X in two phases, the α-Tocopherol has one hydroxyl group, and the corresponding BDE value is equal to 327.0 and 328.6 kJ/mol in the gas and water phases, respectively, which is in excellent agreement with the previous experimental values [177, 193-195] and the theoretical study [197, 198]. while the values of the C-H bonds in the molecule start from 355.0 to 421.3 kJ/mol in the gas phase and from 364.6 to 426.3 kJ/mol in the water phase. In the case of the weakest C-H bond, it was C4-H and located on the heterocyclic ring, while the strongest one was C6-H and located on the methyl group (**Figure 23** *and* ***Figure B3***). The O-H bond has the highest antioxidant potential, but in some cases, C-H bonds can serve as hydrogen donor sites and contribute to the antioxidant effect of the compound. The behavior is similar for the M05-2X/6-311++G(2d,2p), with only a few shifting in the values experienced (***Figure S3, Table S1, and Table S2***).

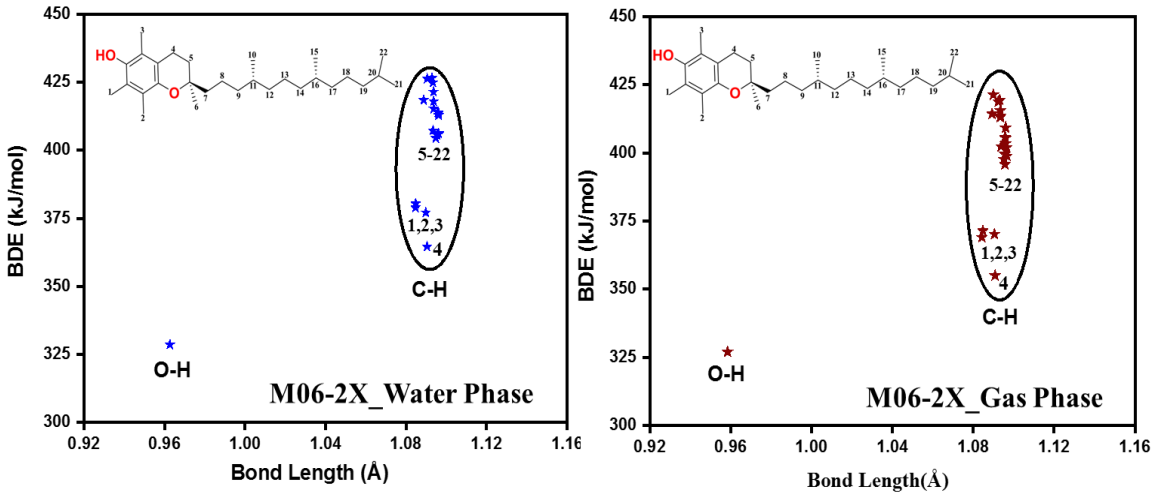

Figure 32. Bond dissociation enthalpy vs bond length plot of α-tocopherol. The calculations were performed in the gas and water phases using the M06-2X/6-311++G(2d,2p) level of theory.

The values of BDE for all possible sites of trolox were also studied (***Table 26***, ***Table 27***, ***Table B 3***, ***Table B4***, ***Figure 33***, *and* ***Figure B4***). Results indicated that in the case of trolox, the two hydroxyl groups O1-H and O2-H are quite far from each other in terms of their antioxidant activity because their BDE is equal to 328.2 and 360.2 kJ/mol in the gas phase, while their values are equal to 332.8 and 363.2 kJ/mol in the water phase. In this case of C-

H bonds, bond dissociation enthalpies in the M06-2X in gas phase cover a range between 359.4 and 427.5 kJ/mol (***Table 26***), while they cover a range from 366.6 and 435.2 kJ/mol (***Table 27***). The smallest one belongs to C4-H, which is located on the heterocyclic ring, and the strongest one is C6-H, which is located on a methyl group (***Figure 33***). It has to be noted that the same behaviour was experienced in both studied species, which is expected due to the structural similarities. There is no difference in the values according to M05-2X/6-311++G(2d,2p) of BDE values (***Figure B4***, ***Table B 3***,*and* ***Table B4***).

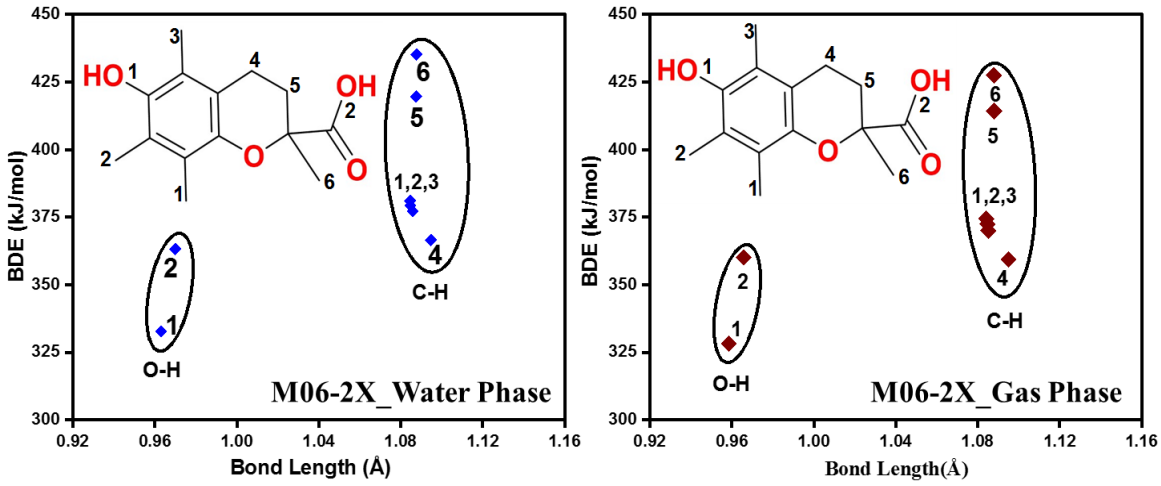

Figure 33. Bond dissociation enthalpy vs bond length plot of trolox. The calculations were performed in the gas and water phases using the M06-2X/6-311++G(2d,2p) level of theory.

The lowest value of BDE belongs to the OH group of the phenol ring of trolox, which is in good agreement with the previous studies [58, 199].

The experimental values of BDEs for the regularly used polymers were collected from the previous literature and compared with the smallest BDEs of trolox and α-tocopherol [94, 95]. We have noticed that the BDE values for polymers are in a range of 393.7 and 406.2 kJ/mol [179], and in both studied species, there is at least one X-H bond that has a smaller BDE than these conventional polymers. Thus, both trolox and α-tocopherol can be applied as antioxidant additives to protect polymers from free radicals.

Single electron transfer proton transfer (SET-PT) has two steps to neutralize radicals. First step, an electron from the antioxidant molecule is transferred, which is followed by a proton transfer. The ionization potential (IP) and proton dissociation enthalpy (PDE) are used in this process to determine the antioxidant potential of the species. The antioxidant capacity of the compounds increases with decreasing IPs and PDE values [58, 94, 95, 160, 161, 194].

IPs and PDE values for α-tocopherol have been computed (***Table 24, Table 25, Table B1, and Table B 2***) in two methods and two phases. As for M06-2X, the results indicate that the IP of tocopherol in the gas phase was higher than the value in the water phase, which is 662.7 kJ/mol in the gas phase and equal to 423.6 kJ/mol in th4e water phase (***Table 24****, and* ***Table 25***). In the gas phase and water phase, the PDE of the O-H bond is equal to 972.9 and 63.7 kJ/mol, respectively. These values are similar to those found in the previous studies [194, 198]. The PDE values of C-H bonds cover a range starting from 1006.1 (C4-H) to 1069.7 kJ/mol (C6-H) in the gas phase while starting from 100.6 to 162.4 kJ/mol in the water phase at M06-2X (***Table 24****,and* ***Table 25***). In the case of the second method (M05-2X), the behavior was the same with a slight change in the values (***Table B1, and Table B 2)***. From the results, we can see that the O-H group is a more potent proton donor in the second step of the SET-PT mechanism of tocopherol than the C-H bonds, which is expected. Consequently, O-H has the highest antioxidant activity than C-H bonds depending on their IP+PDE values. The results corresponding to O-H and C-H bonds for α-tocopherol in both methods agree with the HAT results.

In the case of trolox, the corresponding IP and PDE values were determined (***Table 26, Table 27, Table B 3, and Table B4***) in all of M05-2X and M06-2X. In the M06-2X, it was found that the IP is slightly higher (677.2 kJ/mol) in the gas phase and 436.2 kJ/mol in the water phase compared to α-tocopherol (***Table 26****, and* ***Table 27***). The PDE values of O-H bonds are equal to 961.9 and 991.4 kJ/mol in the gas phase, while they are equal to 56.2 and 86.6 kJ/mol in the water phase, where the lowest bond is the O1-H bond, and the strongest one is O2-H (***Table 24,*** **Table 25***, and* ***Figure 31***). Whereas for C-H bonds, the PDEs are in a range from 993.3 to 1058.5 kJ/mol in the gas phase, and they are in a range starting from 90.0 to 158.6 kJ/mol in the water phase in the M06-2X, where the weakest one refers to the C4-H bond located on the heterocyclic ring, while the strongest one is C6-H, which is located on the methyl group (***Table 24, Table 25*** *, and* **Figure 31**), and it is in good agreement with the previous studies [58]. Moreover, the IP+ PDE results show that O-H activity is higher than C-H activity in all of M06-2X and M05-2X (***Table B 3, and Table B4***). The IP results for α-tocopherol and trolox indicate that the former donates an electron more easily than the latter. All in all, by comparing the lowest values of IP+PDE of trolox and α-tocopherol, the latter has a bit higher antioxidant activity than the former, which is in good agreement with the HAT mechanism.

Sequential proton loss electron transfer (SPLET) is the third antioxidant mechanism to calculate the antioxidant potential of various species. This process is another two-step mechanism, which includes a proton transfer followed by an electron transfer from the antioxidant to the radicals. There are two important parameters that determine the antioxidant ability in this case: proton affinity (PA) and electron transfer enthalpy (ETE). The smaller the PA and ETE, the better the antioxidant is the studied molecule. The calculated values of PA and ETE for all possible sites X-H (X=O or C) bonds of α-tocopherol were collected and compared in two phases by using two methods (***Table 24***, ***Table 25***, ***Table B1***, *and* ***Table B 2***). The O-H bond has the smallest PA+ETE value within the molecule, 1635.6 and 486.5 kJ/mol in the gas phase and water phase, respectively, and it is in good agreement with the previous article [194, 198]. The values of PA +ETE of C-H bonds cover a range between 1668.8 and 1732.7 kJ/mol in the gas phase while in the water phase cover a range between 521.6 to 586.1 (***Table 24***, *and* ***Table 25)***. Where, the weakest C-H bond was located on the heterocyclic ring, while the strongest one was located on the methyl group. As for trolox, PA and ETE values of O-H and C-H bonds have also been computed (***Table 26***, ***Table 27***, ***Table B 3***, *and* ***Table B4***).

There is a special case with trolox, α-tocopherol, and the corresponding anion in the SPL step of the SPLET mechanism in the case of the C6-H (Trolox) and C5-H (α-tocopherol) sites in the gas phase (***Table 24***, *and* ***Table 25)***. Intramolecular rearrangement occurs after the proton transfer (***Figure 34)***, and thus, the SPLET was not comparable with other cases. The proton loss from the C5-H of α-tocopherol and C6-H of Trolox initiated a successive C-O bond break, similar to the situation experienced before [21].

DOI: 10.14750/ME.2025.027

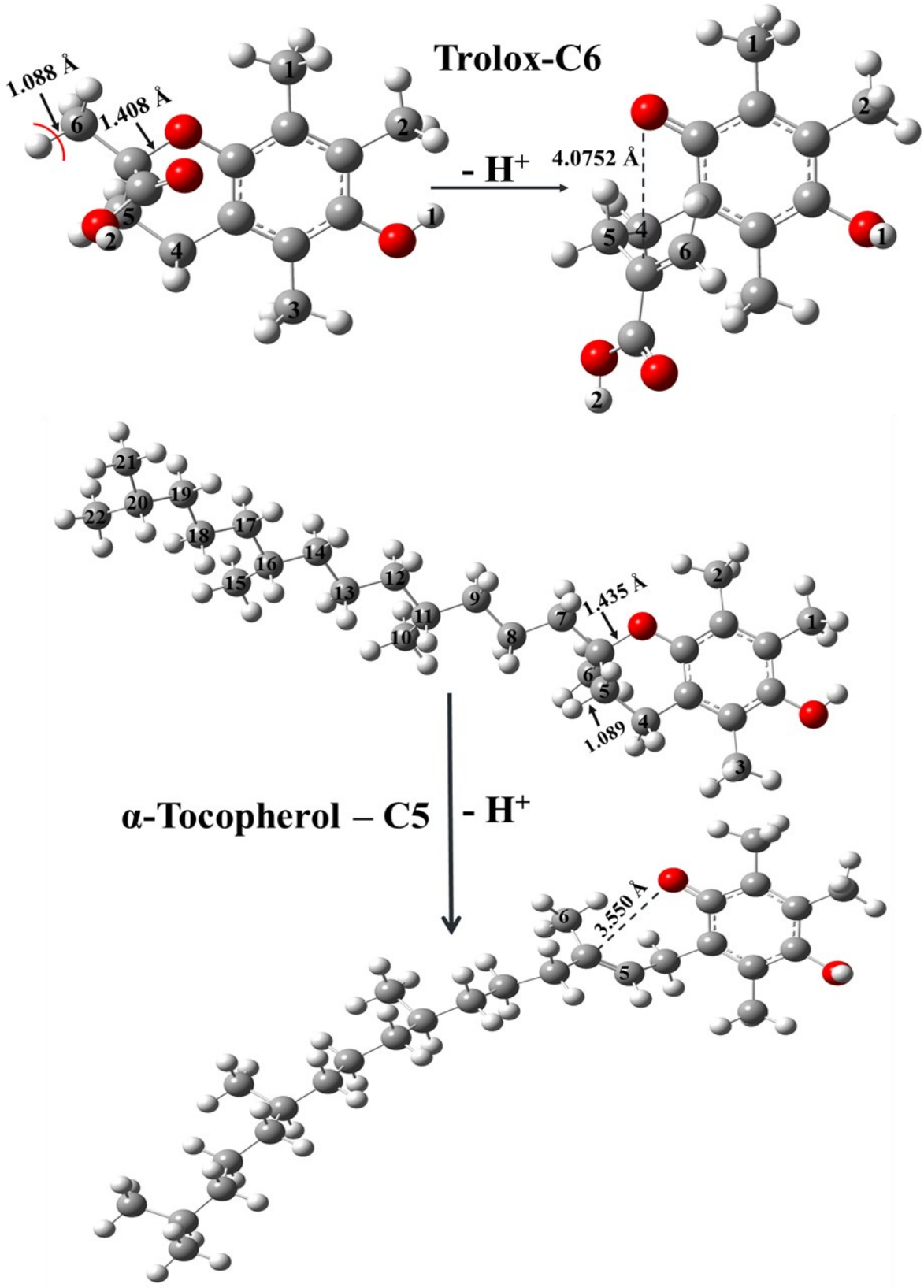

Figure 34. Optimized structures of Trolox, α-tocopherol, and the corresponding an anion in the SPL step of the SPLET mechanism in case of the C5-H of α-tocopherol and C6-H of Trolox site. The species have been computed at the M06-2X/6-311++G(2d,2p) level of theory in the gas phase and the corresponding bond lengths (in Å) are also shown.

DOI: 10.14750/ME.2025.027

From the results, we can see that the antioxidant capability of O-H is bigger than that of C-H bonds for all of α-tocopherol and trolox, but at the same time, there are some C-H bonds, such as C4-H, which may contribute to the antioxidant capability of the species. These results are in good agreement across all mechanisms. If the antioxidant potential of α-tocopherol and trolox is compared, they approximately have the same values, but still, α-tocopherol has higher antioxidant activity.

Table 24. Bond lengths (B.L) (in Å), bond dissociation enthalpy (BDE), ionization potential (IP), proton dissociation enthalpy (PDE), proton affinity (PA) and electron transfer enthalpy (ETE) values in kJ/mol of α-tocopherol computed using in the gas phase the M06-2X/6-311++G(2d,2p) level of theory.

Compound	B.L	BDE	IP	PDE	IP+PDE	PA	ETE	PA+ETE
α-Tocopherol			662.7					
O-H	0.958	327.0		972.9	1635.6	1461.4	174.2	1635.6
C1-H	1.085	371.4		1020.6	1683.3	1564.5	118.0	1682.5
C2-H	1.084	369.1		1019.8	1682.5	1583.4	99.1	1682.5
C3-H	1.090	370.2		1018.6	1681.3	1585.5	95.8	1681.3
C4-H	1.091	355.0		1006.1	1668.8	1569.1	99.6	1668.8
C5-H*	1.089	414.3						
C6-H	1.090	421.3		1069.7	1732.4	1674.3	58.1	1732.4
C7-H	1.093	413.6		1059.3	1722.0	1675.2	49.5	1724.7
C8-H	1.094	402.4		1049.9	1712.6	1668.0	46.3	1714.3
C9-H	1.096	405.6		1054.5	1717.2	1685.7	31.5	1717.2
C10-H	1.093	413.2		1062.6	1725.3	1686.8	38.4	1725.3
C11-H	1.097	398.9		1047.3	1710.0	1673.0	36.5	1709.5
C12-H	1.096	409.2		1057.6	1720.4	1686.5	28.6	1715.1
C13-H	1.096	395.8		1046.2	1709.0	1691.7	15.2	1706.9
C14-H	1.096	405.5		1053.3	1716.0	1700.8	20.8	1721.7
C15-H	1.093	415.6		1064.0	1726.7	1694.0	31.5	1725.5
C16-H	1.097	402.0		1050.4	1713.1	1683.8	29.4	1713.2
C17-H	1.096	403.4		1051.8	1714.5	1693.7	20.2	1713.8
C18-H	1.096	399.6		1047.9	1710.6	1696.7	13.8	1710.5
C19-H	1.096	409.3		1053.6	1716.3	1700.3	15.9	1716.2
C20-H	1.095	397.7		1046.1	1708.8	1697.7	11.2	1708.9
C21-H	1.092	418.8		1067.1	1729.8	1713.9	15.9	1729.9
C22-H	1.093	419.4		1068.3	1731.0	1707.0	25.6	1732.7

* Rearrangement after deprotonation

Table 25. Bond lengths (B.L) (in Å), bond dissociation enthalpy (BDE), ionization potential (IP), proton dissociation enthalpy (PDE), proton affinity (PA) and electron transfer enthalpy (ETE) values in kJ/mol of α-tocopherol computed using in the solvent phase (water) the M06-2X/6-311++G(2d,2p) level of theory.

Compound	B.L	BDE	IP	PDE	IP+PDE	PA	ETE	PA+ETE
α-Tocopherol			423.6					
O-H	0.963	328.6		63.7	487.3	174.1	312.5	486.5
C1-H	1.085	380.4		110.6	534.2	310.8	229.0	539.8
C2-H	1.085	378.9		114.6	538.2	319.7	218.5	538.2
C3-H	1.090	377.1		113.5	537.1	319.8	216.8	536.7
C4-H	1.090	364.6		100.6	524.2	323.8	197.8	521.6
C5-H	1.089	418.5		149.5	573.1	383.6	191.7	575.3
C6-H	1.090	426.3		162.2	585.9	380.7	205.1	585.9
C7-H	1.094	415.3		151.0	574.6	397.3	177.6	574.9
C8-H	1.093	407.3		140.6	564.3	406.0	160.6	566.6
C9-H	1.096	413.9		149.4	573.1	405.9	167.5	573.4
C10-H	1.094	421.4		157.4	581.0	390.6	187.9	578.5
C11-H	1.096	406.3		142.2	565.8	411.7	148.4	560.1
C12-H	1.096	412.9		148.7	572.3	407.3	165.0	572.3
C13-H	1.095	405.5		141.4	565.0	409.7	155.3	565.0
C14-H	1.096	413.1		149.0	572.6	407.7	164.9	572.6
C15-H	1.094	418.0		156.7	580.3	393.8	183.8	577.5
C16-H	1.096	406.1		142.0	565.7	412.3	153.2	565.5
C17-H	1.096	413.0		148.8	572.4	404.5	168.0	572.5
C18-H	1.096	406.0		142.1	565.7	409.9	155.5	565.4
C19-H	1.096	413.7		149.5	573.2	409.0	164.3	573.2
C20-H	1.095	404.5		140.3	564.0	410.2	153.8	564.0
C21-H	1.093	426.5		162.4	586.1	397.3	188.8	586.1
C22-H	1.093	424.9		160.8	584.4	394.8	189.4	584.2

Table 26. Bond lengths (B.L) (in Å), bond dissociation enthalpy (BDE), ionization potential (IP), proton dissociation enthalpy (PDE), proton affinity (PA) and electron transfer enthalpy (ETE) values in kJ/mol of trolox computed using in the gas phase the M06-2X/6-311++G(2d,2p) level of theory.

Compound	B.L	BDE	IP	PDE	IP+PDE	PA	ETE	PA+ETE
Trolox			677.2					
O1-H	0.959	328.2		961.9	1639.1	1460.5	178.8	1639.3
O2-H	0.966	360.2		991.4	1668.6	1406.0	262.4	1668.4
C1-H	1.084	374.5		1007.4	1684.6	1588.0	97.6	1685.6
C2-H	1.085	372.5		1006.5	1683.7	1564.1	119.5	1683.6
C3-H	1.085	370.1		1003.9	1681.2	1584.6	96.5	1681.2
C4-H	1.095	359.4		993.3	1670.5	1566.7	103.8	1670.5
C5-H	1.088	414.3		1048.2	1725.4	1625.2	100.2	1725.4
*C6-H	1.088	427.5						

* Rearrangement after deprotonation

Table 27. Bond lengths (B.L) (in Å), bond dissociation enthalpy (BDE), ionization potential (IP), proton dissociation enthalpy (PDE), proton affinity (PA) and electron transfer enthalpy (ETE) values in kJ/mol of trolox computed using in the solvent phase (water) the M06-2X/6-311++G(2d,2p) level of theory.

Compound	B.L	BDE	IP	PDE	IP+PDE	PA	ETE	PA+ETE
Trolox			436.2					
O1-H	0.963	332.8		56.2	492.3	171.8	320.6	492.3
O2-H	0.970	363.2		86.6	522.8	102.1	420.6	522.8
C1-H	1.085	379.4		103.6	539.8	315.8	222.9	538.8
C2-H	1.085	381.1		104.4	540.5	309.9	230.7	540.6
C3-H	1.086	377.2		100.6	536.8	315.8	221.0	536.8
C4-H	1.095	366.6		90.0	526.2	318.0	208.1	526.2
C5-H	1.088	419.7		143.7	579.8	363.8	215.4	579.2
C6-H	1.088	435.2		158.6	594.8	346.1	248.6	594.7

3.4.2. Experimental Results (α-Tocopherol as an Effective Natural Antioxidant for Polyurethane Foams)

3.4.2.1. Mechanical Tests

A compression force deflection test was carried out according to ASTM D3574 Test C on the different ratios of antioxidant additives (0.0, 0.25, 0.50, 0.75, and 1.0) wt% FPUF/ α-tocopherol samples for each NCO index (1.0 and 1.1). The force was measured at 50% of the original sample height compression after 1 min.

Adding antioxidant additives to the FPUF structure can influence its mechanical properties like the compression force (F). Therefore, this study incorporated α-tocopherol, a natural antioxidant additive, into the FPUF foam structure. The results show that increasing the concentration of α-tocopherol in the foams leads to a decrease in compression force, meaning the foam becomes softer or less resistant to compression. This effect is generally due to the interaction of α-tocopherol with the polymer matrix and the flexibility it introduces. An antioxidant additive like α-tocopherol which has a relatively low molecular weight compound, can act as a plasticizer in the polymer matrix [200]. As a plasticizer, it increases the flexibility of the polymer chains, leading to greater mobility within the matrix. This increased molecular mobility reduces the resistance of foam to compressive forces, making it softer and decreasing its compression force.

As the hardness of the foams with NCO-index 1.1 was higher than 0.1 given that the hard segments were determined by the amount of isocyanate in the foam, the compressive force

(F) also gradually increased from 7.84 N for an NCO index of 1.0 to 10.10 N in the case of the samples with a 1.1 NCO-index (

Table 28). The compressive force (F) of an NCO index of 1.0 with different amounts of antioxidant ranged from 7.84 N to 5.87 N for 0.0 and 1.0% wt, respectively. As for NCO index of 1.1, the compressive force (F) value was 10.10 N (0.0 %wt) of α-tocopherol and 9.27 N (1.0 % wt). That means, the foams with high concentration of antioxidant were softer than the reference.

There are clear differences in the hardness between them, with the F decreasing as the ratio of antioxidants in the foams increases; therefore, softer foams had a higher tocopherol ratio. This means that, if the lower compressive force (F) is required for some applications that need more softer foams, a sample with tocopherol is recommended because it was softer than the reference (foams without tocopherol) and also a sample. with the higher ratios of tocopherol is recommended. The change in foam heights was very small, <1% after the compressive force (F). The compression force was recorded for each NCO-index (***Figure 35***).

Table 28. Compression force deflection test results for Flexible Polyurethane Foam and α-tocopherol as additive (FPUF/ α-tocopherol), h is the sample height after the measurement the F50% (N).

NCO-index-1.0		
α-tocopherol (% wt)	**F50% (N)**	**h (mm)**
0.00	7.84	34.33
0.25	9.37	34.14
0.5	6.86	34.66
0.75	7.06	35.69
1.00	5.87	34.67
NCO- index-1.1		
0.00	10.10	34.55
0.25	11.45	35.70
0.5	11.05	36.21
0.75	10.86	35.21
1.00	9.27	36.63

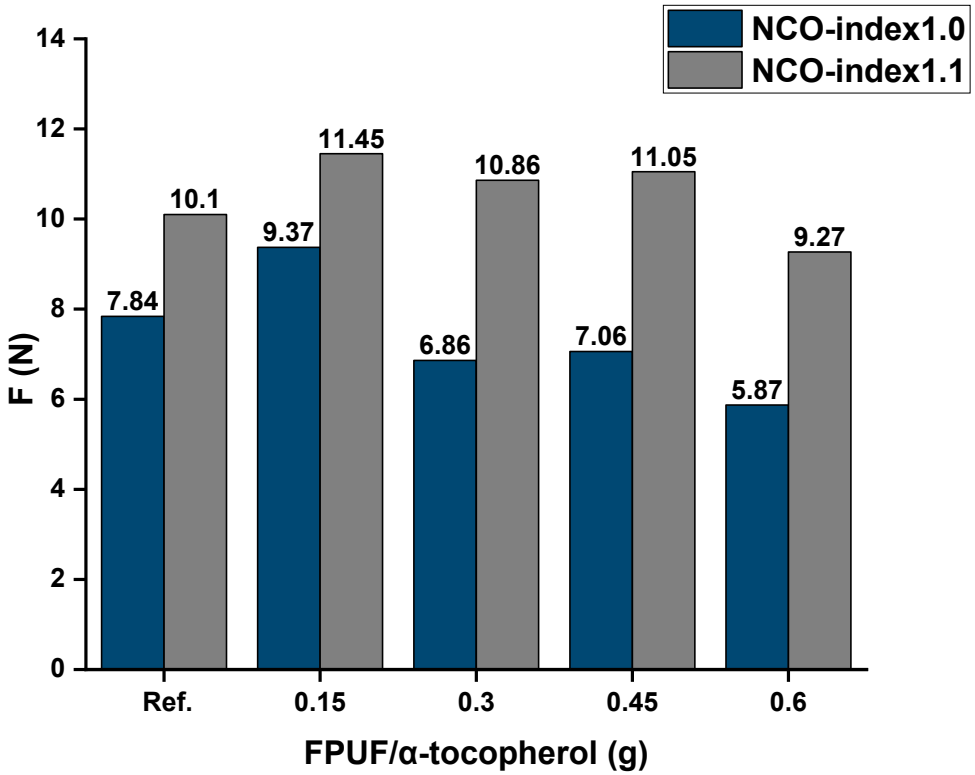

Figure 35. Compression force (F) deflection of composite samples with different ratios (0.0 (Ref), 0.25, 0.50, 0.75, 1.0) FPUF/ α-tocopherol, Ref: foam without α-tocopherol sample.

3.5. Experimental Results (Dehydrochlorination Tests)

3.5.1. Dehydrochlorination Tests for Synthetic Antioxidants (BHA and TBHQ) Additives with PVC

3.5.1.1. Results of the so-called Standard Method

In the current study, BHA, and TBHQ were selected due to their good properties as antioxidant additives [94], with the aim of using a single material to achieve multiple effects. The standard method's dehydrochlorination graphs (***Figure 37)***, which rely on measuring conductivity were prepared. The main aim of including these figures is to make a practical comparison according to the thermal stability of PVC before and after mixing it with the additives and test which antioxidant will do the best to protect the material from degradation. The effect of these molecules as stabilizer on PVC degradation were studied (***Table 29***). The stability of PVC formulations with various BHA, and TBHQ, concentrations (0.0, 0.1, 0.3, 0.5, 1.0, 3.0, 5.0, 10, 20) wt% were examined at high temperatures (***Table 29***). From the results, we can see that the thermal stability (TS) values for all compositions start to increase with increasing antioxidant concentration, but at some point, they start to decrease. For 0.0 to 1.0 wt%, the TS values for BHA range from 19.50 to 22.82 min. From 3.0% to 10.0%, the values start to drop. At 20.0%, we were unable to measure the material due to the strong

smell of the sample, which resembled burnt material. For TBHQ, the TS values range from 22.62 min at 0.1% to 33.03 min at 3.0%, and then the values begin to decrease at the upcoming ratios (5.0, 10.0, and 20.0 wt%) (***Error! Reference source not found.***). It is because the TBHQ began to separate from PVC during the measurement at higher concentrations, forming fibers (***Figure 36***).

Table 29. Thermal stability time for S-5070 PVC with different ratios of BHA, and TBHQ as stabilizer investigated at 180°C.

Thermal Stability time (min)		
Stabilizer Ratios %	**BHA**	**TBHQ**
0.0	19.41	19.41
0.1	20.42	22.62
0.3	20.82	23.62
0.5	21.62	27.82
1.0	22.82	28.42
3.0	21.82	33.03
5.0	21.42	16.61
10.0	21.22	10.21
20.0	*	9.81

*In this ratio, we cannot measure the stability of the system produced with the addition of BHA (very strong smell).

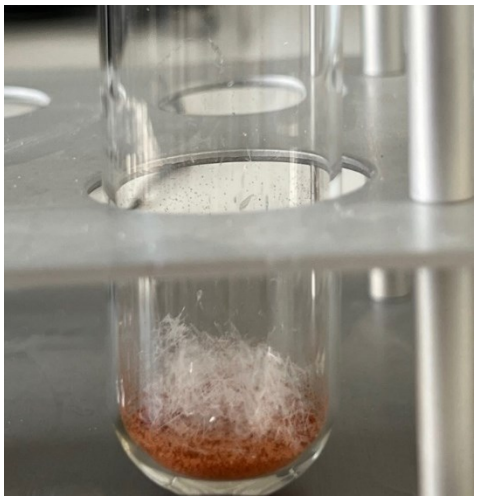

Figure 36. Sample of blend PVC and TBHQ at 5.0, 10.0, 20.0 wt% ratios

DOI: 10.14750/ME.2025.027

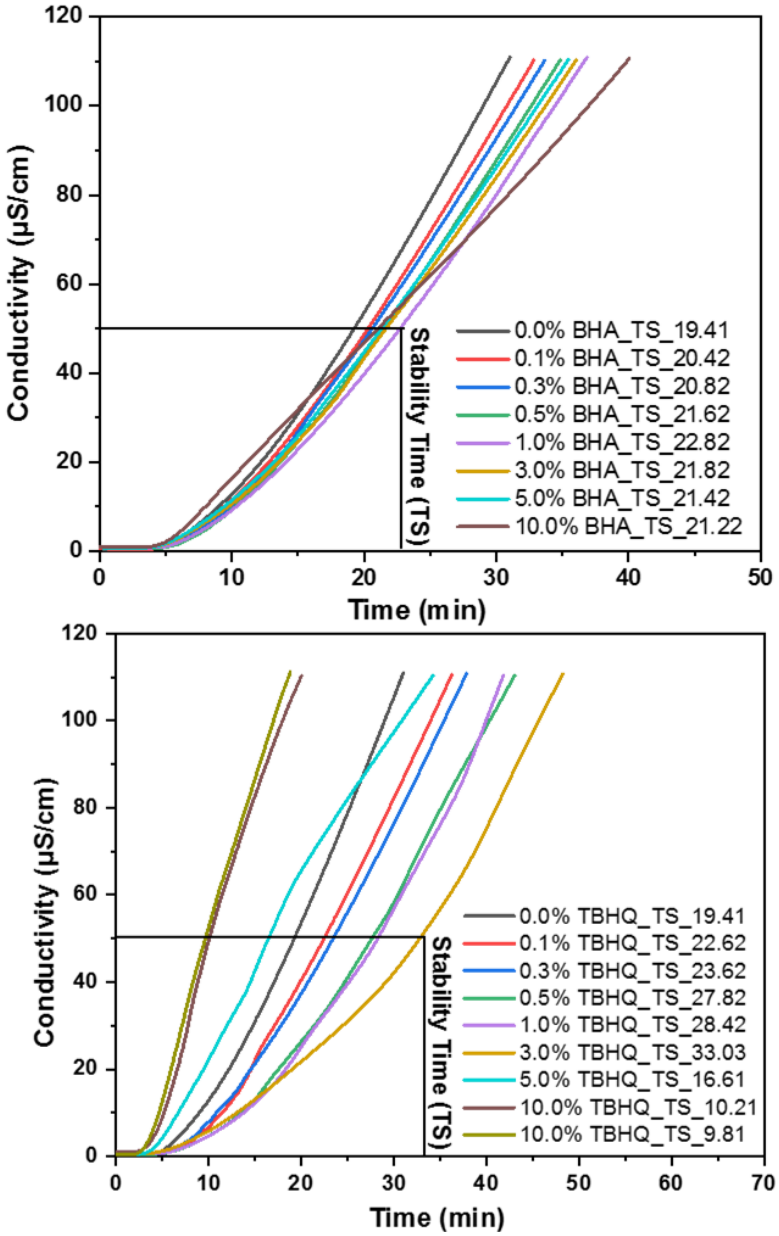

Figure 37. Conductivity of poly (vinyl chloride) contains different ratios (0.0, 0.1, 0.3, 1.0, 3.0, 5.0, 10.0, 20.0 wt.%) of antioxidant additives including BHA, and TBHQ, measured by using the standard method at 180°C for conductivity and thermal stability by using the 895 Professional PVC Thermomat.

3.5.1.2. Results of the Novel Evaluation Method

At high temperatures, the stability of the poly (vinyl chloride) structure diminishes, resulting in a significant release of hydrogen chloride (HCl). As a result, the resistance to polyvinyl chloride begins to decline. (***Figure C1, Figure C2, and Table 30***) represent a dehydrochlorination test (DHC) for PVC at 180 °C with different ratios of BHA, and TBHQ, respectively.

Table 30. Dehydrochlorination (DHC) time for poly (vinyl chloride) with different ratios of BHA, and TBHQ at 180°C.

DHC time (s)		
Stabilizer Ratios %	**BHA**	**TBHQ**
0.0	1861.9	1861.9
0.1	1970.0	2174.2
0.3	2018.0	2270.3
0.5	2090.1	2582.7
1.0	2210.2	2510.5
3.0	2162.2	2894.9
5.0	2126.2	2054.1
10.0	2402.4	1201.2
20.0	*	1129.1

The results show that the dehydrochlorination time for pure PVC and PVC blends with different concentrations of BHA, and TBHQ starts to increase with the concentration of antioxidants, but there is a difference in values for each of the additives. For BHA, the dehydrochlorination time (DHC) ranges from 1861.901 to 2210.256 s between 0.0 to 1.0 wt%, and it begins to decrease at the higher concentrations. As for TBHQ, the DHC time ranges from 1861.901 s at 0.0% to 2894.996 s at 3.0%, and then, the values begin to decrease at the upcoming higher ratios (5.0, 10.0, and 20.0 wt%) (***Table 30***). After adding BHA, and TBHQ, the dehydrochlorination behavior changes, and the structure of PVC becomes more stable with the additives, especially considering TBHQ. All in all, these additives can be applied to protect the polymers and prevent degradation.

3.5.2. Dehydrochlorination Tests for Natural Antioxidants (Curcumin, Ascorbic Acid, and Ascorbic Palmitate) Additives with PVC

3.5.2.1. Results of the so-called Standard Method

In the current study, curcumin, ascorbic acid, and ascorbic palmitate were selected due to their good properties as antioxidant additives [94, 95]. The standard method's dehydrochlorination graphs (***Figure 38***), which rely on measuring conductivity were prepared. The main aim of including these figures is to make a practical comparison according to the thermal stability of PVC before and after mixing it with the additives and test which antioxidant will do the best to protect the material from degradation. The effect

of these molecules as stabilizer on PVC degradation were studied (***Table 31***). The stability of PVC formulations with various curcumin, ascorbic acid, and ascorbic palmitate concentrations (0.0, 0.1, 0.3, 0.5, 1.0, 3.0, 5.0, 10, 20) wt% were examined at high temperatures (***Table 31***).

From the results, we can see that the thermal stability (TS) values for all compositions start to increase with increasing antioxidant concentration. The results indicate that the thermal stability values of Asc acid range from 19.5 to 42.4 min, where the lowest value was for pure PVC and the highest value was for the highest ratio of Asc, respectively. So, we can see that there are clear effects when we compare the thermal stability of pure PVC with the highest ratio of Asc. As for ascorbic palmitate, the TS values range from 19.5 to 36.43 min, where the lowest value was for pure PVC and the highest value was for 1.0 % ratio of Asc. Pal., respectively. After this ratio, the values begin to drop and reach to 25.42 at 20% wt. Regarding curcumin, the TS cover a range from 21.22 to 28.62 minutes, with the lowest value being 0.1% and the highest being 5.0%. After this ratio, the values begin to decrease. The final polymeric compositions, including a halogenated polymeric material (e.g., PVC resin) and a natural antioxidant, exhibit improved thermal stability and, thus, resistance to environmental degradation and aging. And then, these results are considered a new invention in the field of using natural antioxidant as stabilizer with PVC.

Table 31. Thermal stability time for S-5070 PVC with different ratios of Ascorbic acid, ascorbic Palmitate, and curcumin as stabilizer investigated at 180°C.

Thermal Stability time (min)			
Stabilizer Ratios %	**Asc**	**Asc Pal.**	**Curcumin**
0.0	19.41	19.41	19.41
0.1	22.2	30.03	21.22
0.3	28.3	33.63	22.42
0.5	28.5	34.63	22.22
1.0	33.8	36.43	24.82
3.0	36.2	30.23	26.42
5.0	38.9	29.03	28.62
10.0	40.0	25.62	19.62
20.0	42.4	25.42	16.81

DOI: 10.14750/ME.2025.027

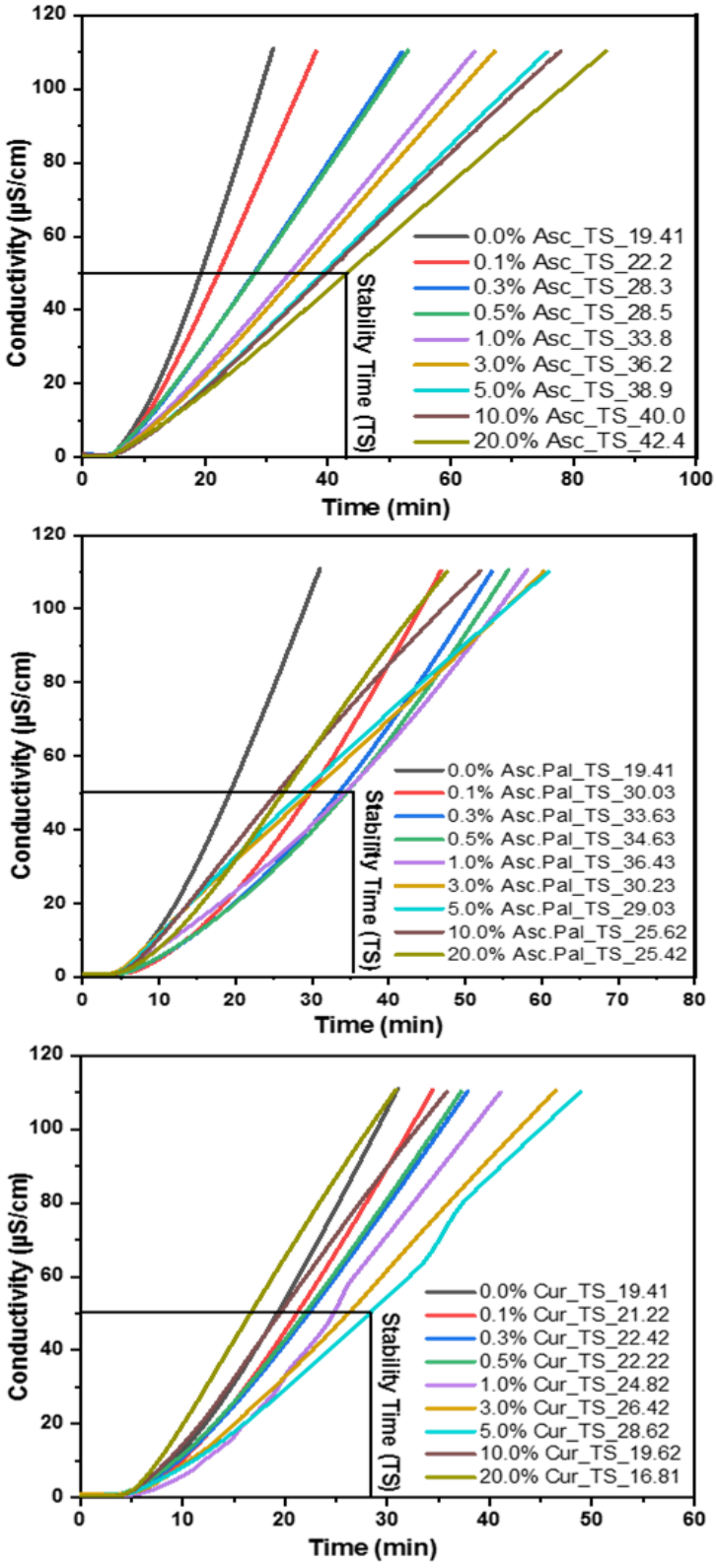

Figure 38. Conductivity of poly (vinyl chloride) contains different ratios (0.0, 0.1, 0.3, 1.0, 3.0, 5.0, 10.0, 20.0 wt.%) of antioxidant additives including Ascorbic acid (Asc), Ascorbyl palmitate (Asc.Pal.), and curcumin (Cur.) measured by using the standard method at 180°C for conductivity and thermal stability by using the 895 Professional PVC Thermomat.

3.5.2.2. Results of the Novel Evaluation Method

At high temperatures, the stability of the poly (vinyl chloride) structure diminishes, resulting in a significant release of hydrogen chloride (HCl). As a result, the resistance to polyvinyl chloride begins to decline. It is demonstrated by ***Figure C3, Figure C4, Figure C5, and Table 32*** which represent dehydrochlorination tests (DHC) for PVC at 180 °C with different ratios of Asc acid, Asc Pal., and curcumin, respectively.

Table 32. Dehydrochlorination (DHC) time for poly (vinyl chloride) with different ratios of Asc acid, Asc Pal., and curcumin at 180°C.

DHC time (s)			
Stabilizer Ratios %	**Asc acid**	**Asc Pal.**	**Curcumin**
0.0	1861.9	1861.9	1861.9
0.1	2282.3	2810.8	2066.1
0.3	3123.2	3207.3	2270.3
0.5	3183.3	3339.4	2234.3
1.0	3831.9	3483.6	2462.5
3.0	4024.1	3615.7	2786.8
5.0	4540.6	3651.7	2931.0
10.0	4672.8	3123.1	2150.2
20.0	5117.3	2858.9	1849.9

The results show that the dehydrochlorination time for pure PVC and PVC blends with different concentrations of Asc acid, Asc pal., and curcumin starts to increase with the concentration of antioxidants, but there is a difference in values for each of the additives. In terms of curcumin and Asc pal., the DHC of curcumin covers a range from 1861.901 s (0.0%) to 2931.035 s (5.0%) and in the case of Asc pal., it covers a range from 1861.901 s (0.0%) to 3651.738 s (5.0%). Above these ratios, the values begin to decrease. As for Asc acid, the DHC starts to increase with the concentration of antioxidants, and it covers a range from 1861.901 s (0.0%) to 5117.357 s (20.0%).

After adding Asc acid, Asc pal., and curcumin, the dehydrochlorination behavior changes, and the structure of PVC becomes more stable with the additives. All in all, these additives can be applied to protect the polymers and prevent degradation.

4. Summary

Antioxidants (AO) are compounds that are used to shield polymers and plastics from the thermal and photo-oxidative effects of aging. Oxidative stress effects living organisms along with food and other commodities' and thus, the importance of antioxidants exceeds the range of polymers. Oxidative stress is a process that involves the attack of free radicals, which are characterized by having an unpaired electron in their outer shell, making them unstable and highly reactive. Free radicals in the body have the capability to damage DNA, cells, and tissues through oxidative stress because they can react swiftly with non-radical species to produce new radicals and propagate free-radical chain reactions. Similar processes can occur with polymeric materials. These harmful reactions can be prevented by antioxidant species, which can donate an electron to free radicals and consequently stabilize and detoxify them. Antioxidant species are divided into two categories: synthetic and natural compounds. Significant environmental concerns have pushed manufacturers to investigate natural alternatives alongside regularly used synthetic materials.

Antioxidant additives and stabilizers are chemical substances frequently employed in many industries, such as food and polymer processing. Despite their distinct goals, we can identify some convergence in their functions, particularly in the realm of polymers and specific materials. One thing they all have in common is that antioxidants can act as stabilizers, particularly when preventing oxidation-induced degradation. In polymers and plastics antioxidants are frequently used to prevent or slow down polymer degradation due to oxidation processes. In this sense, antioxidants are a type of stabilizer that specifically addresses the oxidative degradation of materials. Thus, they aid in the preservation of the material's physical and mechanical qualities throughout time. Furthermore, some stabilizers may have antioxidant properties, and some antioxidants may offer stability against factors beyond oxidation. The specific requirements of the material and the conditions it will encounter determine the choice of additives. For instance, heat, oxidative conditions, and ultraviolet radiation may require stabilizers and antioxidants for a plastic material like PVC to ensure long-term stability.

This doctoral dissertation employs both theoretical and experimental tools to investigate various additives. In the first part, the antioxidant potential of synthetic (BHA, BHT, TBHQ, santowhite, EDTA, and Irganox) and natural (curcumin, L-ascorbic acid, α-tocopherol, and

trolox) antioxidant additives have been studied by using computational chemical tools to compare their ability to donate H atoms to free radicals and thus, prevent the degradation of polymers. The most probable radical scavenging sites have been explored based on DFT calculations carried out by using the B3LYP, M06, M05-2X, and M06-2X functionals in combination with different bases sets, including 6-31G(d), 6-311G(d), 6-311+G(d, p), and 6-311++G(2d, p), in the gas and solvent (water) phases. To compare the antioxidant potential of different groups (X-H, where X = O and C), three major free radical scavenging (RS) mechanisms (HAT, SETPT, and SPLET) have been considered, and the corresponding bond dissociation enthalpy (BDE), ionization potential (IP), proton dissociation enthalpy (PDE), proton affinity (PA), and electron transfer enthalpy (ETE) values have been calculated for each potential hydrogen donor site of the studied species. All in all, the results indicate that the O-H bonds are more potent radical scavenging sites for all species, but some C-H bonds also have significant antioxidant potential depending on their position in the structures. Furthermore, not surprisingly, the hydrogen atoms, which are located in methyl groups, are easier to remove than their benzylic counterparts. Based on the computed BDE values of the C-H and O-H bonds of the additives, BHT has the highest antioxidant potential among synthetic antioxidants, while Asc has the highest antioxidant potential among the natural additives.

By comparing the bond dissociation enthalpy values of commonly used polymers (e.g., PE, PP) from the literature with the lowest BDE values of the studied antioxidant additives, it was found that there is at least one X-H bond in the investigated species that has a lower bond dissociation enthalpy value than the polymeric materials. As a result, these additives can shield polymers and stop material deterioration due to oxidative stress. So, we decided to test these molecules in the laboratory with polymers including PVC and polyurethane to enhance their properties.

In the experimental part, we employed BHA, TBHQ, Asc acid, Asc. pal., and curcumin as heat stabilizers in PVC and α-tocopherol in polyurethane formulation due to their good characteristics, with the aim of using a single material to achieve multiple effects. The effect of the employed additives as stabilizers on PVC degradation was explored by measuring the change of dehydrochlorination. It was found that the structure of PVC becomes more stable with the additives. The impact of α-tocopherol on the polyurethane foam was also investigated. It is a fact that α-tocopherol can be considered as a protective, antioxidant

agent. But other effects have not been considered before. As the ratio of α -tocopherol in the foams increased, the mechanical properties of the foam sample changed, and the compressive force decreased. However, a change in foam hardness was observed in all cases. This was likely caused by the presence of antioxidant in the foam structure. All in all, the studied species can be applied to protect and prevent the degradation of polymeric materials and also fine-tune the (*e.g.* mechanical) properties of the polymeric product.

5. Limitations and Future Outlook

5.1. Limitations

Computer limitations: The Density Functional Theory (DFT) and other computer methods used to investigate the antioxidant power of the additives depend on the functionals and basis sets that are used. The study used several different functionals, including B3LYP, M06, M05-2X, and M06-2X. However, computational issues like the size of the method, basis set and solvent effects could make the results take long time.

In addition, the size of molecules also affects and is a consideration limitation during the work because if the size of the molecules is huge, in this case it will take a long time to finish the calculation and give us results. In some cases, some calculations were resubmitted many times to complete.

In the experimental part: The laboratory testing of additives on PVC and polyurethane demonstrated promising results; the long-term effects and environmental conditions under which the polymers are used could alter the behaviour of antioxidants. The study mostly looks at conditions in the lab, which might not fully reflect how polymers and additives interact in the real world, especially when it comes to UV exposure, mechanical stress, and respect to aging.

5.2. Future Outlook

In the future, research should explore a broader range of antioxidant additives, including newer natural antioxidants and bio-based alternatives. As the need for environmentally friendly solutions grows, it is important to investigate the potential of antioxidants that come from natural sources, like flavonoids, polyphenols, and essential oils. These might work just as well or better than synthetic antioxidants.

While the laboratory tests show promising results, future studies should focus on real-world applications and the long-term stability of the polymer-additive systems. For instance, the effectiveness of antioxidants in protecting against oxidative stress in polymers exposed to UV radiation, heat, moisture, and mechanical stress over extended periods of time should be investigated.

DOI: 10.14750/ME.2025.027

6. New scientific results

My Ph.D. dissertation has been focused on the computational and experimental study of natural and synthetic antioxidant polymer additives. The following main conclusions are drawn as new scientific results:

1st Thesis

The antioxidant potential of synthetic additives, including BHA, BHT, TBHQ, Santowhite, and Irganox, as well as natural antioxidants such as curcumin, ascorbic acid, α-tocopherol, and Trolox, has been systematically evaluated using both computational modeling and experimental studies. It was shown that natural antioxidants are just as good, or even better, at fighting free radicals and preventing the oxidative stress. Based on the bond strength values of the C-H and O-H bonds in the additives, BHT is the best synthetic antioxidant, and ascorbic acid is the best natural antioxidant. These findings suggest that natural antioxidants can serve as viable, environmentally friendly alternatives to synthetic stabilizers for polymer protection against oxidative stress-induced deterioration.

2nd Thesis

The effect of ascorbic acid as stabilizer on PVC degradation was studied (***Table 2T***). The stability of PVC formulations with various ascorbic acid concentrations (0.0, 0.1, 0.3, 0.5, 1.0, 3.0, 5.0, 10, 20 wt%) was examined (***Table 2T***). The results indicate that the thermal stability values of PVC/ascorbic acid increased with increasing antioxidant content compared to the pure PVC. The natural antioxidant has a clear effect on the stability of the system (***Figure 2T***). As a results, polymeric formulations (PVC and ascorbic acid) with improved thermal stability and resistance to environmental degradation and aging was achieved.

Table 2T. Thermal stability time (TS) for S-5070 PVC with different ratios of ascorbic acid as stabilizer investigated at 180°C.

Stabilizer Ratios %	**TS (min)** **Asc**
0.0	19.41
0.1	22.20
0.3	28.30
0.5	28.50
1.0	33.80

DOI: 10.14750/ME.2025.027

3.0	36.20
5.0	38.90
10.0	40.00
20.0	42.40

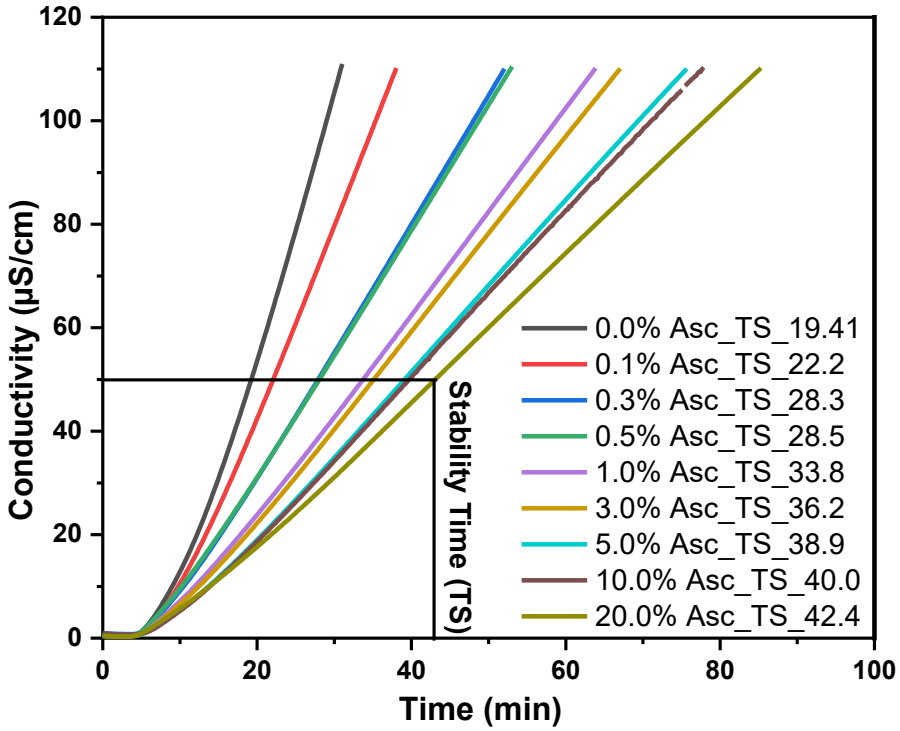

Figure 2T. The conductivity of S-5070 PVC type poly (vinyl chloride) samples containing different ratios (0.0, 0.1, 0.3, 1.0, 3.0, 5.0, 10.0, 20.0 wt.%) of ascorbic acid as stabilizer measured by using the standard method at 180°C for conductivity and thermal stability by using the 895 Professional PVC Thermomat.

3rd Thesis

The effect of ascorbyl palmitate (Asc. Pal.), a fat-soluble derivative of ascorbic acid, as stabilizer on PVC degradation was studied (***Table 3T***). The stability of PVC formulations with various Asc. Pal. concentrations (0.0, 0.1, 0.3, 0.5, 1.0, 3.0, 5.0, 10, and 20 wt%) was examined at high temperatures (***Table 3T***). The results indicate that the thermal stability values of Asc. Pal. range from 19.41 to 36.43 min, where the lowest value was for pure PVC and the highest value was for a 1.0 % ratio of Asc. Pal., respectively. Above 1%, the values start to decrease, reaching a value of 25.42 at 20% weight (***Figure 3T***). Thus, a clear comparison of the thermal stability of pure PVC with samples mixed with Asc. Pal reveals distinct effects, and the thermal stability has been enhanced by the addition of the antioxidant. This means that the formulation with the

DOI: 10.14750/ME.2025.027

antioxidant now exhibits improved thermal stability, thereby an enhanced resistance to environmental degradation and aging was achieved.

Table 3T. Thermal stability time (TS) for S-5070 PVC with different ratios of ascorbyl palmitate as stabilizer investigated at 180°C.

Stabilizer Ratios %	**TS (min)** **Asc Pal.**
0.0	19.41
0.1	30.03
0.3	33.63
0.5	34.63
1.0	36.43
3.0	30.23
5.0	29.03
10.0	25.62
20.0	25.42

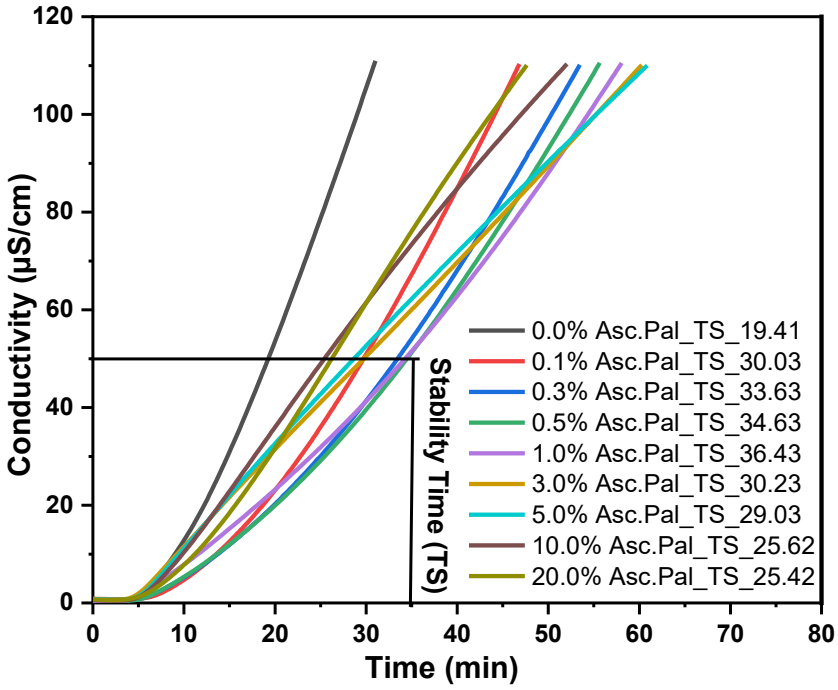

Figure 3T. The conductivity of S-5070 PVC poly (vinyl chloride) samples containing different ratios (0.0, 0.1, 0.3, 1.0, 3.0, 5.0, 10.0, 20.0 wt.%) of ascorbyl palmitate as stabilizer measured by using the standard method at 180°C for conductivity and thermal stability by using the 895 Professional PVC Thermomat.

7. Scientific publications

❖ **Publications in International Journals Related to the Subject of the Dissertation**

1. **Dalal K. Thbayh**, and Béla Fiser, "Computational study of synthetic and natural polymer additives—Antioxidant potential of BHA, TBHQ, BHT, and curcumin." Polymer Degradation and Stability 201 (**2022**): 109979, DOI: https://doi.org/10.1016/j.polymdegradstab.2022.109979. (Q1; IF=6.3)
   Number of Independent Citations: 39

2. **Dalal K. Thbayh**, Edina Reizer, Mousumi U. Kahaly, Béla Viskolcz, and Béla Fiser. "Antioxidant potential of santowhite as synthetic and ascorbic acid as natural polymer additives." Polymers 14, no. 17 (**2022**): 3518. DOI: https://doi.org/10.3390/polym14173518. (Q1; IF=5.0)
   Number of Independent Citations: 12

3. **Dalal K. Thbayh**, Marcin Palusiak, Béla Viskolcz, and Béla Fiser. "Comparative study of the antioxidant capability of EDTA and Irganox." Heliyon 9, no. 5 (**2023**). DOI: https://doi.org/10.1016/j.heliyon.2023.e16064. (Q1; IF=3.4)
   Number of Independent Citations: 8

4. **Dalal K. Thbayh,** Dóra Mentes, Zsanett R. Boros, Marcin Palusiak, László Farkas, Béla Viskolcz, and Béla Fiser "α-Tocopherol and Trolox as Effective Natural Additives for Polyurethane Foams: A DFT and Experimental Study" Molecules 29, no. 24 (**2024**) 6037. DOI: https://doi.org/10.3390/molecules29246037 (Q1; IF=4.2).
   Number of Independent Citations: 1

❖ **Publications in Local Journals Related to the Subject of the Dissertation**

1. **Dalal K. Thbayh,** Anita Rágyanszki, and Béla Fiser. "Antioxidant potential of butylated hydroxytoluene (BHT)–A theoretical study." Materials Science & Engineering 46, 1, **2021,** 63–69, doi:org/10.32974/mse.2021.007.
   Number of Independent Citations: 4

2. **Dalal K. Thbayh**, Edina Reizer, Mousumi U. Kahaly, Béla Viskolcz, and Béla Fiser, "Theoretical study of the antioxidant potential of santowhite as synthetic polymer additives", Symposium on Polyurethane Innovation - SPI 2022, Conference publications, **2022**, 203, 36-43.

3. **Dalal K. Thbayh**, Béla Fiser, "Antioxidant additives and their potential to enhance the properties of polymers", Doktorandusz Almanach, Faculty of Materials and Chemical Engineering, University of Miskolc, **2022**, 1, 83-91.

4. **Dalal K. Thbayh**, Béla Viskolcz, Béla Fiser, "A Theoretical Study of the Applicability of Natural Antioxidant Additives with Polymers" Symposium on Polyurethane Innovation - SPI 2023, Conference publications, **2023**, 1, 28-36.

5. **Dalal K. Thbayh**, Béla Fiser, "Insights into the Antioxidant Capability for the Synthetic Additives_ butylated hydroxyanisole (BHA)", Doktorandusz Almanach,

Faculty of Materials and Chemical Engineering, University of Miskolc, **2023**, 1, 70-75.

6. **Dalal K. Thbayh**, Kitti Bartha, Csaba Kónya, Peter Bagi, R. Zsanett Boros, Laszlo Farkas, and Béla Fiser," Exploring the potential of ethylenediaminetetraacetic acid as a stabilizer for polyvinyl chloride", Doktorandusz Almanach, Faculty of Materials and Chemical Engineering, University of Miskolc, **2024**, 1, 173-178.

7. **Dalal K. Thbayh**, Béla Viskolcz, Béla Fiser, "Theoretical and Experimental Study of Antioxidant Additives" Symposium on Polymer(s) Innovation (SPI) & Energy, Mitigation, Storage, Conference publications, **2024**, 1, 12-19.

❖ **Further Publications during my PhD studies**

1. Malik, Fatima H., and **Dalal K. Thbayh**. "Chitosan doping by Nicotine as the active layer in the Solar Cell." University of Aden Journal of Natural and Applied Sciences, vol. 25, no. 2 (2021) 331-339. DOI: https://doi.org/10.47372/uajnas.2021.n2.a10.

2. Hadeer Q. Waleed, **Dalal K. Thbayh**, Amal Zarrami, Julie Mallouhi, Pecsmány Dániel, Reizer Edina, Rachid Hadjadj, Fiser Béla, ″Hogyan tervezhetünk jobb polimereket szuperszámítógépek segítségével?″ HPC ECHO, Tudománytól Innovációig, **2021**, 10-12.

3. Hadeer Q. Waleed, **Dalal K. Thbayh**, Amal Zarrami, Julie Mallouhi, Pecsmány Dániel, Reizer Edina, Rachid Hadjadj, Fiser Béla, ″Hogyan tervezhetünk jobb polimereket szuperszámítógépek segítségével? ″ HPC ECHO, Tudománytól Innovációig, **2021**, 10-12.

4. Talib, Rawnaq A., **Dalal K. Thbayh**, and Kahtan A. Mohammed. "Study the Optical and Morphological Properties of Prepared PANI/TiO2 Nanocomposites." In Materials Science Forum, **2022**, vol. 1065, pp. 101-108. Trans Tech Publications Ltd, DOI: https://doi.org/10.4028/p-s6y8z3. (Q4; IF= 0.5)
   Number of Independent Citations: 7

5. Talib, R. A., K. A. Mohammed, and **D. K. Thbayh**. "Study the structural and electrical properties of prepared PANI/TiO2 nanocomposites for electronic devices." Journal of Ovonic, **(2022)**, vol.18, no. 3, pp. 389-394, DOI: https://doi.org/10.15251/JOR.2022.183.389. (Q4; IF= 1.165)
   Number of Independent Citations: 5

6. Zakaraia, Dimah, **Dalal K. Thbayh**, Béla Fiser, and Michael C. Owen. "Investigating Collagen as a Biomaterial by Molecular Dynamics Simulations." Hungarian Materials and Chemical Sciences and Engineering 47, no. 1 (**2023**): 118-127. DOI: https://doi.org/10.32974/mse.2022.012.
   Number of Independent Citations: 1

7. Rachid Hadjadj, Imre G. Csizmadia, Hadeer Q. Waleed, **Dalal K. Thbayh**, Béla Viskolcz, Béla Fiser, ″Monoethanolamine assisted CO2 hydrogenation to methanol – A computational study, ″Molecular Catalysis, (**2024**), Vol. 559, pp.114091, DOI: 10.1016/j.mcat.2024.114091. (Q2; IF= 4.6).

8. Muhsen, M. C., Mohammed, A. J., AL-Malki, Z. T., **D. K. Thbayh**, Investigation on the influence of waste-based fillers on the mechanical and thermal characteristics of rigid polyurethane foams. EUREKA: Physics and Engineering, **2024**, 4, 173–183. https://doi.org/10.21303/2461-4262.2024.003419. (Q3; IF= 1.17)

9. Saleh M Bufarwa, Reem M El-Sefait, **Dalal K Thbayh**, Mustapha Belaidi, Rehab K Al-Shemary, Rema M Abdusamea, Marei M El-Ajaily, Béla Fiser, Hanan A Bader, Abdulsalam A Saleh, Mohamad M Bufarwa, Antituberculosis, antimicrobial, antioxidant, cytotoxicity and anti-inflammatory activity of Schiff base derived from 2,3-diaminophenazine moiety and its metal(II) complexes: structural elucidation, computational aspects, and biological evaluation, Reviews in Inorganic Chemistry, (**2024**), https://doi.org/10.1515/revic-2024-0007. (Q2; IF= 4.1)
   Number of Independent Citations: 4

10. Kifayah K. Thbayh, Rafid M. AlBadr, Kareema M. Ziadan, **Dalal K. Thbayh**, Shaimma M. Mohi, Béla Fiser, Fabrication and Characterization of Novel Glass-Ionomer Cement Prepared from Oyster Shells. Scientific Reports, (**2024**) 14:24083 https://doi.org/10.1038/s41598-024-75040-w (D1; IF= 3.8).
11. Bufarwa, Saleh M., Mustapha Belaidi, Leila M. Abbass, and **Dalal K. Thbayh**. "Anticancer Activity, DFT, Molecular Docking, ADMET, and Molecular Dynamics Simulations Investigations of Schiff Base Derived From 2, 3-Diaminophenazine and Its Metal Complexes." *Applied Organometallic Chemistry* 39, no. 1 (**2025**): e7953. DOI: https://doi.org/10.1002/aoc.7953 (Q2; IF= 3.7).
    Number of Independent Citations: 1

❖ **Conferences (Oral and Poster Presentations)**

1. A Miskolci Egyetem Kémiai Intézetének (KI, MAK, ME) és a MAB Elméleti és Fizikai Kémiai Munkabizottságának közös rendezvénye
   Oral presentation/Online,Miskolc, Hungary, 2021.05.11.
   "***Computational studies of natural and synthetic antioxidant additives***"

2. Symposium on Polyurethane Innovation SPI 2021
   Oral presentation/Online, Miskolc, Hungary, 2021.08.24.
   "Antioxidant additives for Polyurethanes"

3. Hungarian Science Day New result in materials science
   Oral presentation/Miskolc, Hungary, 2021.11.08.
   "Computational study of the antioxidant potential of natural and synthetic additives for polymer application"

4. 25th Spring Wind Conference
   Poster presentation/Pécs, Hungary, 2022.05.08-06
   "***Computational study of synthetic and natural antioxidant additives***"

5. 10th Visegrad Symposium on Biomolecular Interactions
   Poster presentation/Nove Hrady, Czech Republic, 2022.06.22-19
   "Theoretical investigation of antioxidant potential of BHA, TBHQ, BHT, and curcumin"

6. Symposium on Polyurethane Innovation SPI 2022
   Oral presentation/Miskolc, Hungary, 2022.08.26
   "Computational Study of the Applicability of Ascorbic Acid as Antioxidant Polymer Additive"
7. Hungarian Science Day
   Oral presentation/Miskolc, Hungary, 2022.11.09.
   "Computational Study of the Natural and Synthetic Antioxidant Additives"

8. 10th Doctoral Symposium on chemistry
   Poster presentation/Lodz, Poland, 2023.05.19-18
   "Antioxidant activity of EDTA and Irganox as synthetic additives"

9. 11th Visegrad Symposium on Biomolecular Interactions
   Poster presentation/Szidonia Castle, Hungary, 2023.06. 23-20
   "Antioxidant activity of EDTA and Irganox as synthetic additives"

10. Symposium on Polyurethane Innovation SPI 2023
    Oral presentation/Miskolc, Hungary, 2023.08.24.
    "A theoretical Study of the Applicability of Natural Antioxidant Additives with Polymers"

11. Basics & Application of Computational Chemistry in Action (BACCA), Erasmus+ Blended Intensive Programme, virtual session
    Oral presentation/Online, 2024.04.04
    "Theoretical Investigation on the Applicability of Synthetic and Natural Antioxidant Additives with Polymers"

12. XXVII. Tavaszi Szél Konferencia 2024
Oral poster/ Budapest, Hungary, 2024.05.05-03
"The Applicability of Curcumin and Ascorbic Acid as Natural Antioxidant Additives"

13. 11th Doctoral Symposium on chemistry in Lodz
    Poster presentation/Lodz, Poland, 2024.05.17-16
"An examination of the applicability of natural antioxidant additives: A theoretical study"

14. Basics & Application of Computational Chemistry in Action (BACCA), Erasmus+ Blended Intensive Programme, virtual session
    Poster presentation/Lodz, Poland, 2024.06.03
"The Applicability of Curcumin and Ascorbic Acid as Natural Antioxidant Additives"

15. 12th Visegrad Symposium on Biomolecular Interactions
Poster presentation/ Piešťany, Slovakia, 2024.06.26-23
"Theoretical study of the applicability of natural antioxidant additives"

References

1. Scott, G., *Polymers and the Environment*. 1999: Royal Society of Chemistry. *ISNB: 0-85404-578-3*.
2. Ulbricht, M.J.P., *Advanced functional polymer membranes*. Polymer, 2006. **47**(7): p. 2217-2262 DOI: https://doi.org/10.1016/j.polymer.2006.01.084.
3. Pendergast, MaryTheresa .M., and E.M. Hoek, A review of water treatment membrane nanotechnologies. Energy & Environmental Science, 2011. 4(6): p. 1946-1971.
4. Ratner, Buddy D., Allan S. Hoffman, Frederick J. Schoen, and Jack E. Lemons. Biomaterials science: an introduction to materials in medicine. Elsevier, 2004.
5. Agarwal, S., J.H. Wendorff, and A. Greiner, Use of electrospinning technique for biomedical applications. Polymer, 2008. 49(26): p. 5603-5621 doi:10.1016/j.polymer.2008.09.014.
6. Vilela, F., et al., *Conjugated porous polymers for energy applications*. Energy & Environmental Science, 2012. **5**(7): p. 7819-7832 DOI: doi:10.1039/C2EE22002D.
7. Tomlinson, E.P., M.E. Hay, and B.W.J.M. Boudouris, Radical polymers and their application to organic electronic devices. Macromolecules, 2014. 47(18): p. 6145-6158 DOI: https://doi.org/10.1021/ma5014572.
8. Mülhaupt, Rolf, Green polymer chemistry and bio-based plastics: dreams and reality. Macromolecular Chemistry and Physics, 2013. 214(2): p. 159-174 DOI: 10.1002/macp.201200439.
9. Cheng, H., et al., *Green polymer chemistry: a brief review*. American Chemical Society, 2013: p. 1-12 DOI: DOI: 10.1021/bk-2013-1144.ch001.
10. Jiang, Shanxue, and Bradley P. Ladewig, Green synthesis of polymeric membranes: Recent advances and future prospects. 2020. 21: p. 1-8 DOI: https://doi.org/10.1016/j.cogsc.2019.07.002.
11. Ebewele, R.O., Polymer science and technology. 2000: CRC press. https://doi.org/10.1201/9781420057805.
12. Song, B., A.-J. Qin, and B.Z.J. Tang, Green Monomer of CO 2 and Alkyne-based Four-component Tandem Polymerization toward Regio-and Stereoregular Poly (aminoacrylate) s. Chinese Journal of Polymer science, 2021. 39(1): p. 51-59 DOI: https://doi.org/10.1007/s10118-020-2454-2.
13. Wang, Jia, Anjun Qin, and Ben Zhong Tang, Multicomponent Polymerizations Involving Green Monomers. Macromolecular Rapid Communications, 2020: p. 2000547 DOI: 10.1002/marc.202000547.
14. Grignard, B., et al., *Advances in the use of CO 2 as a renewable feedstock for the synthesis of polymers*. he Royal Society of Chemistry 2019. **48**(16): p. 4466-4514 DOI: DOI: 10.1039/c9cs00047j.
15. Lu, X.-B. and D.J.J.C.S.R. Darensbourg, *Cobalt catalysts for the coupling of CO 2 and epoxides to provide polycarbonates and cyclic carbonates*. Chemical Society Reviews, 2012. **41**(4): p. 1462-1484 DOI: doi:10.1039/C1CS15142H.
16. Ugi, I., et al., *Ugi reactions with trifunctional α-amino acids, aldehydes, isocyanides and alcohols*. Elsevier Science Ltd, 1996. **52**(35): p. 11657-11664 DOI: https://doi.org/10.1016/0040-4020(96)00647-3.

17. Plastikos, H.G.L., Robert Scott, A Greek-English Lexicon, at Perseus. Perseus.tufts.edu. Retrieved on 2011-07-01.
18. Massy, J., *A Little Book about BIG Chemistry: The Story of Man-Made Polymers*. 2017: Springer.
19. Mohanty, A., et al., *Biofibres, biodegradable polymers and biocomposites: An overview.* Macromolecular Materal. Eng., 2000. **276**(1): p. 1-24 DOI: https://doi.org/10.1002/(SICI)1439-2054(20000301)276:1<1::AID-MAME1>3.0.CO;2-W.
20. Sheldon, R.A. and M.J.G.C. Norton, *Green chemistry and the plastic pollution challenge: towards a circular economy.* The Royal Society of Chemistry Advances, 2020. **22**(19): p. 6310-6322 DOI: DOI: 10.1039/D0GC02630A.
21. Schutyser, W., et al., *Chemicals from lignin: an interplay of lignocellulose fractionation, depolymerisation, and upgrading.* 2018. **47**(3): p. 852-908 DOI: DOI: 10.1039/c7cs00566k.
22. Wang, Z., M.S. Ganewatta, and C.J.P.i.P.S. Tang, *Sustainable polymers from biomass: Bridging chemistry with materials and processing.* Progress in Polymer Science, 2020. **101**: p. 101197 DOI: https://doi.org/10.1016/j.progpolymsci.2019.101197.
23. Song, R., et al., *Current development of biodegradable polymeric materials for biomedical applications.* Drug design, development and therapy, 2018. **12**: p. 3117 DOI: https://doi.org/10.2147/DDDT.S165440.
24. Teo, A.J., et al., *Polymeric biomaterials for medical implants and devices.* ACS Biomaterials Science & Engineering is published by the American Chemical Society, 2016. **2**(4): p. 454-472 DOI: https://doi.org/10.1021/acsbiomaterials.5b00429.
25. Lu, D. and C. Wong, *Materials for advanced packaging*. Vol. 181. 2009: Springer.
26. Ilyas, R. and S.J.C.A.C. Sapuan, *Biopolymers and biocomposites: chemistry and technology.* Current Analytical Chemistry, 2020. **16**(5): p. 500-503 DOI: https://doi.org/10.2174/1573411016052006030953 11.
27. Cao, X., et al., *Green composites reinforced with hemp nanocrystals in plasticized starch.* Journal of Applied Polymer Science, 2008. **109**(6): p. 3804-3810 DOI: DOI 10.1002/app.28418.
28. Asyraf, M., et al., *Potential Application of Green Composites for Cross Arm Component in Transmission Tower: A Brief Review.* Hindawi, International Journal of Polymer Science, 2020. **2020** DOI: https://doi.org/10.1155/2020/8878300.
29. Asyraf, M., et al., *Creep test rig for cantilever beam: Fundamentals, prospects and present views.* 2020. **14**(2): p. 6869-6887.
30. Asyraf, M., et al., *Fundamentals of creep, testing methods and development of test rig for the full-scale crossarm: a review.* Jurnal Teknologi, 2019. **81**(4) DOI: https://doi.org/10.11113/jt.v81.13402.
31. Vieira, P.R., et al., *Experimental fatigue behavior of pultruded glass fibre reinforced polymer composite materials.* Composites Part B, 2018. **146**: p. 69-75 DOI: doi:10.1016/j.compositesb.2018.03.040.
32. Berezina, N. and S.M. Martelli, *Bio-based polymers and materials*. 2014.

33. Iwata, T.J.A.C.I.E., *Biodegradable and bio-based polymers: future prospects of eco-friendly plastics*. Angew. Chemistry. Int., 2015. **54**(11): p. 3210-3215 DOI: DOI: 10.1002/anie.201410770.
34. Abdulbari, H.A., et al., *Bio-polymers for improving liquid flow in pipelines—A review and future work opportunities*. Journal of Industrial and Engineering Chemistry, 2014. **20**(4): p. 1157-1170 DOI: http://dx.doi.org/10.1016/j.jiec.2013.07.050.
35. Lu, S., et al., *MicroRNA-4262 activates the NF-κB and enhances the proliferation of hepatocellular carcinoma cells*. nternational Journal ofBiological Macromolecules, 2016. **86**: p. 43-49 DOI: doi: http://dx.doi.org/doi:10.1016/j.ijbiomac.2016.01.019.
36. Hernández, N., et al., *The battle for the "green" polymer. Different approaches for biopolymer synthesis: bioadvantaged vs. bioreplacement*. Organic & Biomolecular Chemistry, 2014. **12**(18): p. 2834-2849 DOI: DOI: 10.1039/c3ob42339e.
37. Duarte, A.R.C., et al., *Ionic liquids as foaming agents of semi-crystalline natural-based polymers*. Green Chemistry, 2012. **14**(7): p. 1949-1955 DOI: DOI: 10.1039/c2gc16652f.
38. Isikgor, F.H. and C.R.J.P.C. Becer, *Lignocellulosic biomass: a sustainable platform for the production of bio-based chemicals and polymers*. Polymer Chemistry, 2015. **6**(25): p. 4497-4559 DOI: DOI: 10.1039/C5PY00263J.
39. Zhang, C., et al., *Recent advances in vegetable oil-based polymers and their composites*. Progress in Polymer Science, 2017. **71**: p. 91-143 DOI: doi:http://dx.doi.org/doi:10.1016/j.progpolymsci.2016.12.009.
40. Turag, M., M. Rajib, and R. Uddin, *Production of Bio-Fuel & Bio-Plastic from Vegetable Waste as a Sustainable Waste Management*. 2019, Department of Mechanical and Production Engineering, Islamic University of ....
41. Lu, L., et al., *Chemical recycling technologies for PVC waste and PVC-containing plastic waste: A review*. Waste Management, 2023. **166**: p. 245-258 DOI: https://doi.org/10.1016/j.wasman.2023.05.012.
42. Wilkes, C.E., et al., *PVC handbook*. Vol. 184. 2005: Hanser Munich.
43. Zhang, M., et al., *Dioxins and polyvinylchloride in combustion and fires*. Waste Management & Research, 2015. **33**(7): p. 630-643 DOI: DOI: 10.1177/0734242X15590651.
44. Folarin, O.M. and E. Sadiku, *Thermal stabilizers for poly (vinyl chloride): A review*. Int. J. Phys. Sci, 2011. **6**(18): p. 4323-4330 DOI: DOI: 10.5897/IJPS11.654.
45. van Es, D.S., et al., *The compatibility of (natural) polyols with heavy metal-and zinc-free poly (vinyl chloride): Their effect on rheology and implications for plate-out*. Polymer Degradation and stability, 2008. **93**(1): p. 50-58 DOI: https://doi.org/10.1016/j.polymdegradstab.2007.10.016.
46. Huang, J., et al., *Thermal decomposition mechanisms of poly (vinyl chloride): A computational study*. Waste Management, 2018. **76**: p. 483-496 DOI: https://doi.org/10.1016/j.wasman.2018.03.033.
47. Yu, J., et al., *Thermal degradation of PVC: A review*. Waste management, 2016. **48**: p. 300-314 DOI: http://dx.doi.org/10.1016/j.wasman.2015.11.041.

48. Sabaa, M.W. and R.R. Mohamed, *Organic thermal stabilizers for rigid poly (vinyl chloride). Part XIII: Eugenol (4-allyl-2-methoxy-phenol).* Polymer degradation and stability, 2007. **92**(4): p. 587-595 DOI: https://doi.org/10.1016/j.polymdegradstab.2007.01.015.
49. Levchik, S.V. and E.D. Weil, *Overview of the recent literature on flame retardancy and smoke suppression in PVC.* Polymers for Advanced Technologies, 2005. **16**(10): p. 707-716 DOI: https://doi.org/10.1002/pat.645.
50. Ambrogi, V., et al., *Additives in polymers*, in *Modification of polymer properties*. 2017, Elsevier. p. 87-108.
51. Kockott, D., *Natural and artificial weathering of polymers.* Polymer Degradation and Stability, 1989. **25**(2-4): p. 181-208 DOI: https://doi.org/10.1016/S0141-3910(89)81007-9.
52. Marturano, V., P. Cerruti, and V. Ambrogi, *Polymer additives* Physical Sciences Reviews, 2017. **2**(6) DOI: doi:10.1515/psr-2016-0130.
53. Bockhorn, H., et al., *Kinetic study on the thermal degradation of polypropylene and polyethylene.* Journal of Analytical and Applied Pyrolysis, 1999. **48**(2): p. 93-109 DOI: https://doi.org/10.1016/S0165-2370(98)00131-4.
54. Calzonetti, J.A., C.J.J.R.c. Laursen, and technology, *Patents of Charles Goodyear: His international contributions to the rubber industry.* 2010. **83**(3): p. 303-321 DOI: https://doi.org/10.5254/1.3525687.
55. Zhang, Z., et al., *Enhanced morphology and hydrophilicity of PVDF flat membrane with modified CaCO3@ SMA additive via thermally induced phase separation method.* Journal of Industrial and Engineering Chemistry, 2022. **107**: p. 444-455 DOI: https://doi.org/10.1016/j.jiec.2021.12.016.
56. Paoli, M.A.D. and W.R.J.P. Waldman, *Bio-based additives for thermoplastics.* Polímeros, 2019. **29**(2) DOI: https://doi.org/10.1590/0104-1428.06318.
57. Fang, L., et al., *Influence of lanthanum stearate as a co-stabilizer on stabilization efficiency of calcium/zinc stabilizers to polyvinyl chloride.* Polymer degradation and stability, 2009. **94**(5): p. 845-850 DOI: doi:10.1016/j.polymdegradstab.2009.01.024.
58. Boulebd, H., *Comparative study of the radical scavenging behavior of ascorbic acid, BHT, BHA and Trolox: experimental and theoretical study.* Journal of Molecular Structure, 2020. **1201**: p. 127210 DOI: https://doi.org/10.1016/j.molstruc.2019.127210.
59. Benassi, R., et al., *Theoretical study on Curcumin: A comparison of calculated spectroscopic properties with NMR, UV–vis and IR experimental data.* Journal of Molecular Structure, 2008. **892**(1-3): p. 168-176 DOI: doi:10.1016/j.molstruc.2008.05.024.
60. Kirschweng, B., et al., *Efficiency of curcumin, a natural antioxidant, in the processing stabilization of PE: concentration effects.* Polymer Degradation and Stability, 2015. **118**: p. 17-23 DOI: http://dx.doi.org/10.1016/j.polymdegradstab.2015.04.006.
61. Schubert, M.A., et al., *Comparison of two antioxidants for poly (etherurethane urea) in an accelerated in vitro biodegradation system.* Journal of Biomedical Materials Research: An Official Journal of The Society for Biomaterials and The Japanese Society for Biomaterials, 1997. **34**(4): p. 493-505 DOI:

https://doi.org/10.1002/(SICI)1097-4636(19970315)34:4%3C493::AID-JBM10%3E3.0.CO;2-E.

62. Bruens, C., et al., *New performance additives from DSM*. 1999. **7**(8): p. 581-587.
63. Hahladakis, J.N., et al., *An overview of chemical additives present in plastics: Migration, release, fate and environmental impact during their use, disposal and recycling*. Journal of Hazardous Materials, 2018. **344**: p. 179-199.
64. Rezaeisadat, M., A.-K. Bordbar, and R. Omidyan, *Molecular dynamics simulation study of curcumin interaction with nano-micelle of PNIPAAm-b-PEG co-polymer as a smart efficient drug delivery system*. Journal of Molecular Liquids, 2021. **332**: p. 115862 DOI: https://doi.org/10.1016/j.molliq.2021.115862.
65. Rajan, V.K., C. Ragi, and K. Muraleedharan, *A computational exploration into the structure, antioxidant capacity, toxicity and drug-like activity of the anthocyanidin "Petunidin"*. Heliyon, 2019. **5**(7): p. e02115 DOI: https://doi.org/10.1016/j.heliyon.2019.e02115.
66. Nagarajan, S., et al., *Antioxidant activity of synthetic polymers of phenolic compounds*. Polymers, 2020. **12**(8): p. 1646 DOI: doi:10.3390/polym12081646.
67. Scott, G., *Antioxidants*. Bulletin of the Chemical Society of Japan, 1988. **61**(1): p. 165-170.
68. Maraveas, C., I.S. Bayer, and T. Bartzanas, *Recent advances in antioxidant polymers: From sustainable and natural monomers to synthesis and applications*. Polymers, 2021. **13**(15): p. 2465 DOI: https:// doi.org/10.3390/polym13152465.
69. Alov, P., I. Tsakovska, and I. Pajeva, *Computational studies of free radical-scavenging properties of phenolic compounds*. Current topics in medicinal chemistry, 2015. **15**(2): p. 85-104.
70. Leelaphiwat, P., et al., *Effects of nisin and EDTA on morphology and properties of thermoplastic starch and PBAT biodegradable films for meat packaging*. Food Chemistry, 2022. **369**: p. 130956 DOI: https://doi.org/10.1016/j.foodchem.2021.130956.
71. Neha, K., et al., *Medicinal prospects of antioxidants: A review*. European journal of medicinal chemistry, 2019. **178**: p. 687-704 DOI: https://doi.org/10.1016/j.ejmech.2019.06.010.
72. Spiegel, M., et al., *On the Scavenging Ability of Scutellarein against the OOH Radical in Water and Lipid-like Environments: A Theoretical Study*. Antioxidants, 2022. **11**(2): p. 224 DOI: https://doi.org/10.3390/ antiox11020224.
73. Al-Farsi, M., et al., *Color, flavonoids, phenolics and antioxidants of Omani honey*. Heliyon, 2018. **4**(10): p. e00874 DOI: doi: 10.1016/j.heliyon.2018. e00874.
74. Li, D., et al., *Polyphenols, anthocyanins, and flavonoids contents and the antioxidant capacity of various cultivars of highbush and half-high blueberries*. Journal of Food Composition and Analysis, 2017. **62**: p. 84-93 DOI: http://dx.doi.org/10.1016/j.jfca.2017.03.006.
75. Li, M.-J., et al., *Accurate bond dissociation enthalpies of popular antioxidants predicted by the ONIOM-G3B3 method*. Journal of Molecular Structure: THEOCHEM, 2007. **815**(1-3): p. 1-9 DOI: https://doi.org/10.1016/j.theochem.2007.03.012.

76. Mahmood, K., et al., *Synthesis and characterization of chitin/curcumin blended polyurethane elastomers*. International journal of biological macromolecules, 2018. **113**: p. 150-158 DOI: https://doi.org/10.1016/j.ijbiomac.2018.01.031.
77. Galano, A., et al., *Role of the reacting free radicals on the antioxidant mechanism of curcumin*. Chemical Physics, 2009. **363**(1-3): p. 13-23 DOI: doi:10.1016/j.chemphys.2009.07.003.
78. Sharma, O., *Antioxidant activity of curcumin and related compounds*. Biochemical pharmacology, 1976. **25**(15): p. 1811-1812 DOI: https://doi.org/10.1016/0006-2952(76)90421-4.
79. Soudamini, K., et al., *Inhibition of lipid peroxidation and cholesterol levels in mice by curcumin*. Indian journal of physiology and pharmacology, 1992. **36**: p. 239-239.
80. Xiao, Y., et al., *Curcumin inhibits acute vascular inflammation through the activation of heme oxygenase-1*. Oxidative medicine and cellular longevity, 2018. **2018** DOI: https://doi.org/10.1155/2018/3295807.
81. Srimal, R. and B. Dhawan, *Pharmacology of diferuloyl methane (curcumin), a non-steroidal anti-inflammatory agent*. Journal of pharmacy and pharmacology, 1973. **25**(6): p. 447-452 DOI: https://doi.org/10.1111/j.2042-7158.1973.tb09131.x.
82. Nagabhushan, M. and S.V. Bhide, *Nonmutagenicity of curcumin and its antimutagenic action versus chili and capsaicin*. Nutrition and Cancer, , 1986 DOI: http://dx.doi.org/10.1080/01635588609513894.
83. Njus, D. and P.M. Kelley, *Vitamins C and E donate single hydrogen atoms in vivo*. FEBS letters, 1991. **284**(2): p. 147-151 DOI: https://doi.org/10.1016/0014-5793(91)80672-P.
84. Buettner, G.R., *The pecking order of free radicals and antioxidants: lipid peroxidation, α-tocopherol, and ascorbate*. Archives of biochemistry and biophysics, 1993. **300**(2): p. 535-543 DOI: https://doi.org/10.1006/abbi.1993.1074.
85. Tu, Y.-J., D. Njus, and H.B. Schlegel, *A theoretical study of ascorbic acid oxidation and HOO/O 2− radical scavenging*. Organic & biomolecular chemistry, 2017. **15**(20): p. 4417-4431 DOI: https://doi.org/10.1039/C7OB00791D.
86. Pereira, R., et al., *Comparative Analysis between Synthetic Vitamin E and Natural Antioxidant Sources from Tomato, Carrot and Coriander in Diets for Market-Sized Dicentrarchus labrax*. Antioxidants, 2022. **11**(4): p. 636 DOI: https://doi.org/10.3390/antiox11040636.
87. Tomassi, G. and V. Silano, *An assessment of the safety of tocopherols as food additives*. Food and Chemical Toxicology, 1986. **24**(10-11): p. 1051-1061 DOI: https://doi.org/10.1016/0278-6915(86)90288-7.
88. additives, E.P.o.F. and N.S.a.t. Food, *Scientific Opinion on the re-evaluation of tocopherol-rich extract (E 306), α-tocopherol (E 307), γ-tocopherol (E 308) and δ-tocopherol (E 309) as food additives*. EFSA Journal, 2015. **13**(9): p. 4247 DOI: https://doi.org/10.2903/j.efsa.2015.4247.
89. Silva, M.M. and F.C. Lidon, *An overview on applications and side effects of antioxidant food additives*. Emirates Journal of Food and Agriculture, 2016: p. 823-832 DOI: doi: 10.9755/ejfa.2016-07-806.

90. Poljšak, B., et al., *Role of the vitamin E model compound Trolox in the prevention of Cr (VI)-induced cellular damage.* Toxicological & Environmental Chemistry, 2006. **88**(1): p. 141-157 DOI: https://doi.org/10.1080/02772240500456680.
91. Ross, L., et al., *Partitioning and antioxidant action of the water-soluble antioxidant, Trolox, between the aqueous and lipid phases of phosphatidylcholine membranes: 14C tracer and product studies.* Biochimica et Biophysica Acta (BBA)-Biomembranes, 1995. **1237**(1): p. 77-85.
92. Marcos, B., et al., *Development of biodegradable films with antioxidant properties based on polyesters containing α-tocopherol and olive leaf extract for food packaging applications.* Food Packaging and Shelf Life, 2014. **1**(2): p. 140-150 DOI: https://doi.org/10.1016/j.fpsl.2014.04.002.
93. Al-Malaika, S., S. Issenhuth, and D. Burdick, *The antioxidant role of vitamin E in polymers V. Separation of stereoisomers and characterisation of other oxidation products of dl-α-tocopherol formed in polyolefins during melt processing.* Polymer degradation and stability, 2001. **73**(3): p. 491-503 DOI: https://doi.org/10.1016/S0141-3910(01)00137-9.
94. Thbayh, D.K. and B. Fiser, *Computational study of synthetic and natural polymer additives–Antioxidant potential of BHA, TBHQ, BHT, and curcumin.* Polymer Degradation and Stability, 2022: p. 109979 DOI: https://doi.org/10.1016/j.polymdegradstab.2022.109979.
95. Thbayh, D.K., et al., *Antioxidant Potential of Santowhite as Synthetic and Ascorbic Acid as Natural Polymer Additives.* Polymers, 2022. **14**(17): p. 3518.
96. Thbayh, D.K., et al., *Comparative study of the antioxidant capability of EDTA and Irganox.* Heliyon, 2023. **9**(5).
97. Moon, J.-K. and T. Shibamoto, *Antioxidant assays for plant and food components.* Journal of agricultural and food chemistry, 2009. **57**(5): p. 1655-1666 DOI: https://doi.org/10.1021/jf803537k.
98. Brand-Williams, W., M.-E. Cuvelier, and C. Berset, *Use of a free radical method to evaluate antioxidant activity.* LWT-Food science and Technology, 1995. **28**(1): p. 25-30 DOI: https://doi.org/10.1016/S0023-6438(95)80008-5.
99. Fathi-Karkan, S., et al., *A critical review of fibrous polyurethane-based vascular tissue engineering scaffolds.* Journal of Biological Engineering, 2022. **16**(1): p. 1-18 DOI: https://doi.org/10.1186/s13036-022-00286-9.
100. Zaharescu, T., et al., *Prevention of degradation of γ-irradiated EPDM using phenolic antioxidants.* Chemical Papers, 2016. **70**(4): p. 495-504 DOI: https://doi.org/10.1515/chempap-2015-0214.
101. Let, M.B., C. Jacobsen, and A.S. Meyer, *Ascorbyl palmitate, γ-tocopherol, and EDTA affect lipid oxidation in fish oil enriched salad dressing differently.* Journal of agricultural and food chemistry, 2007. **55**(6): p. 2369-2375 DOI: https://doi.org/10.1021/jf062675c.
102. Yu, Z., et al., *Development and antioxidation of metal ion chelating packaging film.* Food Packaging and Shelf Life, 2022. **32**: p. 100846 DOI: https://doi.org/10.1016/j.fpsl.2022.100846.
103. Leszczynski, J., *Handbook of computational chemistry*. Vol. 3. 2012: Springer Science & Business Media.
104. Lashkaripour, *A. Introduction to Quantum Chemistr : The Schrödinger Equation.* 2021.

105. Aslanova, H., N. Zeynalov, and D. Tagiyev, *CLASSIFICATION, ADVANTAGES AND DISADVANTAGES OF COMPUTER MODELING METHODS AND THEIR APPLICATION IN THE PREDICTION OF MULTIPLE PROCESSES*. DOI: doi.org/10.32737/0005-2531-2024-2-5-15.
106. Cramer, C.J. and F. Bickelhaupt, Essentials of computational chemistry. angewandte chemie-international edition in english , 2003. 42(4): p. 381-381.
107. Espinosa-Garcia, J., M. Monge-Palacios, and J. Corchado, *Constructing potential energy surfaces for polyatomic systems: Recent progress and new problems*. Advances in physical chemistry, 2012. **2012**(1): p. 164752 DOI: https://doi.org/10.1155/2012/164752.
108. Schlegel, H.B., *Exploring potential energy surfaces for chemical reactions: an overview of some practical methods*. Journal of computational chemistry, 2003. **24**(12): p. 1514-1527 DOI: https://doi.org/10.1002/jcc.10231.
109. Frisch, M., et al., *gaussian 09, Revision d. 01, Gaussian*. Inc., Wallingford CT, 2009. **201**.
110. Foresman, J.B.F., ,, *A.Exploring Chemistry with Electronic Structure Methods Third Edition*. Gaussian Inc., 2015.
111. Moeller, T., *Chemistry: with inorganic qualitative analysis*. 2012: Elsevier.
112. Sözbilir, M., *Students' ideas and misunderstanding of enthalpy and spontaneity: a review of selected researches*. Hacettepe Üniversitesi Eğitim Fakültesi Dergisi, 2004. **26**(26).
113. Hill, T.L., *An introduction to statistical thermodynamics*. 1986: Courier Corporation.
114. Eyube, E.S., P. Notani, and H. Samaila, *Analytical prediction of enthalpy and Gibbs free energy of gaseous molecules*. Chemical Thermodynamics and Thermal Analysis, 2022. **6**: p. 100060 DOI: https://doi.org/10.1016/j.ctta.2022.100060.
115. Boyd, D.B., K.B. Lipkowitz, and T.R. Cundari, *Reviews in Computational Chemistry*. 2008: Wiley-VCH.
116. Lewars, E.G., *Computational chemistry*. Introduction to the theory and applications of molecular and quantum mechanics, 2011. **318**.
117. Santra, B., *Density-functional theory exchange-correlation functionals for hydrogen bonds in water*. 2010, Technische Universität Berlin Berlin.
118. Chidiebere, C., C. Duru, and J.C. Mbagwu, *Application of computational chemistry in chemical reactivity: A review*. Journal of the Nigerian Society of Physical Sciences, 2021: p. 292-297 DOI: 10.46481/jnsps.2021.347.
119. Cohen, A.J., P. Mori-Sánchez, and W. Yang, *Challenges for density functional theory*. Chemical reviews, 2012. **112**(1): p. 289-320 DOI: https://doi.org/10.1021/cr200107z.
120. Hohenberg, P. and W. Kohn, *Density functional theory (DFT)*. Phys. Rev, 1964. **136**(1964): p. B864.
121. Parr, R.G., *Density functional theory*, in *Electron Distributions and the Chemical Bond*. 1982, Springer. p. 95-100.
122. Burke, K., *Perspective on density functional theory*. The Journal of chemical physics, 2012. **136**(15) DOI: https://doi.org/10.1063/1.4704546.
123. Bachrach, S.M., *Computational organic chemistry*. 2014: John Wiley & Sons.

124. Sousa, S.F., P.A. Fernandes, and M.J. Ramos, *General performance of density functionals*. The Journal of Physical Chemistry A, 2007. **111**(42): p. 10439-10452 DOI: https://doi.org/10.1021/jp0734474.
125. Perdew, J.P. and K. Schmidt. *Jacob's ladder of density functional approximations for the exchange-correlation energy*. in *AIP Conference Proceedings*. 2001. American Institute of Physics DOI: https://doi.org/10.1063/1.1390175.
126. Zhao, Y. and D.G. Truhlar, *A density functional that accounts for medium-range correlation energies in organic chemistry*. Organic Letters, 2006. **8**(25): p. 5753-5755 DOI: https://doi.org/10.1021/ol062318n.
127. Slater, J.C., *A simplification of the Hartree-Fock method*. Physical review, 1951. **81**(3): p. 385 DOI: https://doi.org/10.1103/PhysRev.81.385.
128. Perdew, J.P., K. Burke, and M. Ernzerhof, *Generalized gradient approximation made simple*. Physical review letters, 1996. **77**(18): p. 3865 DOI: https://doi.org/10.1103/PhysRevLett.77.3865.
129. Becke, A.D., *Density-functional exchange-energy approximation with correct asymptotic behavior*. Physical review A, 1988. **38**(6): p. 3098.
130. Lee, C., W. Yang, and R.G. Parr, *Development of the Colle-Salvetti correlation-energy formula into a functional of the electron density*. Physical review B, 1988. **37**(2): p. 785.
131. Perdew, J.P. and W. Yue, *Accurate and simple density functional for the electronic exchange energy: Generalized gradient approximation*. Physical review B, 1986. **33**(12): p. 8800 DOI: https://doi.org/10.1103/PhysRevB.33.8800.
132. Peng, H., et al., *SCAN+ rVV10: A promising van der Waals density functional*. arXiv preprint arXiv:1510.05712, 2015 DOI: https://doi.org/10.48550/arXiv.1510.05712.
133. Staroverov, V.N., et al., *Comparative assessment of a new nonempirical density functional: Molecules and hydrogen-bonded complexes*. The Journal of chemical physics, 2003. **119**(23): p. 12129-12137 DOI: https://doi.org/10.1063/1.1626543.
134. Becke, A.D., *Becke's three parameter hybrid method using the LYP correlation functional*. J. Chem. Phys, 1993. **98**(492): p. 5648-5652.
135. Matsushita, Y.-i., K. Nakamura, and A. Oshiyama, *Comparative study of hybrid functionals applied to structural and electronic properties of semiconductors and insulators*. Physical Review B—Condensed Matter and Materials Physics, 2011. **84**(7): p. 075205 DOI: https://doi.org/10.1103/PhysRevB.84.075205.
136. Nayebzadeh, M., et al., *Kinetics and oxidation mechanism of pyrene initiated by hydroxyl radical. A theoretical investigation*. Chemical Physics, 2020. **528**: p. 110522 DOI: https://doi.org/10.1016/j.chemphys.2019.110522.
137. Jasiński, R., *Searching for zwitterionic intermediates in Hetero Diels–Alder reactions between methyl α, p-dinitrocinnamate and vinyl-alkyl ethers*. Computational and Theoretical Chemistry, 2014. **1046**: p. 93-98 DOI: https://doi.org/10.1016/j.comptc.2014.08.002. .
138. Zhao, Y. and D.G. Truhlar, *The Minnesota density functionals and their applications to problems in mineralogy and geochemistry*. Rev. Mineral. Geochem, 2010. **71**: p. 19-37 DOI: https://doi.org/10.1515/9781501508448-004.

139. Zhao, Y. and D.G. Truhlar, *A new local density functional for main-group thermochemistry, transition metal bonding, thermochemical kinetics, and noncovalent interactions*. The Journal of chemical physics, 2006. **125**(19) DOI: https://doi.org/10.1063/1.2370993.
140. Perlt, E., *Basis sets in computational chemistry*. 2021: Springer.
141. Jensen, F., *Atomic orbital basis sets*. Wiley Interdisciplinary Reviews: Computational Molecular Science, 2013. **3**(3): p. 273-295 DOI: https://doi.org/10.1002/wcms.1123.
142. Davidson, E.R. and D. Feller, *Basis set selection for molecular calculations*. Chemical Reviews, 1986. **86**(4): p. 681-696.
143. Cassady, S.J., et al., *The thermal decomposition of ethane*. Fuel, 2020. **268**: p. 117409 DOI: https://doi.org/10.1016/j.fuel.2020.117409.
144. Rassolov, V.A., et al., *6-31G* basis set for third-row atoms*. Journal of Computational Chemistry, 2001. **22**(9): p. 976-984 DOI: https://doi.org/10.1002/jcc.1058.
145. Schäfer, A., H. Horn, and R. Ahlrichs, *Fully optimized contracted Gaussian basis sets for atoms Li to Kr*. The Journal of chemical physics, 1992. **97**(4): p. 2571-2577 DOI: https://doi.org/10.1063/1.463096.
146. Weigend, F. and R. Ahlrichs, *Balanced basis sets of split valence, triple zeta valence and quadruple zeta valence quality for H to Rn: Design and assessment of accuracy*. Physical Chemistry Chemical Physics, 2005. **7**(18): p. 3297-3305 DOI: https://doi.org/10.1039/B508541A.
147. Veszprémi, T., et al., *Fundamentals of Group Theory*. Quantum Chemistry: Fundamentals to Applications, 1999: p. 3-27.
148. Beck, A.D., *Density-functional thermochemistry. III. The role of exact exchange*. J. Chem. Phys, 1993. **98**(7): p. 5648-6.
149. Vosko, S.H., L. Wilk, and M. Nusair, *Accurate spin-dependent electron liquid correlation energies for local spin density calculations: a critical analysis*. Canadian Journal of physics, 1980. **58**(8): p. 1200-1211 DOI: https://doi.org/10.1139/p80-159. .
150. Zhao, Y. and D.G. Truhlar, *The M06 suite of density functionals for main group thermochemistry, thermochemical kinetics, noncovalent interactions, excited states, and transition elements: two new functionals and systematic testing of four M06-class functionals and 12 other functionals*. Theoretical chemistry accounts, 2008. **120**(1): p. 215-241 DOI: 10.1007/s00214-007-0310-x.
151. Zhao, Y., N.E. Schultz, and D.G. Truhlar, *Design of density functionals by combining the method of constraint satisfaction with parametrization for thermochemistry, thermochemical kinetics, and noncovalent interactions*. Journal of chemical theory and computation, 2006. **2**(2): p. 364-382 DOI: https://doi.org/10.1021/ct0502763. .
152. de Souza, G.L. and K.A. Peterson, *Benchmarking antioxidant-related properties for gallic acid through the use of DFT, MP2, CCSD, and CCSD (T) approaches*. The Journal of Physical Chemistry A, 2021. **125**(1): p. 198-208 DOI: https://doi.org/10.1021/acs.jpca.0c09116.
153. Santos, J.L., et al., *Probing structural properties and antioxidant activity mechanisms for eleocarpanthraquinone*. Journal of Molecular Modeling, 2020. **26**(9): p. 1-8 DOI: https://doi.org/10.1007/s00894-020-04469-3. .

154. Pandithavidana, D.R. and S.B. Jayawardana, *Comparative Study of Antioxidant Potential of Selected Dietary Vitamins*.
155. Lu, Y., et al., *Reaction mechanism of ferulic acid scavenging OH and NO2 radicals: a theoretical study*. Structural Chemistry, 2022: p. 1-7 DOI: https://doi.org/10.1007/s11224-021-01855-2.
156. Maciel, E.N., et al., *A computational study on the reaction between fisetin and 2, 2-diphenyl-1-picrylhydrazyl (DPPH)*. Journal of Molecular Modeling, 2019. **25**(4): p. 1-8 DOI: https://doi.org/10.1007/s00894-019-3969-8.
157. Maciel, E.N., et al., *Examining the reaction between antioxidant compounds and 2, 2-diphenyl-1-picrylhydrazyl (DPPH) through a computational investigation*. Journal of Molecular Modeling, 2018. **24**(8): p. 1-12 DOI: https://doi.org/10.1007/s00894-018-3745-1.
158. Zheng, Y.-Z., et al., *Theoretical studies on the antioxidant activity of pinobanksin and its ester derivatives: Effects of the chain length and solvent*. Food chemistry, 2018. **240**: p. 323-329 DOI: http://dx.doi.org/10.1016/j.foodchem.2017.07.133.
159. Thbayh, D.K., A. Rágyanszki, and B. Fiser, Antioxidant potential of butylated hydroxytoluene (BHT) – A theoretical study. Materials Science and Engineering, 2021. 46(1): p. 63-69 DOI: https://doi.org/10.32974/mse.2021.007.
160. Spiegel, M., *Current Trends in Computational Quantum Chemistry Studies on Antioxidant Radical Scavenging Activity*. Journal of Chemical Information and Modeling, 2022 DOI: https://doi.org/10.1021/acs.jcim.2c00104.
161. Wang, L., et al., *Effects of nitro-and amino-group on the antioxidant activity of genistein: a theoretical study*. Food chemistry, 2019. **275**: p. 339-345 DOI: https://doi.org/10.1016/j.foodchem.2018.09.108.
162. Marković, Z., et al., *Revisiting the solvation enthalpies and free energies of the proton and electron in various solvents*. Computational and Theoretical Chemistry, 2016. **1077**: p. 11-17 DOI: http://dx.doi.org/10.1016/j.comptc.2015.09.007.
163. Fifen, J.J., *Thermodynamics of the electron revisited and generalized*. Journal of Chemical Theory and Computation, 2013. **9**(7): p. 3165-3169 DOI: https://doi.org/10.1021/ct400212t.
164. Fifen, J.J., Z. Dhaouadi, and M. Nsangou, *Revision of the thermodynamics of the proton in gas phase*. The Journal of Physical Chemistry A, 2014. **118**(46): p. 11090-11097 DOI: https://doi.org/10.1021/jp508968z.
165. Najafi, M., M. Zahedi, and E. Klein, *DFT/B3LYP study of the solvent effect on the reaction enthalpies of homolytic and heterolytic OH bond cleavage in mono-substituted chromans*. Computational and Theoretical Chemistry, 2011. **978**(1-3): p. 16-28 DOI: doi:10.1016/j.theochem.2010.04.002.
166. TAGHI, Z.M. and F. Fakhimi, *Kinetics Study of Degradation and Stabilizing Effect of Organic Thermal Stabilizers (EDTA, 1,2 Propane Diol, Benzoic Acid, and Phenol) for Rigid Polyvinyl Chloride*. 2005.
167. Ruijian, X., Z. Dafei, and Z. Deren, *Effect of organotin stabiliser on the thermal stabilisation of PVC: Part II—Structure changes in PVC and the mechanism of stabilisation*. Polymer degradation and stability, 1990. **28**(3): p. 323-330 DOI: https://doi.org/10.1016/0141-3910(90)90071-E.

168. Spiliopoulos, G., M. Statheropoulos, and G. Parissakis, *Mass spectrometric study of the stabilization of PVC with dioctyltin dithioglycolic acid ester*. European polymer journal, 1989. **25**(9): p. 989-991 DOI: https://doi.org/10.1016/0014-3057(89)90125-0.
169. PVC Thermomat, Metrohm Magyarország Kft., Hungary, 2018. .
170. Moslem, A.I., *Flame Retarding-Stabilizing Behavior of Plasticized Poly (vinyl chloride) Containing Novel Heavy Metal Free Modifier*. 2021, Miskolci Egyetem.
171. Foxboro, I., *Table of conductivity vs. concentration for common solutions*. 1999.
172. Rimarčík, J., et al., *Study of the solvent effect on the enthalpies of homolytic and heterolytic N–H bond cleavage in p-phenylenediamine and tetracyano-p-phenylenediamine*. Journal of Molecular Structure: THEOCHEM, 2010. **952**(1-3): p. 25-30 DOI: doi:10.1016/j.theochem.2010.04.002.
173. Thong, N.M., et al., *Theoretical investigation on the bond dissociation enthalpies of phenolic compounds extracted from Artocarpus altilis using ONIOM (ROB3LYP/6-311++ G (2df, 2p): PM6) method*. Chemical Physics Letters, 2014. **613**: p. 139-145 DOI: http://dx.doi.org/10.1016/j.cplett.2014.08.067.
174. Thong, N.M., et al., *Antioxidant properties of xanthones extracted from the pericarp of Garcinia mangostana (Mangosteen): a theoretical study*. Chemical Physics Letters, 2015. **625**: p. 30-35 DOI: http://dx.doi.org/10.1016/j.cplett.2015.02.033.
175. Lee, C.Y., et al., *Computational Study of Ortho-Substituent Effects on Antioxidant Activities of Phenolic Dendritic Antioxidants*. Antioxidants, 2020. **9**(3): p. 189 DOI: doi:10.3390/antiox9030189.
176. Alberto, M.E., et al., *A physicochemical examination of the free radical scavenging activity of Trolox: mechanism, kinetics and influence of the environment*. Physical chemistry chemical physics, 2013. **15**(13): p. 4642-4650 DOI: https://doi.org/10.1039/C3CP43319F.
177. Luo, Y.-R., *Comprehensive handbook of chemical bond energies*. 2007: CRC press.
178. Leopoldini, M., N. Russo, and M. Toscano, *The molecular basis of working mechanism of natural polyphenolic antioxidants*. Food Chemistry, 2011. **125**(2): p. 288-306 DOI: doi:10.1016/j.foodchem.2010.08.012.
179. Zuquan, J., *Carbon—hydrogen bond dissociation energies and stretching frequencies*. Journal of Molecular Structure: THEOCHEM, 1985. **123**(3-4): p. 443-455 DOI: https://doi.org/10.1016/0166-1280(85)80185-8.
180. Vo, Q.V., et al., *Density functional theory study of the role of benzylic hydrogen atoms in the antioxidant properties of lignans*. Scientific reports, 2018. **8**(1): p. 1-10 DOI: https://doi.org/10.1038/s41598-018-30860-5.
181. Li, M., et al., *A DFT study on reaction of eupatilin with hydroxyl radical in solution*. International Journal of Quantum Chemistry, 2013. **113**(7): p. 966-974 DOI: https://doi.org/10.1002/qua.24060.
182. Pérez-González, A. and A. Galano, *On the• OH and• OOH scavenging activity of 3-methyl-1-pyridin-2-yl-5-pyrazolone: Comparisons with its parent compound, edaravone*. International Journal of Quantum Chemistry, 2012. **112**(21): p. 3441-3448 DOI: https://doi.org/10.1002/qua.24046.

183. Škorňa, P., et al., *Thermodynamic study of vitamin B6 antioxidant potential*. Computational and Theoretical Chemistry, 2016. **1077**: p. 32-38 DOI: http://dx.doi.org/10.1016/j.comptc.2015.10.010.
184. Xue, Y., et al., *Density functional theory study of the structure–antioxidant activity of polyphenolic deoxybenzoins*. Food chemistry, 2014. **151**: p. 198-206 DOI: http://dx.doi.org/10.1016/j.foodchem.2013.11.064.
185. Wang, Y.-N., et al., *Kinetics and mechanism of the oxidation of ascorbic acid in aqueous solutions by a trans-dioxoruthenium (VI) complex*. Inorganic Chemistry, 2009. **48**(1): p. 400-406 DOI: https://doi.org/10.1021/ic8015904
186. Wang, G., et al., *Theoretical study on the structural and antioxidant properties of some recently synthesised 2, 4, 5-trimethoxy chalcones*. Food chemistry, 2015. **171**: p. 89-97 DOI: http://dx.doi.org/10.1016/j.foodchem.2014.08.106.
187. Leopoldini, M., et al., *Detailed investigation of the OH radical quenching by natural antioxidant caffeic acid studied by quantum mechanical models*. Journal of Chemical Theory and Computation, 2011. **7**(12): p. 4218-4233 DOI: https://doi.org/10.1021/ct200572p.
188. Pandithavidana, D.R. and S.B. Jayawardana, *Comparative study of antioxidant potential of selected dietary vitamins; computational insights*. Molecules, 2019. **24**(9): p. 1646 DOI: https://doi.org/10.3390/molecules24091646.
189. Zavala-Oseguera, C., et al., *OH radical gas phase reactions with aliphatic ethers: a variational transition State Theory Study*. The Journal of Physical Chemistry A, 2009. **113**(50): p. 13913-13920 DOI: https://doi.org/10.1021/jp906144d.
190. Galano, A. and J.R. Alvarez-Idaboy, *Guanosine+ oh radical reaction in aqueous solution: A reinterpretation of the uv− vis data based on thermodynamic and kinetic calculations*. Organic Letters, 2009. **11**(22): p. 5114-5117 DOI: https://doi.org/10.1021/ol901862h.
191. Fiser, B.l., et al., *Antioxidant potential of glutathione: a theoretical study*. The Journal of Physical Chemistry B, 2011. **115**(38): p. 11269-11277 DOI: https://doi.org/10.1021/jp2049525.
192. Molski, M., *Theoretical study on the radical scavenging activity of gallic acid*. Heliyon, 2023: p. e12806 DOI: https://doi.org/10.1016/j.heliyon.2023.e12806.
193. Wayner, D., et al., *Application of Photoacoustic Calorimetry to the Measurement of the OH Bond Strength in Vitamin E (alpha-and delta-Tocopherol) and Related Phenolic Antioxidants (1)*. The Journal of organic chemistry, 1996. **61**(18): p. 6430-6433.
194. Klein, E., V. Lukeš, and M. Ilčin, *DFT/B3LYP study of tocopherols and chromans antioxidant action energetics*. Chemical physics, 2007. **336**(1): p. 51-57 DOI: doi:10.1016/j.chemphys.2007.05.007.
195. Lucarini, M., et al., *Bond dissociation energies of O− H bonds in substituted phenols from equilibration studies*. The Journal of organic chemistry, 1996. **61**(26): p. 9259-9263 DOI: https://doi.org/10.1021/jo961039i.
196. Rohman, R., R. Nath, and R. Kar, *Revisiting the hydrogen atom transfer reactions through a simple and accurate theoretical model: Role of hydrogen bond energy in polyphenolic antioxidants*. Computational and Theoretical Chemistry, 2023. **1223**: p. 114097 DOI: https://doi.org/10.1016/j.comptc.2023.114097.

197. Wright, J.S., et al., *Theoretical calculation of substituent effects on the O− H bond strength of phenolic antioxidants related to vitamin E*. Journal of the American Chemical Society, 1997. **119**(18): p. 4245-4252 DOI: https://doi.org/10.1021/ja963378z.
198. Baj, A., et al., *Synthesis, DFT calculations, and in vitro antioxidant study on novel carba-analogs of vitamin E*. Antioxidants, 2019. **8**(12): p. 589 DOI: https://doi.org/10.3390/antiox8120589.
199. Ardalan, P., T. Ardalan, and M. Momen Heravi, *A DFT Study on Antioxidant Activity of Trolox and Substituted Trolox and Their Radicals*. Applied Chemistry, 2013. **8**(29): p. 45-50 DOI: 10.22075/CHEM.2013.2463.
200. Tsioptsias, C., et al., *Effect of an Antioxidant and a Compatibilizer on the Mechanical Properties of Virgin and Thermally Aged Polypropylene Drawn Fibers*. Textiles, 2022. **2**(3): p. 499-510 DOI: https://doi.org/10.3390/textiles2030028.

DOI: 10.14750/ME.2025.027

Appendix A

Comparative Study of the Antioxidant Capability of EDTA and Irganox

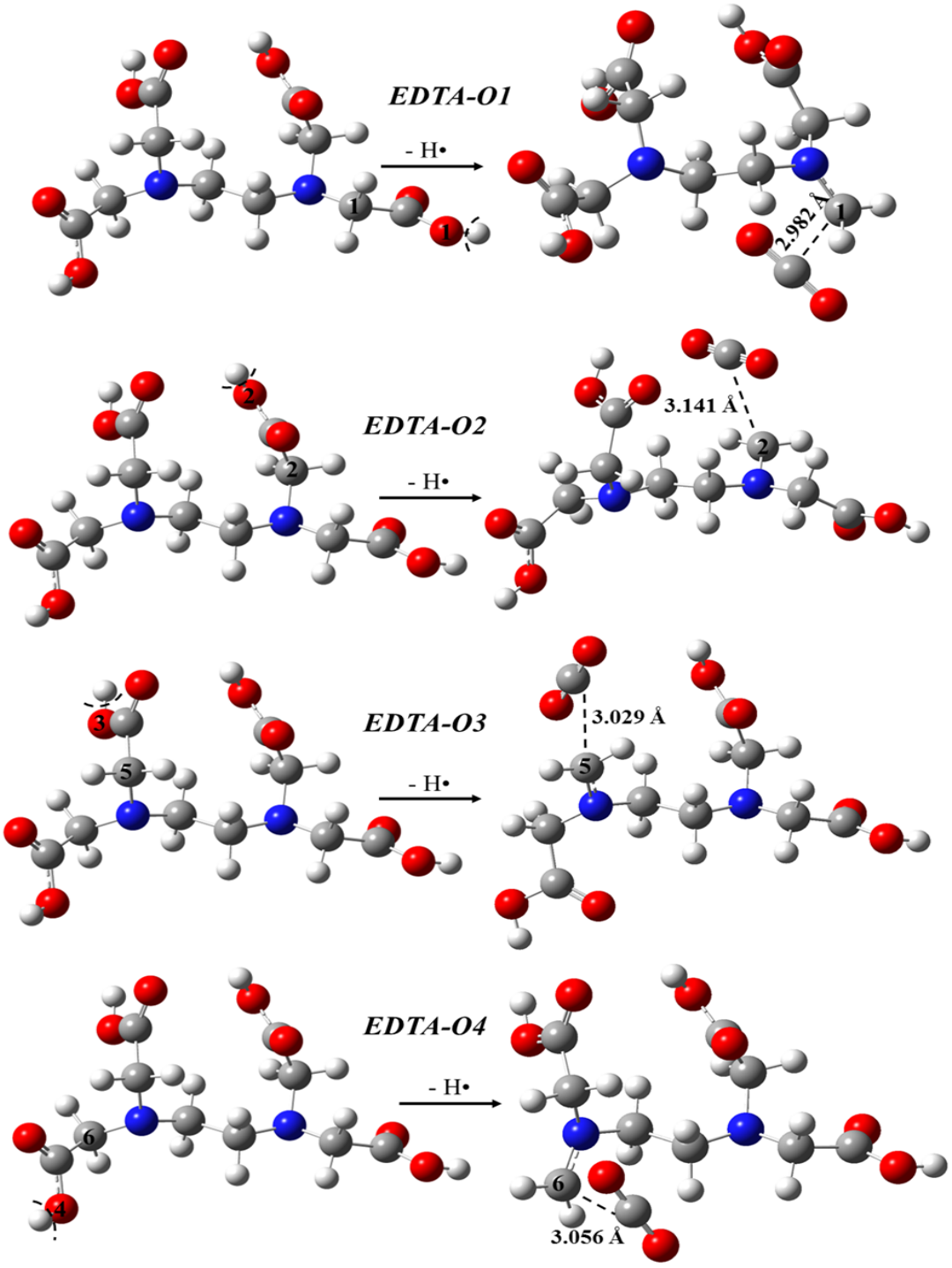

Figure A1. Optimized structures of ethylenediaminetetraacetic acid (EDTA) and the corresponding radical species after H-atom transfer in the hydrogen atom transfer (HAT) mechanism in case of the O1-H, O2-H, O3-H, and O4-H sites. The species have been computed at the M05-2X/6-311++G(2d,2p) level of theory in the gas phase and specific geometrical parameters are also shown (in Å).

DOI: 10.14750/ME.2025.027

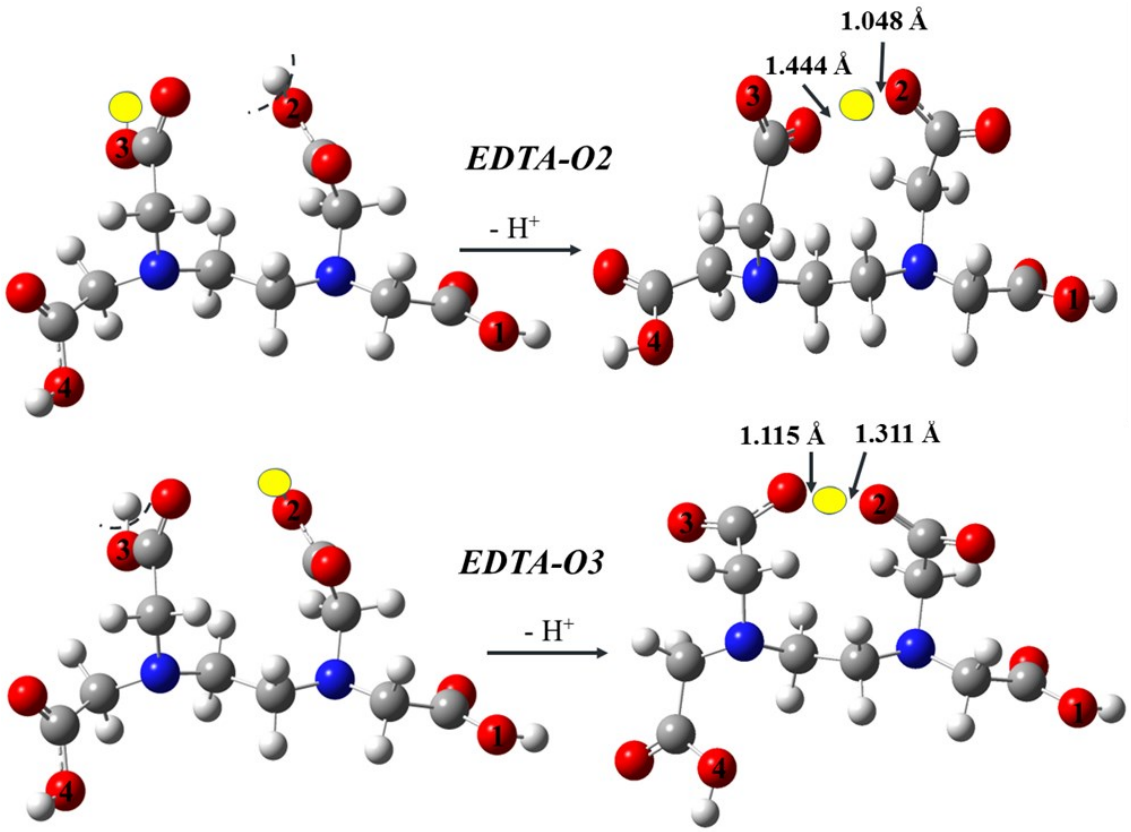

Figure A2. Optimized structures of ethylenediaminetetraacetic acid (EDTA) and the corresponding anionic species after proton loss in the first step of the SPLET mechanism in the cases of the O2-H and O3-H donor sites. The species have been computed at the M05-2X/6-311++G(2d,2p) level of theory in the gas phase and the corresponding specific geometric parameters are also shown (in Å).

Table A1. The ionization potential (IP), proton dissociation enthalpy (PDE), proton affinities (PAs) and electron transfer enthalpies (ETE) values in kJ/mol for ethylenediaminetetraacetic acid (EDTA) and Irganox model calculated at the M05-2X/6-311++G(2d,2p) level of theory in gas phase.

Compound	IP	PDE	IP+PDE	PA	ETE	PA+ETE
EDTA	702.1					
O1-H		967.7	1669.7	1407.1	268.8	1676.0
O2-H		959.7	1661.8	1321.8*	385.7*	1707.4*
O3-H		959.9	1662.0	1295.5*	401.5*	1697.0*
O4-H		962.7	1664.7	1388.7	271.1	1659.8
C1-H		918.8	1620.9	1504.3	137.8	1642.0
C2-H		922.4	1624.5	1466.4	165.7	1632.1
C3-H		975.0	1677.1	1624.4	58.0	1682.4
C4-H		960.3	1662.3	1624.2	55.5	1679.7
C5-H		922.5	1624.5	1402.6	248.2	1650.8
C6-H		922.0	1624.1	1483.6	143.4	1627.0
Irganox	730.5					
O-H		915.2	1645.7	1409.5	236.2	1645.7
C1-H		1041.6	1772.1	1639.6	132.5	1772.1

DOI: 10.14750/ME.2025.027

C2-H	1043.4	1773.9	1626.5	147.4	1773.9
C3-H	1006.5	1737.0	1669.6	67.4	1737.0
C4-H	1005.6	1736.2	1707.7	28.5	1736.2
C5-H	941.8	1672.3	1578.5	93.3	1671.9
C6-H	966.8	1697.3	1526.3	171.0	1697.3
C7-H	995.7	1726.3	1674.7	51.6	1726.3

* Rearrangement after deprotonation

DOI: 10.14750/ME.2025.027

Appendix B

Insights into the Antioxidant Potential of α-Tocopherol and Trolox

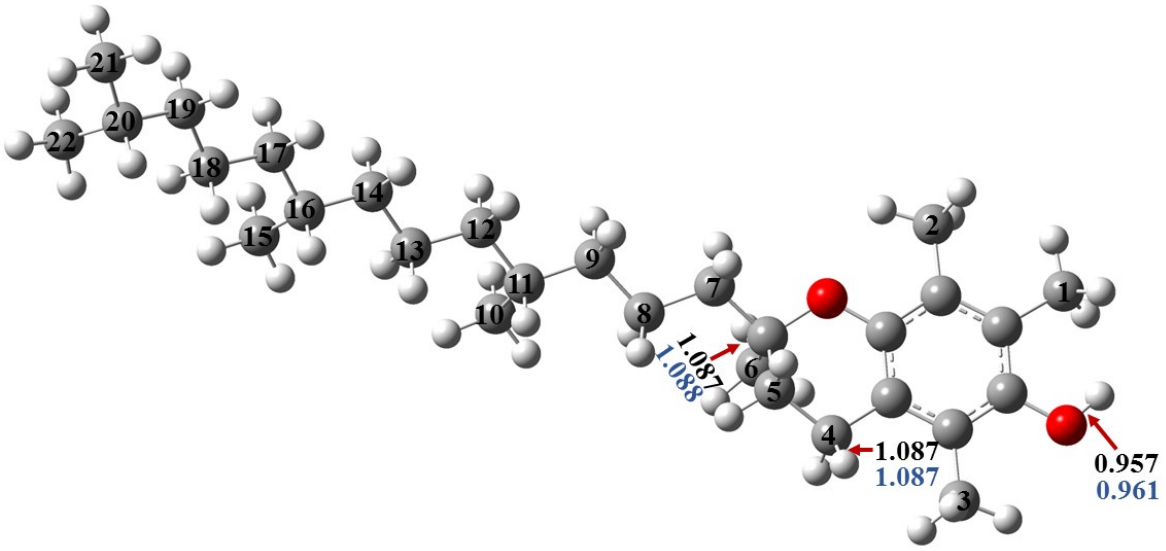

Figure B 1. Optimized geometries of the studied natural antioxidant additives α-Tocopherol (vitamin E). Geometry optimizations have been carried out at the M05-2X/6-311++G(2d,2p) level of theory in gas and water phase, and the appropriate bond lengths (in Å) for the strongest and weakest X-H (X=O, C) bond are also displayed in the black (gas) and blue (water) phases.

Table B1. Bond lengths (B.L) (in Å), Bond dissociation enthalpy (BDE), ionization potential (IP), proton dissociation enthalpy (PDE), proton affinities (PAs) and electron transfer enthalpies (ETE) values in kJ/mol for α-Tocopherol (vitamin E) calculated at the M05-2X/6-311++G(2d,2p) level of theory in gas phase.

Compound	B.L	BDE	IP	PDE	IP+PDE	PA	ETE	PA+ETE
α-Tocopherol			664.5					
O-H	0.957	324.7		974.1	1638.7	1460.7	178.0	1638.7
C1-H	1.082	367.9		1017.5	1682.1	1566.8	115.1	1681.8
C2-H	1.081	367.0		1016.5	1681.0	1591.4	89.8	1681.2
C3-H	1.087	365.6		1017.4	1681.9	1593.1	88.8	1681.9
C4-H	1.087	353.1		1002.5	1667.0	1576.6	90.4	1667.0
C5-H*	1.086	410.6						
C6-H	1.087	422.9		1072.3	1736.8	1680.2	58.9	1739.0
C7-H	1.090	411.0		1060.4	1724.9	1685.3	39.6	1724.9
C8-H	1.090	399.6		1048.9	1713.4	1680.4	33.0	1713.4
C9-H	1.092	405.9		1055.4	1719.9	1695.1	24.8	1719.9
C10-H	1.090	411.1		1060.5	1725.0	1696.8	28.3	1725.0
C11-H	1.093	400.8		1051.9	1716.4	1686.6	25.4	1712.0
C12-H	1.093	405.1		1051.8	1716.3	1697.1	24.4	1721.5
C13-H	1.092	400.9		1050.4	1714.9	1700.1	15.0	1715.1
C14-H	1.092	407.9		1057.4	1721.9	1700.8	20.8	1721.7
C15-H	1.090	413.7		1065.5	1730.1	1701.0	26.3	1727.3

DOI: 10.14750/ME.2025.027

C16-H	1.093	399.9	1049.8	1714.4	1697.0	18.1	1715.1
C17-H	1.093	408.7	1055.4	1720.0	1706.1	15.5	1721.6
C18-H	1.092	397.8	1047.3	1711.8	1707.4	5.2	1712.6
C19-H	1.093	405.6	1058.1	1722.6	1709.5	10.0	1719.6
C20-H	1.092	401.0	1050.1	1714.7	1708.4	6.3	1714.7
C21-H	1.090	418.4	1067.9	1732.4	1724.6	7.8	1732.4
C22-H	1.093	416.9	1066.4	1730.9	1711.1	19.8	1730.9

* Rearrangement after deprotonation

Table B 2. Bond lengths (B.L) (in Å), Bond dissociation enthalpy (BDE), ionization potential (IP), proton dissociation enthalpy (PDE), proton affinities (PAs) and electron transfer enthalpies (ETE) values in kJ/mol for α-Tocopherol (vitamin E) calculated at the M05-2X/6-311++G(2d,2p) level of theory in solvent phase (water).

Compound	**B.L**	**BDE**	**IP**	**PDE**	**IP+PDE**	**PA**	**ETE**	**PA+ETE**
α-Tocopherol			438.7					
O-H	0.961	326.6		67.6	506.3	172.1	335.2	507.3
C1-H	1.082	373.0		110.9	549.6	318.2	235.9	554.1
C2-H	1.082	374.1		114.7	553.4	325.2	227.8	553.1
C3-H	1.087	372.5		112.9	551.6	325.0	226.2	551.2
C4-H	1.087	360.2		100.9	539.6	329.8	209.8	539.6
C5-H	1.086	415.3		156.7	595.4	388.1	206.6	594.7
C6-H	1.088	427.6		168.2	606.9	380.5	223.9	604.5
C7-H	1.091	415.0		155.8	594.5	402.8	189.5	592.3
C8-H	1.090	407.8		148.4	587.0	413.0	173.3	586.2
C9-H	1.093	413.3		153.9	592.6	417.2	175.4	592.7
C10-H	1.091	420.9		159.8	598.5	401.1	199.6	600.7
C11-H	1.093	406.6		147.4	586.1	421.8	164.2	585.9
C12-H	1.093	412.2		152.8	591.5	415.8	175.7	591.5
C13-H	1.092	402.6		143.2	581.9	418.7	163.0	581.7
C14-H	1.093	412.8		153.4	592.1	415.9	175.9	591.9
C15-H	1.091	422.4		158.9	597.6	401.6	195.9	597.6
C16-H	1.093	407.3		147.0	585.7	422.4	160.3	582.8
C17-H	1.093	412.8		153.5	592.2	416.0	175.8	591.8
C18-H	1.092	403.3		141.0	579.7	418.6	163.8	582.4
C19-H	1.093	413.5		154.2	592.9	417.9	174.6	592.5
C20-H	1.091	404.8		143.0	581.7	423.1	161.0	584.1
C21-H	1.090	426.7		167.3	606.0	405.2	200.8	606.0
C22-H	1.090	424.9		165.9	604.6	402.2	202.1	604.2

DOI: 10.14750/ME.2025.027

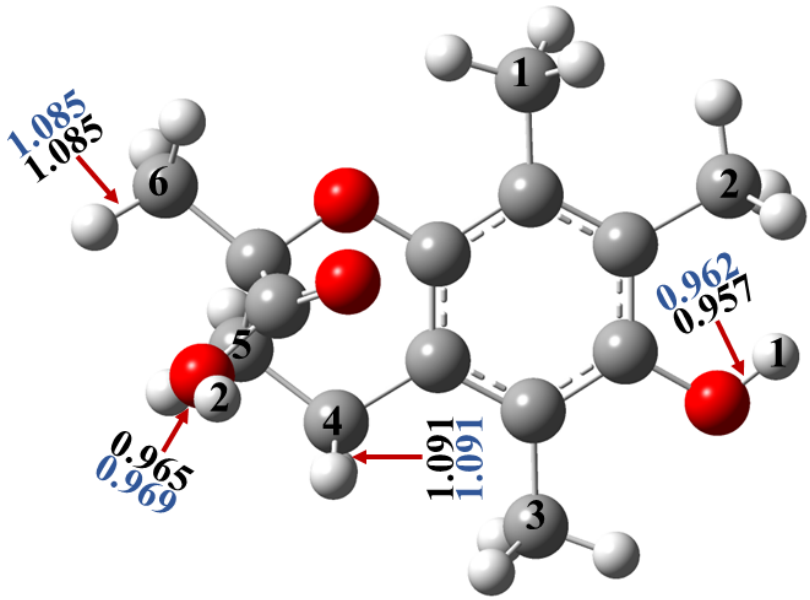

Figure B2. Optimized geometries of the studied natural antioxidant additives Trolox. Geometry optimizations have been carried out at the M05-2X/6-311++G(2d,2p) level of theory in gas and water phase, and the appropriate bond lengths (in Å) for the strongest and weakest X-H (X=O, C) bond are also displayed in the black (gas) and blue (water) phases.

Table B 3. Bond dissociation enthalpy (BDE), ionization potential (IP), proton dissociation enthalpy (PDE), proton affinities (PAs) and electron transfer enthalpies (ETE) values in kJ/mol for Trolox calculated at the M05-2X/6-311++G(2d,2p) level of theory in gas phase.

Compound	B.L	BDE	IP	PDE	IP+PDE	PA	ETE	PA+ETE
Trolox			674.7					
O1-H	0.957	326.9		966.9	1641.7	1461.2	179.7	1640.9
O2-H	0.965	367.5		1029.5	1704.2	1403.1	279.2	1682.3
C1-H	1.081	368.9		1008.1	1682.9	1592.6	90.3	1682.8
C2-H	1.082	367.9		1007.2	1682.0	1567.6	114.2	1681.9
C3-H	1.082	365.5		1004.7	1679.4	1588.7	90.7	1679.4
C4-H	1.091	354.5		993.7	1668.5	1570.6	97.9	1668.5
C5-H	1.085	413.6		1052.8	1727.6	1629.1	98.5	1727.6
C6-H*	1.085	425.1						

* Rearrangement after deprotonation

Table B4. Bond dissociation enthalpy (BDE), ionization potential (IP), proton dissociation enthalpy (PDE), proton affinities (PAs) and electron transfer enthalpies (ETE) values in kJ/mol for Trolox calculated at the M05-2X/6-311++G(2d,2p) level of theory in solvent phase (water).

Compound	B.L	BDE	IP	PDE	IP+PDE	PA	ETE	PA+ETE
Trolox			450.9					
O1-H	0.962	332.7		61.6	512.5	172.4	338.9	511.4
O2-H	0.969	358.2		86.2	537.1	100.7	436.4	537.1
C1-H	1.082	374.6		103.6	554.5	321.3	232.6	553.9
C2-H	1.082	376.6		105.0	555.9	315.8	240.0	555.9
C3-H	1.083	372.4		102.0	552.9	319.3	232.4	551.7

DOI: 10.14750/ME.2025.027

C4-H	1.091	362.3	90.7	541.6	321.7	220.0	541.6
C5-H	1.084	420.1	149.0	599.9	369.2	230.2	599.4
C6-H	1.085	435.8	165.3	616.1	349.5	265.6	615.1

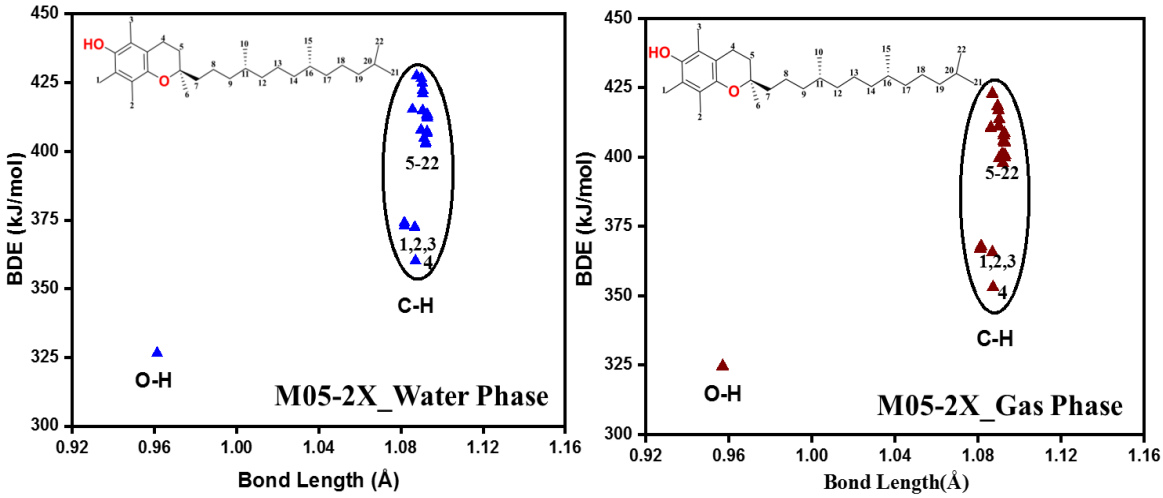

Figure B3. Bond dissociation enthalpy (BDE) vs bond length plot for studied natural antioxidant additive α-Tocopherol (vitamin E). The calculations have been carried out at the M05-2X/6-311++G(2d,2p) level of theory in the gas and water phases.

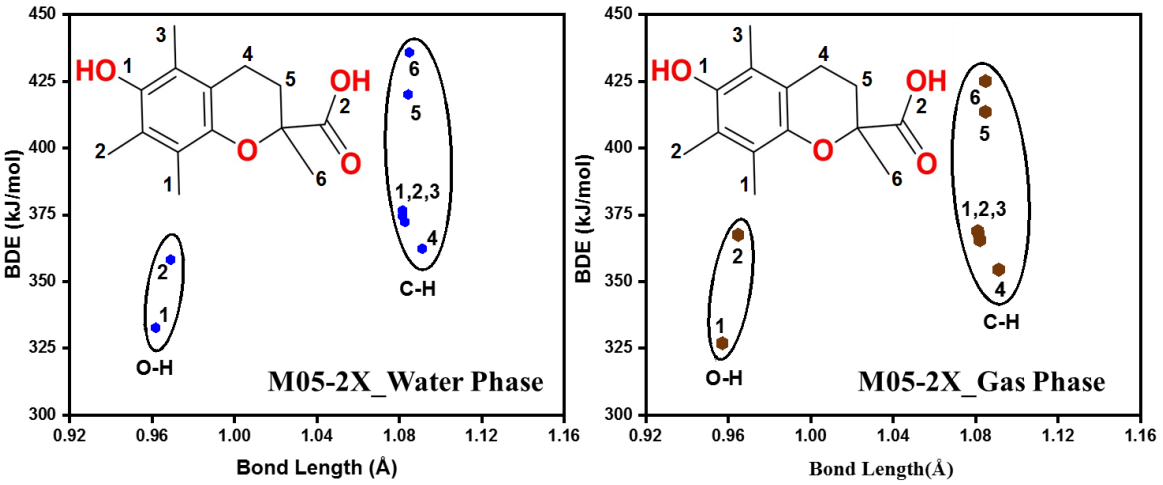

Figure B4. Bond dissociation enthalpy (BDE) vs bond length plot for studied natural antioxidant additive Trolox. The calculations have been carried out at the M05-2X/6-311++G(2d,2p) level of theory in the gas and water phases.

DOI: 10.14750/ME.2025.027

Appendix C

Experimental Results (Dehydrochlorination Tests)

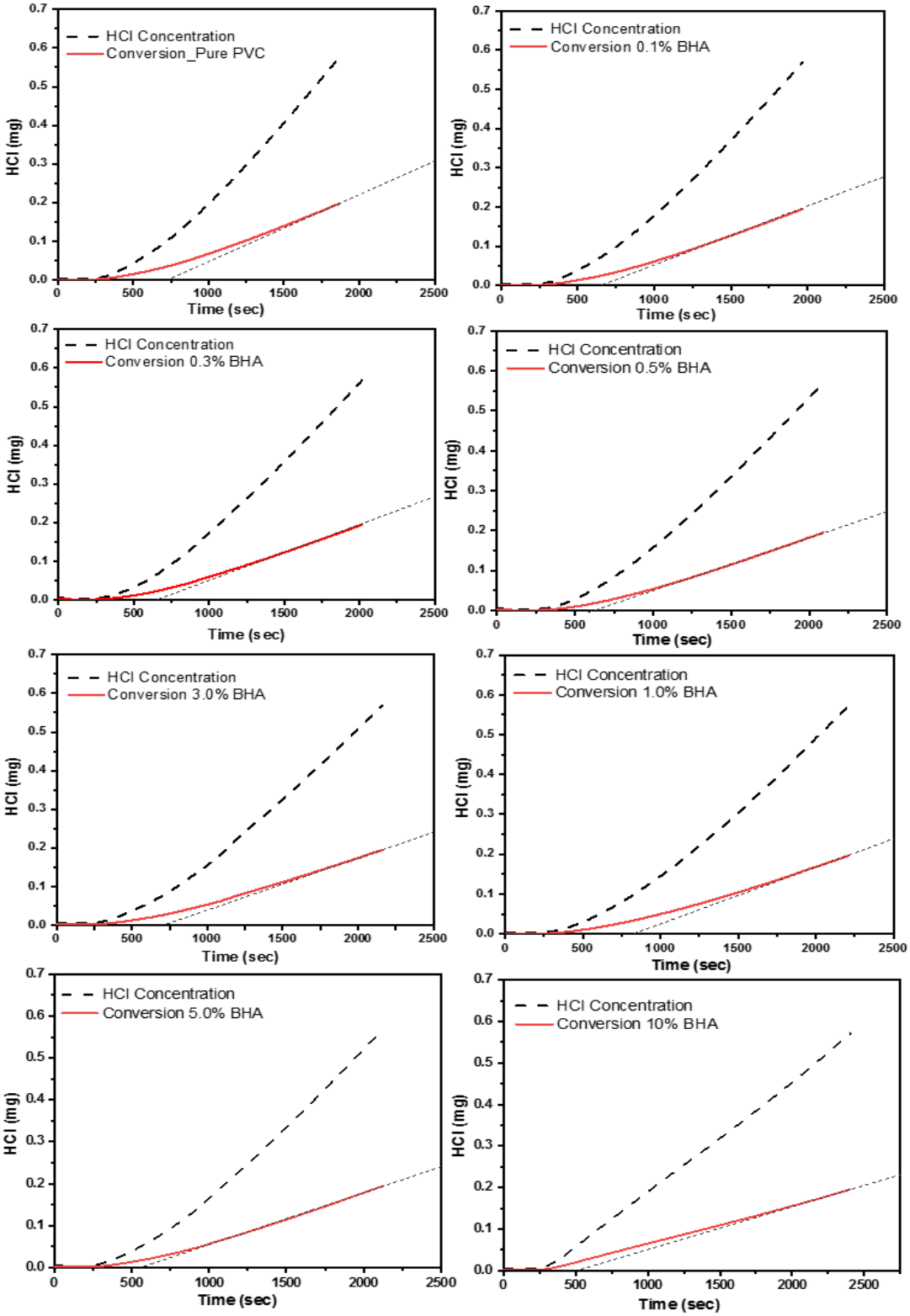

Figure C1. Dehydrochlorination test of poly (vinyl chloride) mixed with different ratios (0.0, 0.1, 0.3, 1.0, 3.0, 5.0, 10.0, 20.0 wt.%) of BHA and tested at 180°C by using the 895 Professional PVC Thermomat.

DOI: 10.14750/ME.2025.027

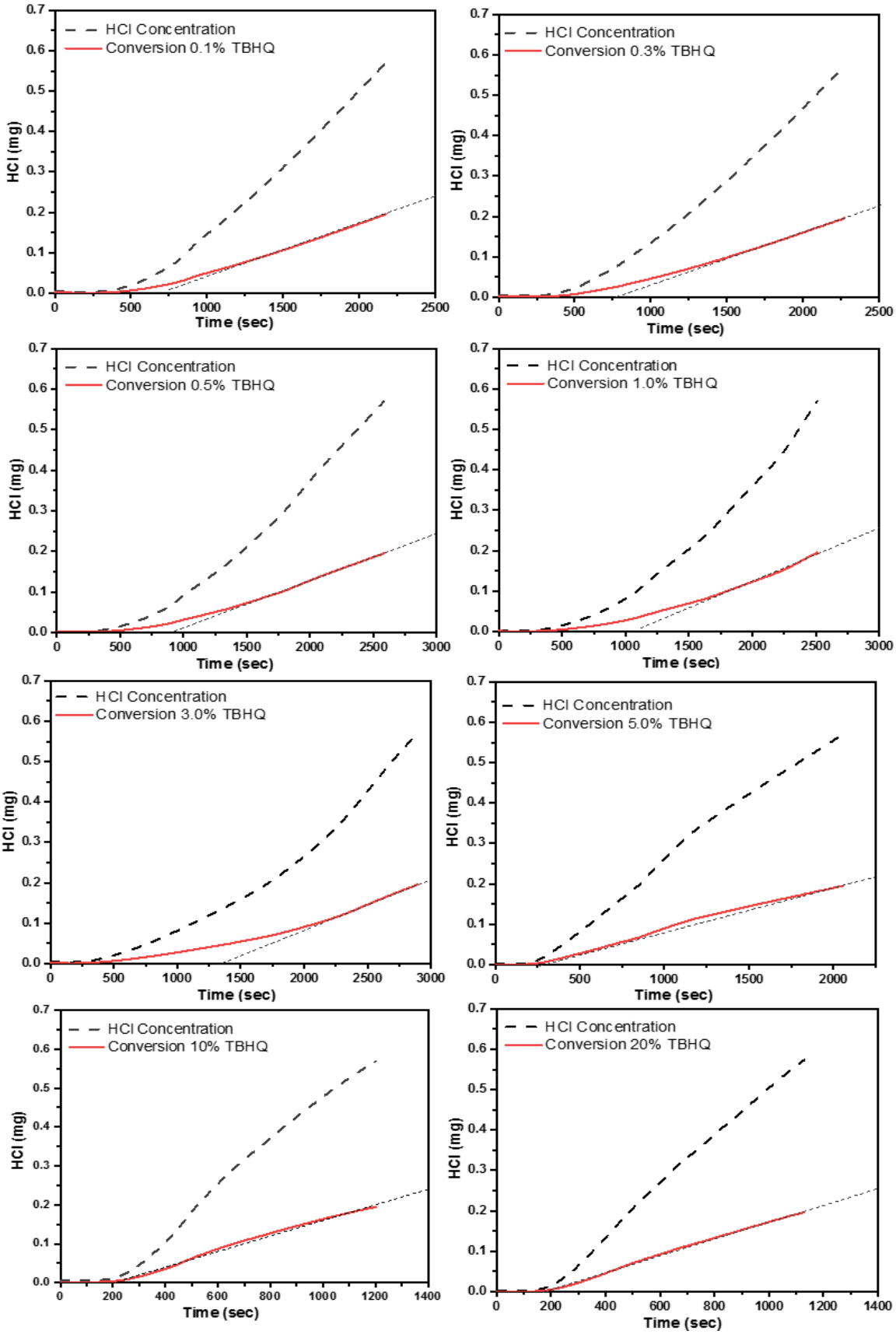

Figure C2. Dehydrochlorination test of poly (vinyl chloride) mixed with different ratios (0.0, 0.1, 0.3, 1.0, 3.0, 5.0, 10.0, 20.0 wt.%) of TBHQ and tested at 180°C by using the 895 Professional PVC Thermomat.

DOI: 10.14750/ME.2025.027

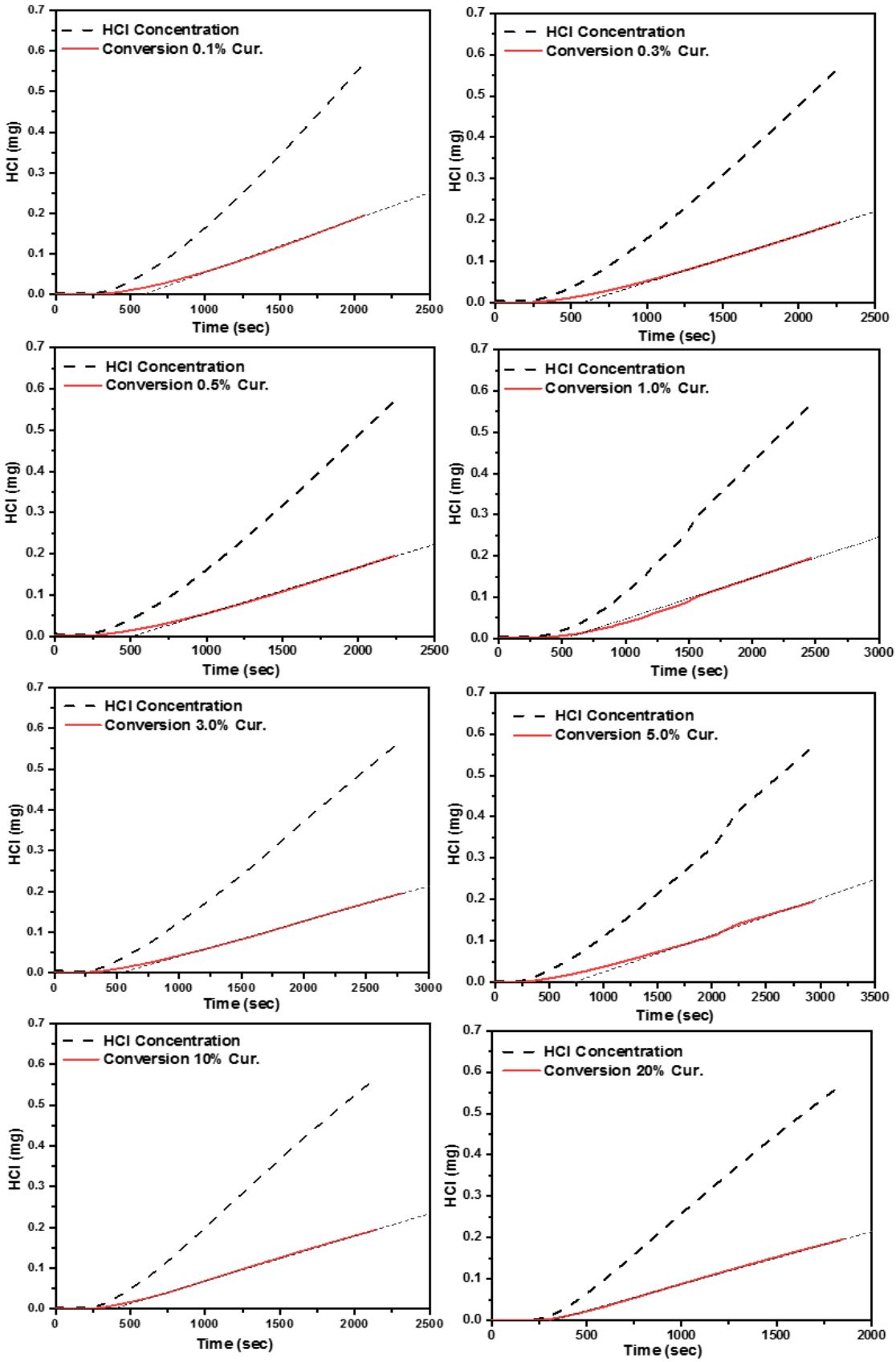

Figure C3. Dehydrochlorination test of poly (vinyl chloride) mixed with different ratios (0.0, 0.1, 0.3, 1.0, 3.0, 5.0, 10.0, 20.0 wt.%) of curcumin and tested at 180°C by using the 895 Professional PVC Thermomat.

DOI: 10.14750/ME.2025.027

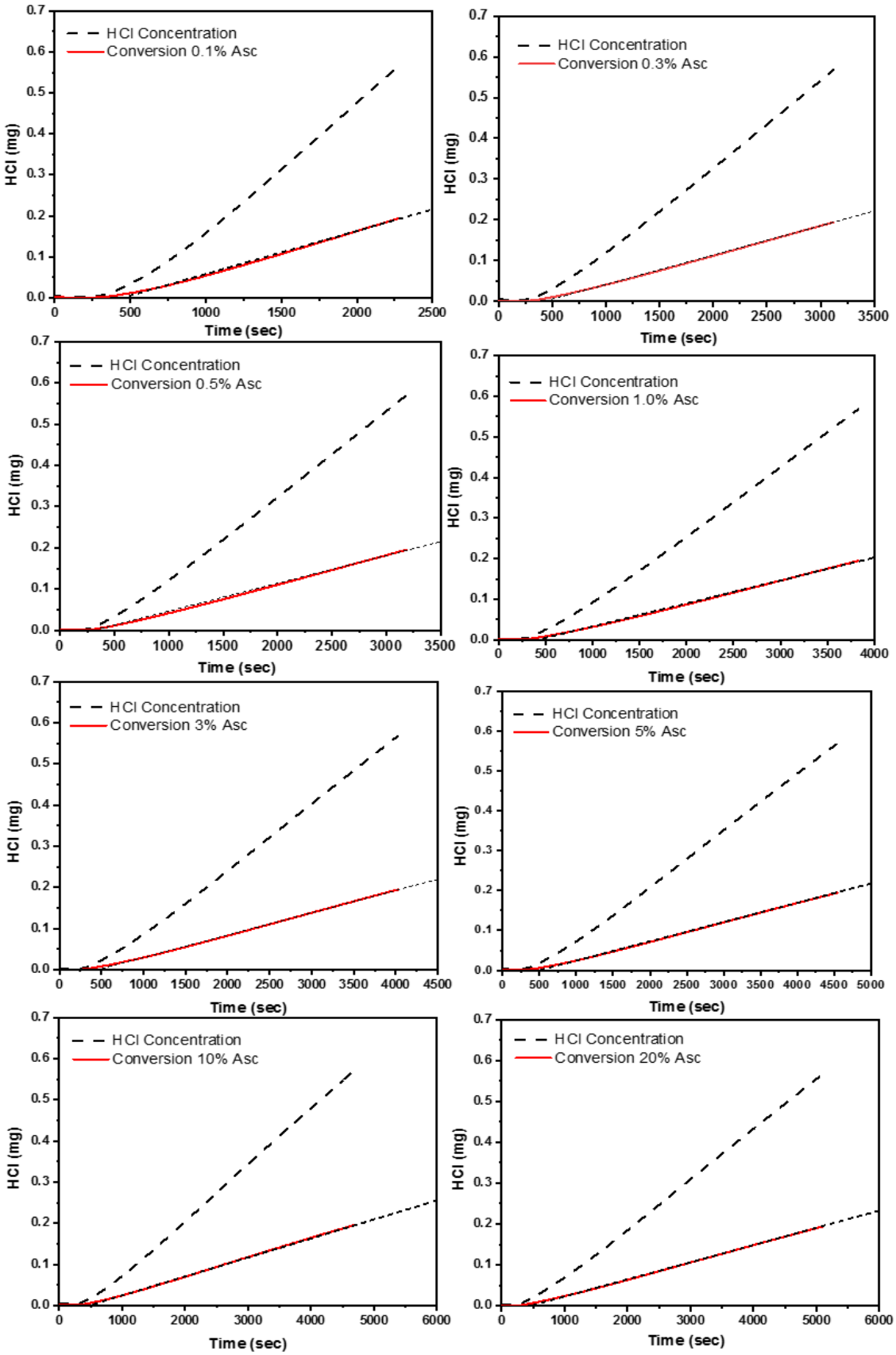

Figure C4. Dehydrochlorination test of poly (vinyl chloride) mixed with different ratios (0.0, 0.1, 0.3, 1.0, 3.0, 5.0, 10.0, 20.0 wt.%) of Asc and tested at 180°C by using the 895 Professional PVC Thermomat.

DOI: 10.14750/ME.2025.027

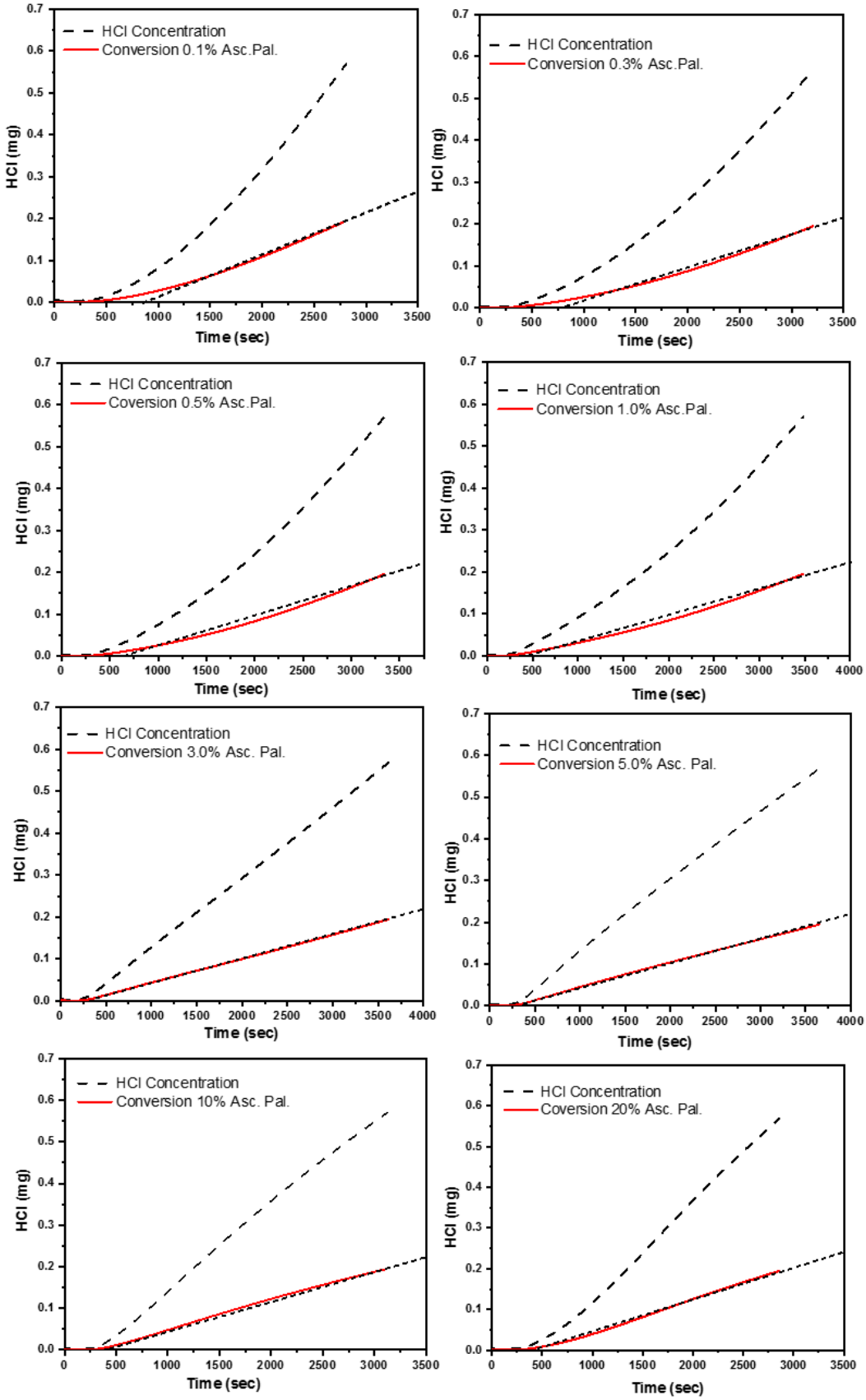

Figure C5. Dehydrochlorination test of poly (vinyl chloride) mixed with different ratios (0.0, 0.1, 0.3, 1.0, 3.0, 5.0, 10.0, 20.0 wt.%) of Asc. Pal. and tested at 180°C by using the 895 Professional PVC Thermomat.